INFLUENCE OF CONCRETE THICKNESS ON THE NATURAL FIRE RESISTANCE OF COMPOSITE SLABS

Sirine Amira

Final report of the thesis presented to the

Université libre de Tunis - ULT

Polytechnic Institute of Bragança – IPB

For the fulfilment of the requirements for a Master's Degree in

Construction Engineering

December, 2020

INFLUENCE OF CONCRETE THICKNESS ON THE NATURAL FIRE RESISTANCE OF COMPOSITE SLABS

Sirine Amira

Final report of the thesis presented to the

Université libre de Tunis - ULT

Polytechnic Institute of Bragança – IPB

For the fulfilment of the requirements for a Master's Degree in

Construction Engineering

In the scope of the double degree program with the

Université libre de Tunis - ULT

Supervised by:

Prof. Dr. Paulo Alexandre Gonçalves Piloto (IPB)

Prof. Dr. Carlos Jorge da Rocha Balsa (IPB)

Prof. Dr. Youssfi Ismail(ULT)

December, 2020

ACKNOWLEDGEMENT

I would like to thank all the people who contributed to the success of my thesis and who helped me in writing this report

First of all, I would like to thank my parents, grandparents, my sister and my brother, for their constant support and their confidence in me. Without their encouragement, this work could not have been carried out successfully.

Special thanks to my supervisors at IPB, Professor Paulo Alexandre Gonçalves Piloto and Professor Carlos Jorge da Rocha Balsa, for their invaluable support, patience and guidance throughout the development of this work. Thank you for sharing the expertise and providing important advice that made this project possible.

Professor Yousfi Ismail, my supervisor at ULT, is cordially thanked for his help and dedication. In addition, I would like to thank professor Khzemi Issam Din for encouraging me on this trip, as well as all the professors of the IPB and the ULT, for helping me to build knowledge throughout my graduation.

ABSTRACT

This work studies the thermal behavior of composite slabs under controlled test conditions, which correspond to a natural fire from below. This composite solution consists of a concrete coating poured onto a steel deck. Concrete is usually reinforced with a steel mesh, but it can also contain individual steel bars.

This composite solution is widely used in all types of buildings and requires fire resistance in accordance with regulations and standards.

The composite slab must meet the fire safety requirements of the building code. The fire resistance of these items is usually evaluated using standard fire resistance tests. Test samples are being prepared in agreement with fire resistance criteria on the stability (R), integrity standards (E) and insulation (I) must be considered. Annexe D of EN 1994-1-2 provides guidelines for the calculation of fire resistance (I) and temperature of steel and unprotected parts of steel decks exposed to fire. However, over the past two decades, no revisions have been made to these methods.

The main work developed in this thesis consists in the development of numerical models for thermal analysis, using the MATLAB software. In order to study the effects of different parameters on the fire resistance (I) of the composite slab a total of 96 numerical simulations were carried out considering the perfect contact and an air gap between the steel deck and the concrete topping.

The results show that the calculation rules given in European standards are generally conservatives and do not consider important parameters. This work provides improved equations for estimating the fire resistance (I) in function of the effective thickness.

Keywords: composite slab; fire resistance; heat transfer; finite element method, numerica lsimulation, Matlab

RESUMO

Este trabalho estuda o comportamento térmico de lajes mistas em condições de ensaio controladas, que correspondem a um incêndio natural vindo de baixo. Esta solução composta consiste em um revestimento de concreto derramado sobre uma plataforma de aço. O concreto geralmente é reforçado com uma tela de aço, mas também pode conter barras de aço individuais.

Esta solução composta é amplamente utilizada em todos os tipos de edifícios e requer resistência ao fogo de acordo com os regulamentos e normas.

A laje mista deve atender aos requisitos de segurança contra incêndio do código de construção. A resistência ao fogo desses itens é geralmente avaliada usando testes padrão de resistência ao fogo. As amostras de teste estão sendo preparadas de acordo com os critérios de resistência ao fogo quanto à estabilidade (R), padrões de integridade (E) e isolamento (I) devem ser considerados. O anexo D da EN 1994-1-2 fornece diretrizes para o cálculo da resistência ao fogo (I) e da temperatura do aço e das partes desprotegidas das plataformas de aço expostas ao fogo. No entanto, nas últimas duas décadas, nenhuma revisão foi feita nesses métodos.

O principal trabalho desenvolvido nesta tese consiste no desenvolvimento de modelos numéricos para análise térmica, utilizando o software MATLAB. Com o objetivo de estudar os efeitos de diferentes parâmetros na resistência ao fogo (I) da laje mista, foram realizadas 96 simulações numéricas considerando o contato perfeito e um entreferro entre o tabuleiro de aço e a cobertura de concreto.

Os resultados mostram que as regras de cálculo fornecidas nas normas europeias são geralmente conservadoras e não consideram parâmetros importantes. Este trabalho fornece equações aprimoradas para estimar a resistência ao fogo (I) em função da espessura efetiva.

Palavras-chave: laje mista; resistência ao fogo; transferência de calor; método dos elementos finitos, simulação numérica, Matlab

INDEX

LIST OF FIGURES

Table List

SYMBOLS

Latin letters

A/L_r	The rib geometry factor
A_t	Total area of enclosure (walls, ceiling and floor, including openings)
A_v	Total are of vertical openings on all walls
b	Thermal absorptivity for the total enclosure
c	Specific heat
c_a	Specific heat of carbon steel
c_{air}	Specific heat of air
c_p	Specific heat of dry concrete
$c_{p,peak}$	Peak of specific heat of concrete according to a certain moisture content
D	Maximum deflection
d	Distance from the extreme fibre of the cold design compression zone to the extreme fibre of the cold design tensile zone
d'_{reb}	Concrete cover for rebar
E	Integrity criterion
E_b	Maximum amount of thermal radiation which can be emitted from a surface
h_1	Height of the concrete part of a composite slab above the steel deck
h_2	Height of the concrete part of a composite slab within the steel deck
h_3	Thickness of the screed situated on top of the concrete
h_{eff}	Effective thickness of a composite slab
h_{eq}	Weighted average of window heights on all walls
$\dot{h}_{net}$	Design value of the net heat flux per unit area
$\dot{h}_{cd}$	Conduction heat flux
$\dot{h}_{net,cv}$	Design value of the net heat flux per unit area by convection
$\dot{h}_{net,r}$	Design value of the net heat flux per unit area by radiation
I	Thermal insulation criterion
L	Clear span of the structural element
l_1, l_2, l_3	Specific dimensions of the trapezoidal or re-entrant steel deck profile
$\vec{n}$	Normal vector
O	Opening factor of the fire compartment
Q	External heat flux
$q_{t,d}$	Design fire load density related to the total surface area A_t

R	Load bearing criterion
s_{mesh}	Anti-crack mesh spacing
T	The temperature
T_∞	Bulk temperature
$\dot{T}$	Time derivative
T_0	Initial temperature
T_{crit}	Critical temperature of the composite slab
T_g	Gas temperature
t	Time
t_a	Air gap thickness
t_d	Thickness of the steel deck profile
t_{fi}	The fire resistance with respect to thermal insulation criterion
$t_{fi,d}$	Design value of standard fire resistance of a member in fire situation
$t_{fi,r}$	Required standard fire resistance in the fire situation
t_{lim}	Time for maximum gas temperature in case of fuel controlled fire
t_{max}	Time for maximum gas temperature
U	Internal energy
u	Moisture content
u_1; u_2	Shortest distance of the centre of the rebar to any point of the webs of the steel deck
u_3	Distance of the centre of the rebar to the lower flange

Greek letters

α	Angle of the web
α_{cv}	Convective heat transfer coefficient
Δ	Variation
ε	Emissivity
ε_f	Emissivity coefficient of the fire
ε_m	Emissivity coefficient related to the surface material of the member
ε_{res}	Resulting emissivity
Φ	View factor
Φ_{low}	View factor of the lower flange
Φ_{up}	View factor of the upper flange
Φ_{web}	View factor of the web
ϕ	Conduction heat flux

ϕ_{reb}	Diameter of the rebar
θ_g	Gas temperature in the vicinity of the fire exposed element
θ_m	Surface temperature of the element
θ_r	Effective radiation temperature of the fire environment
θ	Temperature
θ_a	Temperature of the parts of the steel deck
θ_s	Temperature of the rebars in the rib
Γ	Time factor function of the opening factor O and the thermal absorptivity b
λ	Thermal conductivity
λ_a	Thermal conductivity of carbon steel
λ_{air}	Thermal conductivity of air
λ_c	Thermal conductivity of concrete
ρ	Density
ρ_a	Density of carbon steel
ρ_{air}	Density of air
ρ_c	Density of concrete
σ	Stefan-Boltzmann constant

1. INTRODUCTION

1.1 General

A composite steel-concrete slab consists of cold-formed profiled steel deck which acts as a permanent formwork to the concrete topping. Usually, the concrete is reinforced with individual longitudinal reinforcement bars placed within the ribs and an anti-crack mesh, as illustrated in Figure 1.1. The composite action between the steel and concrete is generally achieved by indentations or embossments in the steel deck [1].

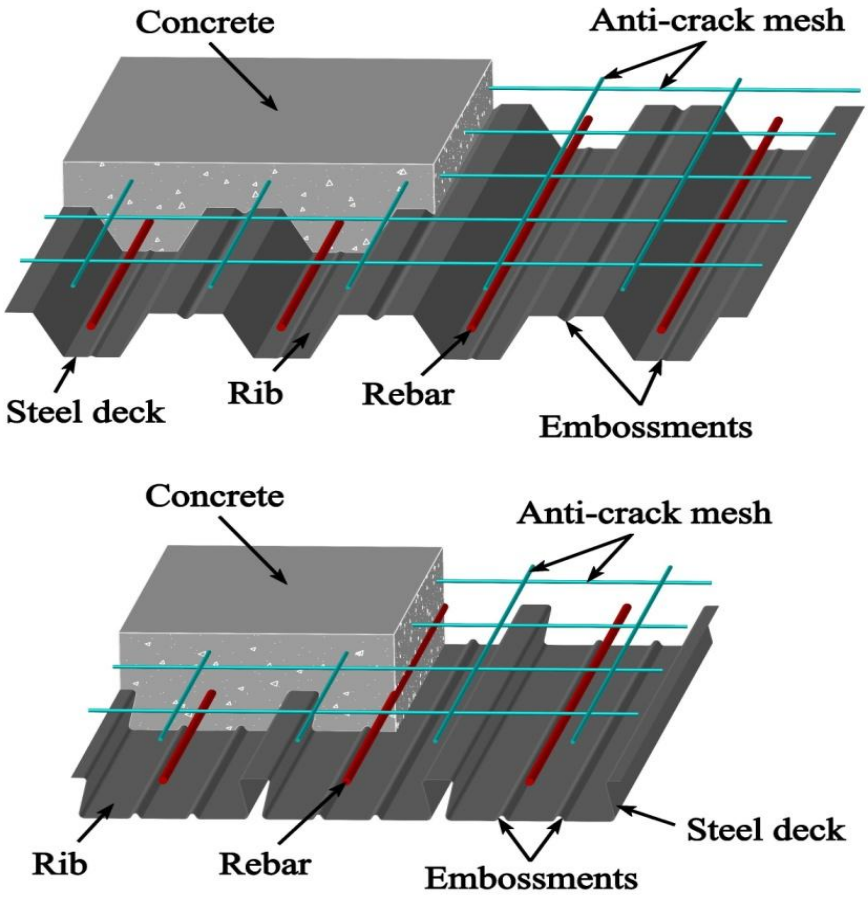

Figure1.1: Typical layout of composite slabs: trapezoidal and re-entrant profiles[1].

The additional steel reinforcing elements incorporated within the concrete layer on composite slabs have several functions such as reinforcing the structure hence allow openings, distributing the effects of concentrated and linear loads, improving the fire resistance and controlling concrete cracking [2].

The steel deck has three different functions: before concrete pouring, it acts as a work platform and safety screen; during casting, the deck serves as permanent shuttering; and after hardening of the concrete, the deck serves as reinforcement [1]. Owing to the relative ease of casting concrete, trapezoidal deck slabs are more popular than re-entering ones [3].

Fire resistance of an assembly or material can be defined as the property to endure fire or protect from it. On structural engineering elements, it is measured by the time and can be associated to the capacity of confining a fire or to maintain performing the structural function during fire exposure, or both. On composite slabs, the fire resistance is principally affected by the thickness of the steel deck, type of aggregate in concrete and the thickness of the concrete layer [4]. Several other aspects may influence on the fire endurance of composite slabs such as the diameter and concrete cover for the reinforcement bars, for example.

The concept of fire safety engineering consists in the prevention of the catastrophic failure of structures during fires. Consequently, the objective is to guarantee that every person in a building can escape safely from a fire [5]. Therefore, the application of protective actions and appropriate fire design is essential to reduce the damage to the whole building and ensure life safety in case of fire.

The employment of composite slabs in construction has been usual in North America for several years and since the 80s, a significant increase has taken place in Europe [6]. Thus, different types of profiled steel deck started to be developed likewise researches concerning the structural and thermal behavior of composite slabs has significantly increased.

Composite slabs have an important paper in preventing the spread of fire in buildings. The fire resistance of this type of building element should be determined according to three different criteria, namely, load bearing (R), integrity (E) and insulation (I).

Presently, several types of profiled steel deck are marketed in Europe with thicknesses usually ranging from 0.7 mm to 1.2 mm. Generally, with the aim of providing protection against corrosion, the steel deck is made from galvanized cold-formed steel with a thin zinc layer applied on both faces [7]. This measure increases considerably the durability of the structure as a whole and hence decreases the number of pathologies.

The overall depth of composite slabs, that is, the height of the steel deck added to the height of the concrete layer typically varies between 100 and 170 mm. The span length usually varies between 2.5 and 4.0 m when the slab is not propped during the construction phase [8].

This type of structural engineering element is mainly used in multi-storey office buildings however, it is common to encounter this structural element in various types of buildings such as airports, industrial constructions, parking spaces and hospitals, among others [2].

After completing the construction stage, the steel deck acts as an external reinforcement. Therefore, this solution requires less additional reinforcement and provides reduced construction time in comparison with conventional flat slabs due to the application of the steel deck as a permanent formwork [9]. In addition, the structural efficiency and the reduction / elimination of propping are other advantages of the use of composite slabs.

Another advantage of the use of composite slabs is the reduction of the dead load of the structure. Owing to the hollow shape of the deck, a significant area of concrete can be saved providing a decrease on the self-weight and therefore resulting in a more economical and efficient building. The flexibility, simplicity of installation / transportation and elevated quality control on the production of the steel deck are other positive points of this solution [10].

Structural elements have to meet fire-safety requirements and additional measures have to be taken if necessary. For composite slabs with profiled steel deck, the direct exposure of the steel deck to fire leads to fast loss of stiffness and strength degradation. Therefore, additional reinforcement is commonly used to increase the fire resistance and comply with the requirements of design codes [11].

An appropriate prediction of the behavior of structural engineering elements in use is essential for a safe and economic design. Large scale fire tests on elements of construction are expensive and time-consuming. As a workaround, numerical methods can provide a rapid and cost effective approach to problems of heat transfer and even afford accurate predictions of the fire performance

An appropriate prediction of the behaviour of structural engineering elements in use is essential for a safe and economic design. Large scale fire tests on elements of construction are expensive and time-consuming. As a workaround, numerical methods can provide a rapid and cost effective approach to problems of heat transfer and even afford accurate predictions of the fire performance of structures [12].

Simplified calculation methods for determining the fire resistance of composite slabs are presented by the European Standard EN 1994 Part 1-2[13]. The calculation rules are suitable for a specific range of unprotected composite slabs with trapezoidal and re-entrant steel deck exposed to fire according to standard temperature-time curves.

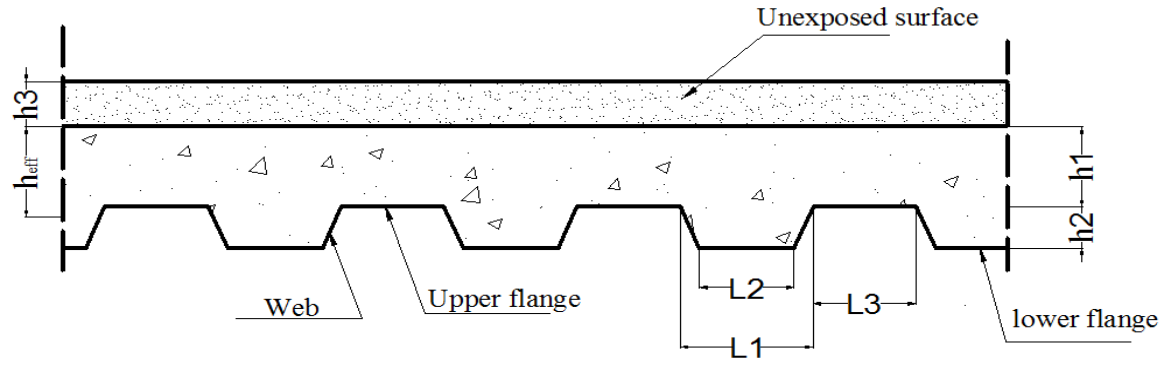

Figure1.2: Schematization of the profile of composite slabs with trapezoidal steel deck (adapted from EN 1994-1-2[13]).

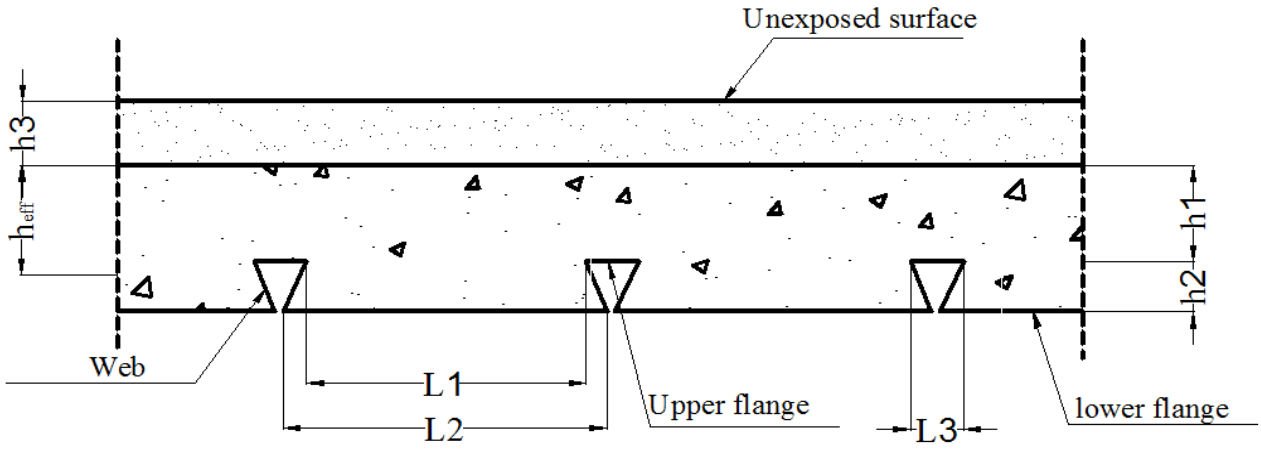

Figure1.3: Schematization of the profile of composite slabs with re-entrant steel deck (adapted from EN1994-1-2[13]).

When exposed to fire, the steel deck heats up quickly, expand and may separate from the concrete lining. The loss of thermal contact between these components can also be attributed to the evaporation of moisture from concrete at a temperature of 100 °C. Indeed, previous research mentioned the separation of the steel deck from the concrete topping. Composite panels exposed to fire increase the thermal resistance of this interface (see, for example, [15]). Foundation work is focused on using different steel deck geometries, concrete thickness and other parameters to numerically simulate the fire behaviour of the composite slab.

1.2 Objectives

The primary objective of fire safety is to protect the life of residents and emergency personnel on the premises. It also aims to protect the environment and limit material (structure and

content) and economic (business continuity) damage. In order to achieve these objectives, various measures must be taken to comply with fire regulations. The main objective of this study is to develop three-dimensional thermal models in order to study the fire behavior of composite steel-concrete slabs with profiled steel deck. To this end, a new tool must be developed on the MATLAB [38] a software for three-dimensional thermal analyzes, the developed finite element models must be validated against the experimental data provided by different authors.

The final goal of this work is to study the influence of different parameters on fire resistance (I), as well as on the temperature of reinforcements and parts of the steel deck of composite slabs. The numerical results should be compared with the simplified calculation methods of EN 1994-1-2 [13] Additionally, new suggested formulas should be proposed for determining the fire resistance of composite slabs from the point of view of thermal; new suggestions can be made for calculating the temperature of parts of the steel deck or concrete topping, which is important for the load-bearing fire resistance.

1.3 Motivation

The increasing use of composite structures in buildings has highlighted the need for a precise and refined analysis of the thermal and structural behavior of these elements in the event of fire. In this way, it is possible to adopt economical solutions while allowing safe and efficient constructions.

The analytical solution of problems involving complex geometries and material properties is generally difficult and often impossible. An alternative for these cases is the application of numerical methods, namely finite element methods(FEM) [16].

Due to the exponential growth of computing over the past decades, several FEM-based computer programs have been developed. Along with the increase in the processing power of computers, complex engineering problems were solved by means of numerical simulations using these programs, as a result, several studies have shown that numerical analyzes are an effective approach to determine the answers. Structures thus providing results.

A large number of digital surveys have provided valuable information and improved knowledge on the behavior of composite slabs with steel decks during exposure to fire. Nevertheless, the majority of these studies have focused on the structural response, using thermal analysis to provide input data for the structural model. Thus, a small number of

studies have systematically studied the temperature gradient in composite slabs under fire and its sensitivity to different parameters [7].

Annex D of EN 1994-1-2 [13] presents a simplified calculation method for the calculation of the fire resistance of unprotected composite slabs subjected to the standard ISO 834 and natural fire curve from below. In recent years, no revision has been made to this method and the range of geometric parameters of profiles marketed today has considerably increased compared to the range used in the decade of 1990. For these reasons, it is estimated that thermal analyzes must be performed in order to assess the accuracy of these calculation rules.

In the present investigation, it is expected that the development of the new tool for the evaluation of fire resistance, together with the results of the numerical simulations, will provide consistent data for the development of future studies. In addition, this work intends to contribute to the community by increasing knowledge about the fire behavior of composite slabs and by promoting scientific development, thus providing increasingly safe buildings.

1.4 Methodology

In order to determine the fire resistance of composite slabs with regard to the thermal insulation criterion, and to calculate the temperature of the steel components, two different resolution methods are used: the simplified calculation method for standards and the advanced calculation method. The latter is based on three-dimensional finite element models.

Two different parametric studies should be performed in order to analyze possible parameters relevant to fire resistance. Commonly used values of concrete thicknesses are selected for the range of parameters studied. A total of (94 numerical simulations) must be performed, including validation analyses. The first parametric study includes slabs (with different air gap *ta* (0.5; 1 and 2 mm), from which the best air gap is choose for the remaining part of the work. The second parametric study is about four different types of composite slabs: two trapezoidal and two reentrants. In addition, the effect of four different concrete thicknesses is analyzed. A perfect thermal contact model should be used in these analyses.

A representative portion of one square meter of each composite slab is selected to perform the numerical analyses. Composite slabs are exposed to fire on the lower surface according to different natural standard fire curves.

1.5 Definitions of a fire

As a physical phenomenon, a fire is defined as the result of combination heat - fuel - oxygen. Once it starts in a compartment, the fire can develop in 4 stages [17, 18]:

- a “pre-flashover” occurs if several materials catch fire. However, in many cases the fire is extinguished due to the small amount of combustible materials or insufficient ventilation. Although this phase lasts longer than the following, no structural damage is observed, which explains why it is most of the time not considered in the thermal response of the room concerned;
- The "initial" phase takes place when all the combustible materials burn. This phase is often caused by human intervention such as opening a window or of a door. This sudden supply of oxygen then allows the fire to spread to any object flammable present in the compartment. We thus define the "flashover" or generalized conflagration as the brief transition from growing fire to fire fully developed, which may result in the appearance of flames at the compartment openings;
- The ignition or combustion phase corresponds to a fully developed fire. The heat transfer rate reaches a peak, causing a very rapid increase in temperature. This is also the period that generates the most material damage;
- The extinction or cooling phase is characterized by a decrease in temperature after some time due to thermal inertia. The last three phases are often represented by different conventional curves of gas temperature as a function of time [17, 18].

1.5 Fire resistance of composite slabs

Typically, experimental fire tests are expensive and time consuming. As an alternative solution, numerical simulation and simple calculation methods can be used to determine the fire resistance of composite panels. The fire resistance of composite panels is only defined by considering the standard fire potential below, which is always decisive in practical situations.

When exposed to fire, the process of determining the cross-sectional temperature field of the composite plate is complicated due to the presence of ribs, resulting in an orthotropic profile with a large temperature gradient. Therefore, calculating the unexposed surface temperature and predicting the fire resistance of composite panels present difficult challenges in the design of fire protection. Figure 1.4 shows the theoretical distribution of temperature and the average temperature obtained in the cross section at the unexposed surface of any composite plate with trapezoidal steel deck.

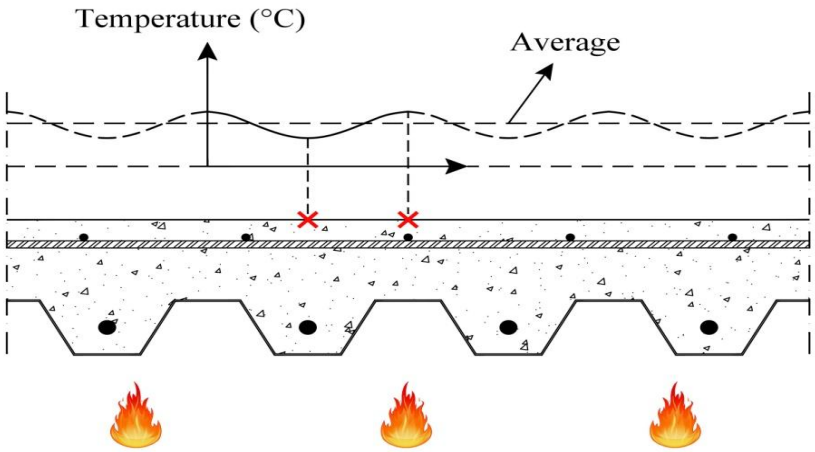

Figure1.4: Theoretical temperature distribution at the unexposed surface of a fire exposed composite slab (adapted from both [1])

1.6 Eurocode 4 – Part 1-2

The first recommendations for the assessment of the fire resistance of composite slabs in Eurocode 4 were based on the model introduced by the European Convention for Constructional Steelwork (ECCS) in 1983 [19]. This model, however, was based on limited experimental data available at the time it was developed hence leading to the adoption of conservative assumptions and uneconomical designs.

In 1990, the first draft of Eurocode 4 "Design of composite steel and concrete structures – Part 1-2: Structural fire design" was presented at a symposium in Luxembourg. Members of the European Community were invited to contribute by sending comments and suggestions. A redrafting started in 1991, but the final version for voting was approved in 1993 [20].

With the aim of enhancing these design rules, substantial research effort was initiated in Europe with the ECSC research project. Several experimental fire tests provided consistent data for the development of improved simple calculation rules. The actual version of Eurocode 4 –Part 1-2 was released in 2005 and incorporated the proposal new rules for the calculation of the fire resistance of composite slabs introduced by Both [1] in 1998.

The simplified calculation method provides guidelines for determining the fire resistance of composite slabs subjected to standard fire conditions according to the thermal insulation criterion (I). The proposed model is based on the slab geometry, partial factors and other parameters, being proper to composite slabs with trapezoidal and re-entrant steel deck. Moreover, these rules are exclusively applicable to composite slabs without any protection against fire, that is, slabs with fire containment measures are not covered.

The simplified calculation method for the fire resistance (I) has a field of application limited to a range of commonly used composite slab geometries from the decade of 1990. Table 1.1 presents the range of applicability of the method of Eurocode 4 for unprotected composite slabs with trapezoidal and re-entrant profiles, valid for slabs with either normal weight concrete or lightweight concrete. The geometric parameters of the slab are illustrated in Figures 1.2 and 1.3.

Table1.1: Field of application of the Annex D of EN 1994-1-2[13].

For trapezoidal steel deck profiles	For re-entrant steel deck profiles
$80.0 \leq L_1 \leq 155.0$ mm	$77.0 \leq L_1 \leq 135.0$ mm
$32.0 \leq L_2 \leq 132.0$ mm	$110.0 \leq L_2 \leq 150.0$ mm
$40.0 \leq L_3 \leq 115.0$ mm	$38.5 \leq L_3 \leq 97.5$ mm
$50.0 \leq h_1 \leq 125.0$ mm	$50.0 \leq h_1 \leq 130.0$ mm
$50.0 \leq h_2 \leq 100.0$ mm	$30.0 \leq h_2 \leq 60.0$ mm

Still with regard to the thermal insulation criterion, the Eurocode 4 considers orthotropic slabs as equivalent solid slabs with an effective thickness (h_{eff}) which depends on the geometry of the steel deck as well as the concrete depth. The standard presents two different formulae for the calculation of h_{eff} and specifies the minimum effective thickness according to standard fire resistance classes. These normative recommendations are discussed in section 3.6.

With respect to the load bearing criterion (R), the Eurocode 4 – Part 1-2 determines that if a composite slab with profiled steel deck, with or without additional reinforcement, is properly designed according to EN 1994-1-1[21] .

This standard also states that the integrity criterion (E) is assumed to be satisfied for composite slabs with profiled steel deck.

1.7 Outline

In this work, Chapter 1 gives an introduces to the research theme and presents the work methodology; a summary of relevant surveys in the field of study; and a brief description of

the concepts regarding the fire resistance of composite slabs. Chapter 2 deals with the description of the different fire curves, heat transfer mechanisms, and the openness factor and experimental tests.

Chapter 3 presents thermal properties of materials and other aspects relating to the fire behavior of composite structures. Chapter 4 describes FEM principles as well as the development of finite element models for the development of numerical simulations using MATLAB software and the numerical validation for the different points in the slab with different air gaps *ta.*

Chapter5, the description and the results of the parametric analyses are presented. A discussion around the influence of each parameter studied is also given in this chapter.

On the basis of the general evaluation of the results, new proposal concerning the calculation of the fire resistance (I) and temperatures of steel components must also be indicated.

The conclusions of the investigation and recommendations for further research can be found in Chapter 6.The Numerical results and Eurocode results for the maximum and average temperatures for each natural curve, type of steel and the different heights of h1 are in the Annexe.

2. FIRE BEHAVIOR OF COMPOSITE STRUCTURES

Before analysing the thermal behavior of composite structural members, it is important to understand the different mechanisms of heat transfer and the different methods of heat transfer. This chapter presents the most relevant concepts related to fire safety engineering, heat transfer, thermal properties of materials, fire resistance standards and other aspects related to the fire behavior of buildings during exposure to fire. The physical parameters that determine the fire situation will affect the duration and severity of the fire, as well as the thermal effect on structural components. The most important factors are the density of the thermal load, the combustion characteristics of the material, the shape and size of the compartment, the ventilation conditions and the thermal performance of the enclosure boundary[22].

According to EN 1991-1-2[23], actions against a burning building are classified as accidental actions. The effects of fire will increase the temperature of the structural elements of the building, affect its performance and cause additional loads and displacements. These consequences can cause the collapse of the frame or even lead to its destruction, which highlights the need to assess the fire behavior of building elements in the event of fire[24].

Basically, the design concept of the fire of a building element can be defined by a transient analysis, meeting the following conditions:

$$t_{fi,d} > t_{fi,r} \quad (2.1)$$

In the in equation above, $t_{fi,d}$ represents the design value of fire resistance and $t_{fi,r}$ is the nominal required fire resistance, both components in compatible units of time. Other parameters must be verified such as the critical temperature and the structural resistance, for example.

Due to the orthotropic ribbed lower portion, composite slabs present a complex temperature distribution across the section during fire exposure. In view of that, the thermal gradient on the unexposed side of the slab is strongly affected by the geometry of the steel deck and the position of the ribs. The thicker portion is subjected to lower temperatures than the thinner portion, see Figure 1.4. The last one plays a substantial role in the thermal insulation criterion of composite slabs.

The critical temperature of the steel components of composite slabs is defined as the average temperature of each steel component (steel deck) at the time of failure concerning the thermal insulation criterion.

2.1 Heat transfer and thermal actions:

In order to better a understanding of the mechanisms of heat transfer, it is necessary to make clear some basic concepts. “Temperature” can be defined as the measure of the amount of kinetic energy present in the molecules of a given substance. In other words, it is a measure of the coldness or warmth of a substance. Çengel and Ghajar [25] define “heat” as the form of energy which can be transferred from one system to another as a consequence of temperature difference.

A thermodynamic analysis deals with the amount of heat transfer as an energy system undergoes a process from one equilibrium state to another. The heat transfer is the science which concerns the determination of the rates of these energy transfers. The heat transfer between two substances requires the existence of temperature differences and occurs from the high-temperature medium to the lower-temperature medium [25].

There are three different modes of heat transfer: conduction, convection and radiation. As a matter of fact, the temperature distribution in a system is dependent on the combined effects of these three modes of heat transfer [26].

In order to calculate the rate of temperature increase in structural components, it is fundamental to determine the amount of heat which affects these components. The Eurocode 1 – Part 1-2 [23] presents thermal actions for temperature analysis, which are given by the net heat flux $\dot{h}_{net}$ (W/m^2) to the boundary surface of the element. On the fire exposed surfaces, the net heat flux is divided into two components: the first considers heat transfer by convection ($\dot{h}_{net,cv}$) and the second by radiation ($\dot{h}_{net,r}$), as presented below.

$$h_{net} = h_{net,cv} + h_{net,r} \quad (2.2)$$

The following subsections present the formulation used to determine each component of the equation above and give a brief description of the three modes of heat transfer.

2.1.1 Conduction

Conduction can be defined as the transfer of energy in the body from particles of higher energy level (higher temperature) to particles of lower energy level (lower temperature) due to

the interaction between particles [25]. Conductive heat transfer can occur in solids, gases or liquids. This phenomenon is governed by the Fourier's law of heat conduction, introduced in 1822. According to this law, the conduction heat flux $\dot{h}_{cd}$ (W/m^2) is directly proportional to the temperature gradient in the direction of the flow of heat $\frac{dT}{dx}$ (K/m), as presented in Equation 2.3.

$$\dot{h_{cd}} = -\lambda . \frac{dT}{dx} \quad (2.3)$$

In the last equation, λ represents the thermal conductivity (W/mK), which is a measure of the capacity of the material to conduct heat. As stated before, the heat is transferred from the higher temperature particles to the lower temperature particles, resulting in a negative temperature variation. In this regard, the negative sign is necessary because the heat transfer in the positive x direction is a positive value

The conduction heat flux is a vector quantity ($\vec{\dot{h}}_{cd}$), therefore, in the three-dimensional space, this component can be written as:

$$\dot{h_{cd}} = -\lambda(\partial x, \partial y, \partial z)^T T \quad (2.4)$$

In the equation above, the vector derivative is the gradient operator (∇) applied to the temperature T.

A good heat conductor presents a high thermal conductivity and a poor heat conductor (insulator) presents a low thermal conductivity. This thermal property varies from material to material and depends on the physical state, chemical constitution and temperature of the material. Consequently, in a transient analysis, it is necessary to determine this property in each time step of the solution.

2.1.2 Convection

Convection heat transfer is defined as the mode of energy transfer between a solid surface and a fluid (liquid or gas) in movement on its boundaries, involving combined effects of conduction and fluid motion. The greater the velocity of the fluid is, the greater the convection heat transfer. Whether there is no bulk fluid motion, the heat transfer between the solid and adjacent fluid is governed by conduction [25].

The convection heat transfer occurs through two different manners, namely the natural (or free) convection and the forced convection. The first takes place if the fluid motion is caused by resulting forces that are induced by temperature differences between its layers. In contrast, the second occurs whether the fluid is forced to flow over a solid by using hydraulic machines such as pumps, for example [26].

The overall effect of convection is well defined through the Newton's law of cooling, which states that the rate of convection heat transfer is proportional to the temperature difference between the surface and fluid temperatures.

The Eurocode 1 – Part 1-2 [23] determines that the net convective heat flux component $\dot{h}_{net,cv}$ (W/m^2) for temperature analysis shall be calculated according to the following equation:

$$h_{net\,,cv} = \alpha_{cv}.\left(\theta_g - \theta_m\right) \quad (2.5)$$

Where, α_{cv} is the coefficient of heat transfer by convection (W/m^{2}K), relevant for nominal temperature-time curves; θ_g represents the gas temperature in the vicinity of the fire exposed element (°C); and θ_m is the surface temperature of the element (°C).

The EN 1991 – 1-2[23] also states that the net convective heat flux on the unexposed surface of separating elements should be calculated with α_{cv} = 4 (W/m^{2}K). Otherwise, this value should be taken as α_{cv} = 9 (W/m^{2}K) when assuming it contains the effects of radiation heat transfer. Regarding the fire exposed surface, the coefficient of heat transfer by convection should be adopted as α_{cv} = 25 (W/m^{2}K) if the element is exposed to the standard fire curve ISO 834 or the external fire curve. In case of surfaces exposed to the hydrocarbon curve, a value of α_{cv} = 50 (W/m^{2}K) should be taken.

It is noteworthy that a mean value is assumed for this coefficient by means of simplification, since the convection heat transfer is complex and depends on several factors such as the velocity field of the fluid.

2.1.3 Radiation

Radiation consists of the energy emitted by matter in the form of electromagnetic waves (photons) due to changes in the electronic configurations of atoms or molecules. In opposition to conduction and convection, this mean of heat transfer does not require a material medium, that is, the heat can also be transferred through regions of vacuum [25].

For heat transfer analyses, the radiation is restricted to the thermal radiation, which is propagated as a result of temperature differences in a system. This means that other forms of electromagnetic radiation do not influence on the temperature distribution. In the heating process of a fire, the radiation is the main mechanism of heat transfer, especially when high temperatures are reached. The radiation heat transfer is a complex phenomenon due to its dependence on the relative positions of the flames [24].

The maximum amount of thermal radiation E_b (W/m^2) which can be emitted from a surface is determined by the Stefan-Boltzmann law. This law states that an idealized surface called blackbody (ideal thermal radiator) emits thermal radiation proportionally to the fourth power of the absolute temperature T (K), as given below.

$$E_b = \sigma . T^4 \qquad (2.6)$$

In the Equation (2.6), σ is a proportionality constant called Stefan-Boltzmann constant, which is equal to 5.67E-8 (W/m^2K^4). This equation is suitable only for radiation emitted by a blackbody, which is of fundamental importance to radiant heat transfer [27].

A blackbody is a perfect radiation emitter and thus, no other body can emit more thermal radiation than a blackbody at the same temperature. Given these points, the radiation emitted by real surfaces must take into consideration an additional factor. This factor is called emissivity (ε), which is a value between 0 and 1 defined as the ratio of the energy emitted by the real surface to the energy emitted by a blackbody, both at the same temperature [28]. For a general surface, the total radiant energy E (W/m^2)can be expressed as:

$$E_b = \sigma . T^4 \qquad (2.7)$$

Commonly, the emissivity of a surface is associated to the wavelength of radiant energy, the surface temperature and the angle of radiation. For simplification purposes, whether the emissivity is independent of these factors, the surface is called a greybody surface. The greybody radiation is applied in fire engineering approaches and calculations.

According to Eurocode 1 – Part 1-2 [23] and considering the concepts presented above, the net radiative heat flux component $\dot{h}_{net,r}$ (W/m^2) for temperature analysis of structural members should be determined according to the following equation:

$$h_{net,r} = \Phi \varepsilon_m . \varepsilon_f . \sigma [(\theta_r + 273)^4 - (\theta_m + 273)^4] \qquad (2.8)$$

In the last equation, Φ (dimensionless) is the view factor, which takes into consideration position and shadow effects; ε_m (dimensionless) represents the surface emissivity of the element; ε_f (dimensionless) represents the emissivity of the fire; σ is the Stefan-Boltzmann constant (W/m^{2}K^4); θ_r is the effective radiation temperature of the fire environment (°C); and θ_m is the surface temperature of the element (°C).

The EN 1992-1-2 [29] states that the emissivity related to the concrete surface should be equal to 0.7. The EN 1993-1-2 [18] determines that the emissivity concerning the steel surface should be taken as 0.7 for carbon steel and taken as 0.4 for stainless steel. Regarding the fire emissivity. The EN 1991-1-2 [23] states that this parameter should be taken as 1.

In the numerical modelling performed in this investigation, the gas temperature is assumed to be the effective radiation temperature of the fire environment, approximated by the Stefan-Boltzmann law. Therefore, considering convection and radiation heat transfer, the net heat flux which affects a structural member under fire conditions can be written as:

$$h_{net} = \alpha_{cv} . (\theta_g - \theta_m) + \Phi . \varepsilon_{res} . 5.67E-8 . [(\theta_g + 273)^4 - (\theta_m + 273)^4] \qquad (2.9)$$

In the equation above, ε_{res} (dimensionless) represents the resulting emissivity, which is the product between the surface emissivity of the member and the emissivity of the fire. This equation represents the boundary conditions applied on the fire exposed surface of the composite slabs numerically tested in this work.

2.2 View factor

The specified view factor (Φ) quantifies the geometric relationship between the radiation emitting surface and the receiving surface which depends on surfaces and orientations, such as the distance between them [30]. The view factor at the bottom flange of the composite slab is given as Φinf = 1.

The view factor of the web and the top flange of the steel deck is less than one, due to the obstruction caused by the ribs of the platform steel. This value can be calculated by developed by H. C. Hottel in the 1950s [25]cross-chain method. This approach is also adopted by the standards EN 1994-1-2 and NBR 14323; however, only the expression for the upper flange view factor is given.

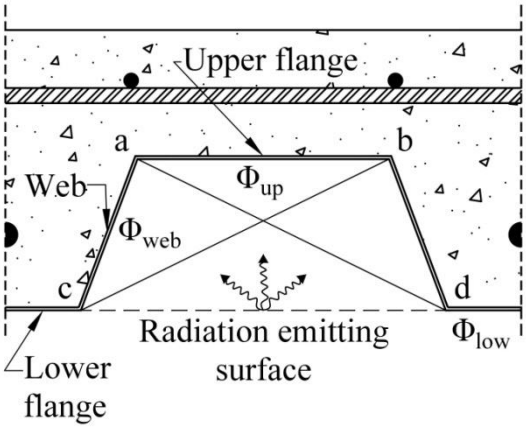

Figure 2.1: Schematic for the calculation of the view factor (adapted from Jiang et al. [9]).

The view factors of the upper flange (Φ_{up}) and web (Φ_{web}) can be calculated as function of the distances between the parts of the steel deck or using the geometric parameters of the composite slab, see Figures 1.2 and 1.3. The expressions for the calculation of these view factors of composite slabs with either trapezoidal or re-entrant profiles are presented in Eqs. 2.10a and 2.10b.

$$\Phi_{up} = \frac{ad + cb - ab - cd}{2.ab} = \frac{\sqrt{h^2{}_2 + \left(l_3 + \frac{l_1 - l_2}{2}\right)^2} - \sqrt{h^2{}_2 + \left(\frac{l_1 - l_2}{2}\right)^2}}{l_3} \quad (2.10a)$$

$$\Phi_{up} = \frac{ac + cd - ad}{2.ac} = \frac{\sqrt{h^2{}_2 + \left(\frac{l_1 - l_2}{2}\right)^2} - (l_3 + l_1 - l_2) - \sqrt{h^2{}_2 + \left(l_3 + \frac{l_1 - l_2}{2}\right)^2}}{2.\sqrt{h^2{}_2 + \left(\frac{l_1 - l_2}{2}\right)^2}} \quad (2.10b)$$

2.3 Fires in multi-storey buildings

Besides consisting in big tragedies and usually resulting in several losses, accidental fires provide an opportunity for humanity to understand the performance of entire buildings when subjected to fire. Thus, the design of buildings is improved as long as the experience from these fires and large-scale fire tests is obtained.

In the first part of the decade of 1990, two fires occurred in multi-storey buildings in England, namely Broad gate and Churchill Plaza. In 1996, a programme of fire tests conducted on an eight-storey composite steel-framed building was finished at the Building Research Establishment's Cardington Laboratory[40].

2.3.1 Fire Test in the University of Manchester

A total of nine identical composite slab strips, comprising trapezoidal metal decking, full weight concrete and steel mesh, were tested. Two of the slabs were tested at room temperature and the remaining seven slabs were tested in different fire scenarios, which included both the heating and cooling stages of a fire. Each strip of slab was 1.2 m wide and 6.45 m long and was supported to create a median span of 4 m with two end overhangs. The overhangs were restrained against any upward vertical movement at a distance of 1.1 m from the vertical supports. For the fire tests, the slabs were heated over the median length of 3 m of the slab [31].

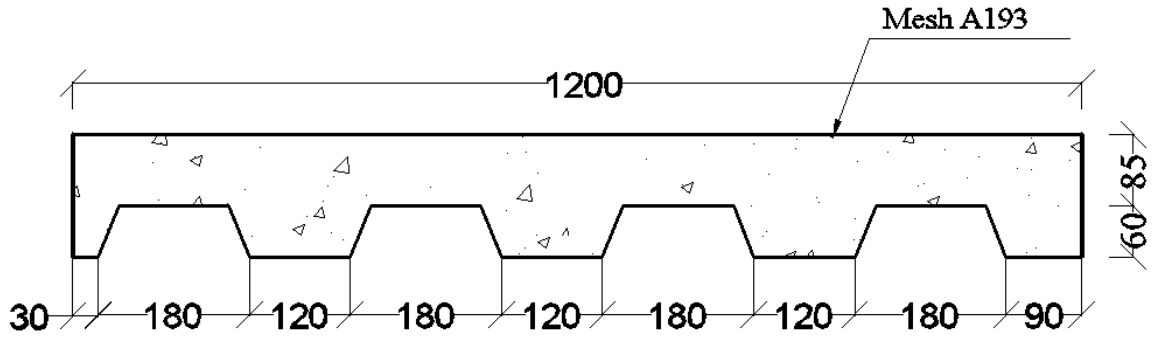

Figure2.2 : Profile of the composite slab specimen

2.3.2 Cardington fire tests

Between 1995 and 1996, a programme of large scale fire tests were carried out in a complete building at the Cardington Laboratory in Bedfordshire, UK. The 8-storeysteel framed

composite building was designed according to the British standard BS 5950 – Part 1 to recreate a typical multi-storey office building [28]. Figure 2.3 illustrates the Cardington multi-storey test frame during the installation of the profiled steel deck of the composite slabs.

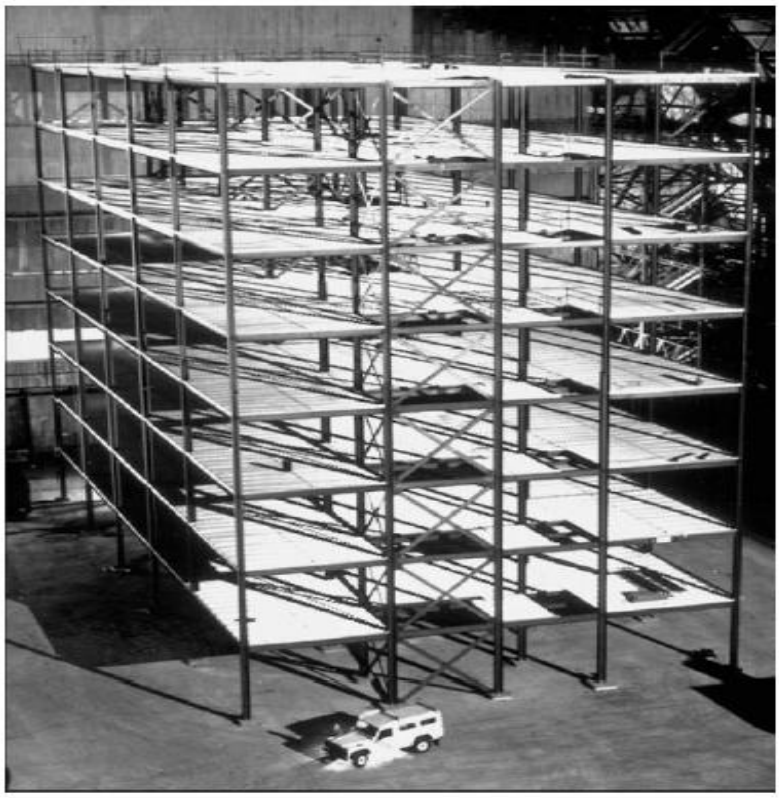

Figure2.3: Composite steel framed building at BRE Cardington[40].

The objective of the six major fire tests was to investigate the behaviour of a real structure when subjected to real fire conditions and provide data for the validation of numerical simulations of structures under fire conditions.

The test building was composed by composite floor slabs with profiled steel deck in composite action with the supporting beams and using cast in situ concrete. Sandbags distributed over each floor were used to impose the loads with load levels that were typically found in office buildings in the UK, see Figure 2.4. Due to mistakes in the placement of the reinforcement, such as the non-overlapping of the mesh in some regions, large cracks occurred in the slabs.

Figure2.4: Cardington fire test steel-framed building max steel temperature 1150°C [40]

Although suffering extensive cracking, the composite floors preserved its integrity and separating function during all the fire tests, presenting an important contribution to the survival of the test frame.

In general, the structural elements presented a good performance and the overall structural stability was retained. It was observed that the fire behaviour of all the elements acting together was different from the performance of single members in standard fire tests. Therefore, the Cardington fire tests evidenced that steel frames with composite floor slabs provided a greater fire resistance than that normally assumed at that time.

2.4 Fire curves

Fires occur with the existence of the three factors in simultaneous: heat source (responsible for the initial ignition); fuel (e.g. paper, oil and wood); and oxygen. Whether one of these factors is missing, the fire does not ignite or reach a significant level.

Although consisting of complex and stochastic events, a fire can be modelled by temperature-time curves. In a structure subjected to elevated temperatures, these curves allow the determination of the maximum temperature reached on the elements and its correspondent

fire resistance as well [33]. A short discussion about some fire curves is presented in the following subsections.

2.4.1 Natural Fire curve:

In real natural fire models, the complete process of fire development can be described as being composed by four different stages, see Figure 2.5. Not necessarily all fires follow this curve, because in some situations it may disappear naturally or do not reach flashover, mainly if the fuel materials are isolated or if there is not enough air to maintain the combustion [34].

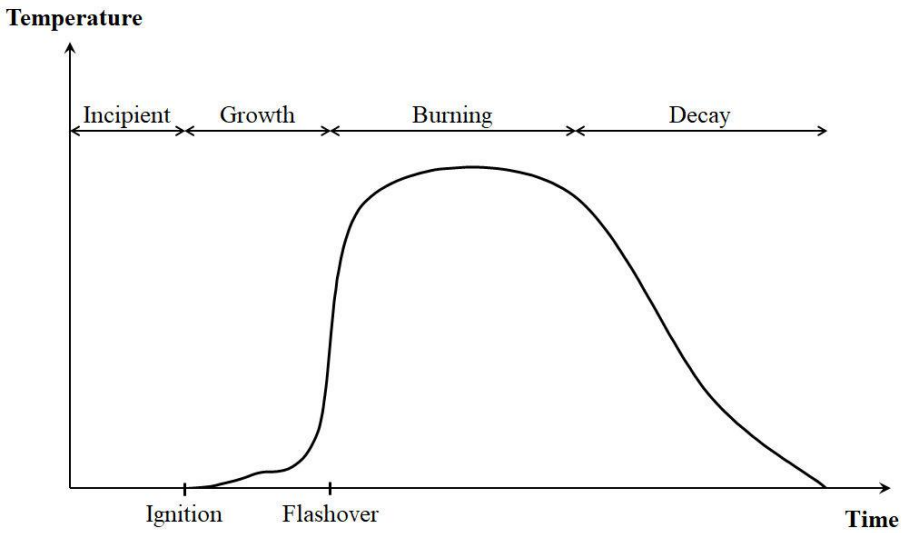

Figure2.5: Fire curve for the complete process of fire development

(adapted from Abu [32]).

The incipient stage is characterized by the heating of potential combustible materials. The transition from the incipient stage to the growth stage is called ignition, representing the start of combustion. In the growth stage, most fires spread slowly on the available combustible surfaces, and then more rapidly as long as the fire grows and there is radiant feedback from flames to other fuel materials. The flashover represents the transition from the growth stage to the burning period, characterized by a rapid increase in the burning rate. In the burning period, the temperatures and radiant heat flux within the compartment are of such level that all exposed surfaces are burning. Finally, after all the fuel materials in the environment have burned out, the temperatures drop and the fire dies in the decay period[34].

These curves are determined from experimental fire tests in compartments using real fire conditions and present an ascending segment (heating phase), and a descending segment (cooling phase). Results of tests evidenced that the parameters that most influence on the

shape of the natural fire curves are the level of fire and ventilation, as well as the thermal properties of the materials of the compartment wall [33].

2.4.2 Nominal standard fire curves ISO 834

In view of the conditioning factors regarding the natural fire curves, standard fire curves were created with the aim of determining a convention for the development of numerical simulations and experimental fire tests. These fire curves present only a heating phase and do not depend on the characteristics of the compartment.

The Eurocode 1 – Part 1-2[23] specifies three different nominal fire curves for the fire design of structures, namely the standard temperature-time curve, the external fire curve and the hydrocarbon curve. These fire curves allow the calculation of the temperature in a fire compartment as function of time. The equations which describe these curves are presented below, where T_g represents the gas temperature (°C), and t is the time (min).

- Standard fire curve (ISO 834):

$$T_g = 20 + 345log_{10}(8t + 1)(2.11)$$

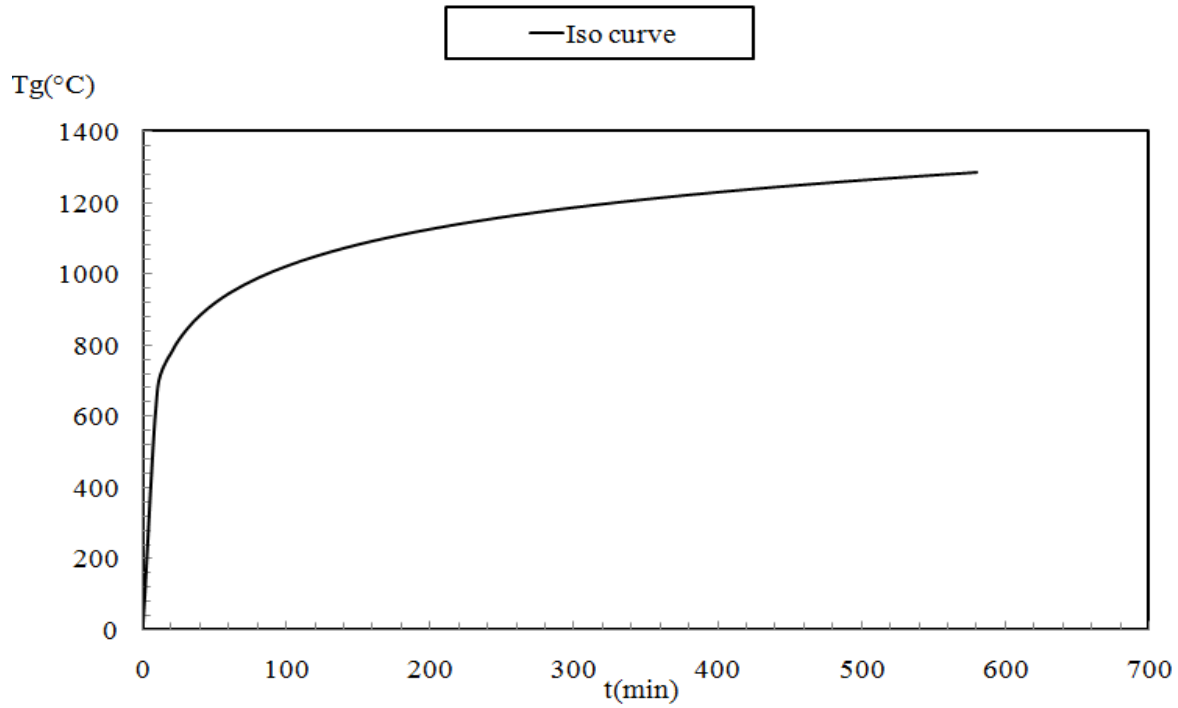

Figure2.6: Nominal time-temperature fire curves.

2.4.3 Parametric temperature-time curves:

In the Annex A of Eurocode 1 – Part 1-2, a model for the determination of parametric temperature-time curves is defined. These curves are valid for fire compartments up to 500 m^2 of floor area, without openings in the roof and for a maximum compartment height of 4 m.

Unlike the nominal fire curves, the parametric curves present both heating and cooling phases, and depend on several factors such as the thermal properties of the boundary of enclosure, fire load density, and area of enclosure, among others. The temperature-time curves in the heating phase shall be calculated according to Eq. 2.12.

$$T_g = 20 + 1325(1 - 0.324e^{-0.2t^*} - 0.204e^{-1.7t^*} - 0.472e^{-19t^*}) \qquad (2.12)$$

In the formula above, T_g is the gas temperature in the fire compartment (°C); and t* represents a fictitious time(h), which should be calculated according to Eq. 2.13, where t is the time (h)

$$t^* = t.\Gamma. \quad (2.13)$$

The factor Γ is dimensionless and must be determined as follows.

$$\Gamma = \left[\frac{O}{b}\right]^2 / \left(\frac{0.04}{1160}\right)^2 \quad (2.14)$$

Where:

$$O = A_v.\sqrt{h_{eq}/A_t} \quad (2.15a)$$

$$b = \sqrt{\rho.c.\lambda} \quad (2.15b)$$

In the equations above, O is the opening factor of the fire compartment ($m^{1/2}$), respecting the limits $0.02 \leq O \leq 0.20$; A_v is the total area of vertical openings on all walls(m^2); h_{eq} is the weighted average of window heights on all walls (m); and A_t is the total area of enclosure including openings (m^2). The factor b is given in $J/m^2s^{1/2}K$, respecting the limits

$100 \leq b \leq 2200$; ρ is the density of boundary of enclosure (kg/m^3); c is the specific heat of boundary of enclosure (J/kgK); and λ is the thermal conductivity of boundary of enclosure (W/mK).

The heating phase of fire occurs until the maximum temperature T_{max}, defined by $t^* = t^*_{max}$. This temperature should be determined using Eqs. 2.16 and 2.12.

$$t^*_{max} = t_{max} . \Gamma \quad (2.16a)$$

$$t_{max} = max\left[0.2.10^{-3}.q_{t,d}/O); t_{lim}\right] \quad (2.16b)$$

In the equations above, t^*_{max}, t_{max} and t_{lim} are given in hours; qt,d is the design value of the fire load density related to the total surface area of the enclosure (MJ/m2), within the limits $50 \leq qt,d \leq 1000$; and tlim is the time limit, which separates the heating phase from the cooling phase as function of the fire growth rate.

The segment of the parametric curves related to the cooling phase of fire presents a decreasing linear relationship between temperature and time. The temperature-time curves in this phase should be calculated using the following equations.

$$T_g = T_{max} - 625.(t^* - t^*_{max} - x) \text{For} t^*_{max} \leq 0.5 \quad (2.17a)$$

$$T_g = T_{max} - 250.(3 - t^*_{max})(t^* - t^*_{max} - x) \quad \text{For } 0.5 \leq t^*_{max} \leq 2 \quad (2.17b)$$

$$T_g = T_{max} - 250.(t^* - t^*_{max} - x) \quad \text{For } t^*_{max} \geq 2 \quad (2.17c)$$

Where:

$$t^*_{max} = \left(0.2.10^{-3}.\frac{q_{t,d}}{O}\right).\Gamma \quad (2.18)$$

In the above equations, t * must be determined according to the equation. 2.13. The factor x is dimension less and given as x = 1.0 if tmax>tlim;or x = (tlim • Γ) / t * max if tmax =tlim.

Figure 2.7 shows examples of parametric curves applying the Eurocode 1 - Part 1-2 method. The parameters used in the analysis is b = 2121.32J/m2s1/2K and tlim = 20 minutes or 0.333 hour (average heat growth rate).

Table2.1: Investigated parameters of the six natural curves.

Natural curves	Av (m²)	qf,d (MJ/m²)	qt,d (MJ/m²)	O (m^1/2)
1	25	1904.593	432.862	0,044
2	25	1904.59269	432.861	0,062
3	35	1961.59728	483.492	0.052
4	70	2212.4297	640.194	0.065
5	100	2213,24297	691.638	0.04
6	150	2602,26904	867.42	0.06

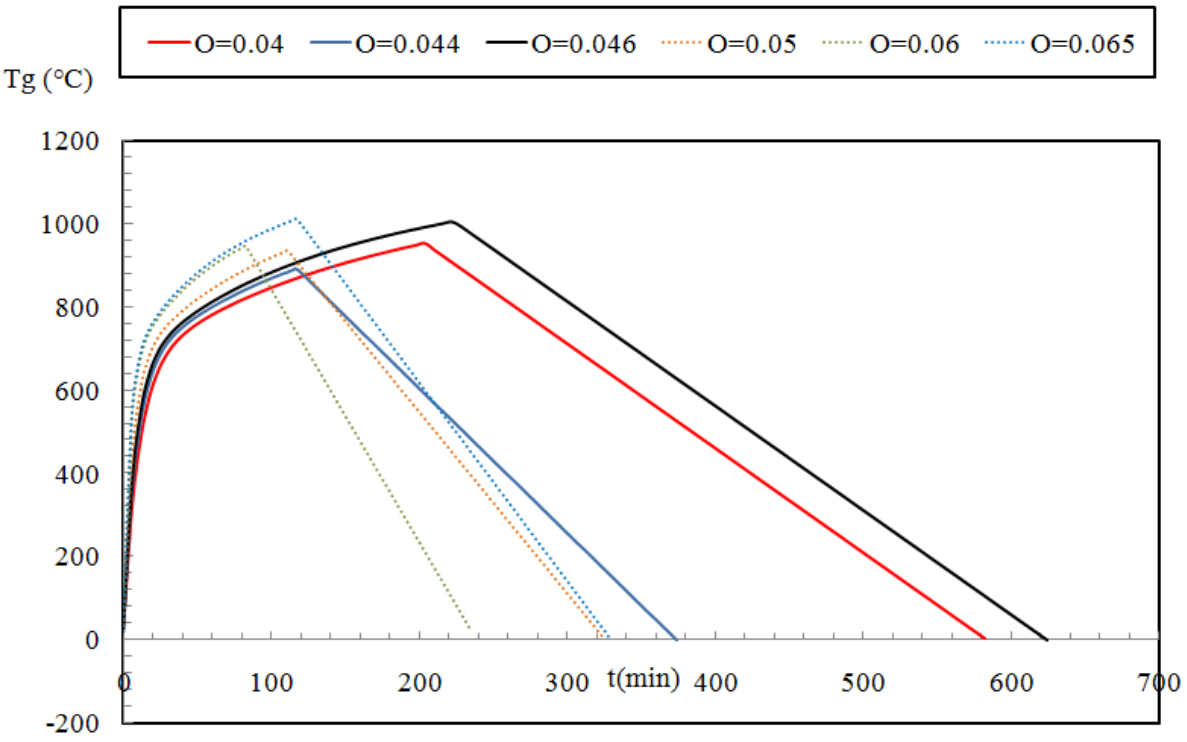

Figure2.7: Natural curves with different opening factor

Regarding the analysis, it can be observed that as the opening factor of the compartment increases, the duration of the heating phase decreases and the maximum temperature increases, leading to more severe fires.

2.5 Fire resistance criteria

Structural elements need to meet fire-safety requirements according to building codes. For composite slabs, the requirements are normally specified by fire ratings of 30, 60, 90 minutes or more. The fire rating of this type of building element is usually made using standard fire tests (CEN - European Committee for Standardization, 2012; CEN - European Committee for Standardization, 2014) and should consider the criteria of Insulation (I), Integrity (E) and Load Bearing (R). Generally, experimental fire tests are expensive and time-consuming. As an alternative solution, the fire resistance can be evaluated by means of numerical simulations and using simplified calculation methods. The fire resistance of the composite slabs is defined with respect to standard fire exposure from below. In this investigation, the fire resistance is investigated with respect to both load bearing (R) and thermal insulation (I) criteria. The thermal insulation criterion (I) is the ability to withstand fire in one side and prevent excessive transmission of heat. The assessment shall be made on the basis of the average temperature rise on the unexposed surface limited to 140 °C above the initial average temperature, or; on the basis of the maximum temperature rise at any point on the unexposed surface limited to 180 °C above the initial average temperature. The integrity criterion (E) is the capacity to withstand fire in one side and resist penetration of hot gases and flames. The assessment should be made on the basis of measuring cracks or openings in excess of given dimensions, or the ignition of a cotton pad, or sustained flaming on the unexposed side. For cast in situ composite slabs, the integrity criterion is normally satisfied provided that the joints are adequately sealed.

2.5.1Load bearing criterion

The load bearing resistance for flexural loaded elements (R) is the ability to support the loading during the test without collapsing. The assessment shall be made on the basis of limiting vertical displacement D (D= L2 /400d [mm]), or limiting rate of vertical displacement (dD/dt= L 2 /9000d [mm/min]), being L the clear span of the testing specimen in millimetres and d is the distance from the extreme fibre of the cold design compression zone to the extreme fibre of the cold design tensile zone of the structural section, in millimetres.

2.5.2 Insulation criterion

The insulation standard (I) can be defined as the ability to resist fire on one side and prevent excessive heat transfer, the goal being to prevent fire caused by any material from spreading onto surfaces, not exposed. In this regard, the temperature change of the unexposed surface is the main consideration of the standard.

The evaluation of the insulation standards must be based on an average temperature rise of the unexposed surface limited to 140 ° C above the initial average temperature; or based on the maximum temperature rise of any point on the unexposed surface limited to 180 ° C above the initial mean temperature. Therefore, the fire resistance (I) is the time (in minutes) required to meet one of these standards, according to the standard[7].

2.5.3 Integrity criterion

The Integrity Standard (E) is having the ability to withstand fire on one side and the ability to resist the penetration of hot gases and flames through cracks and openings. Assessment should be based on the measurement of cracks or openings exceeding a given size; or inflammation of the cotton ball; or continuous burn on the unexposed side. For composite panels cast in situ, as long as the joints are properly sealed, integrity standards can generally be met.

3. THERMAL PROPERTIES OF MATERIALS

3.1 Genral

The temperature variation within a structural element depends on:

- The density of the material ρ;
- The thermal conductivity is “a measure of the ability of a material to conduct heat”[26]
- The specific heat of the material c which represents the quantity of heat necessary for raise the temperature of 1 kg of this material by 1 °C.

The thermal properties of steel [37]. are known, which allows us to present only the laws of this material. Concrete [29] is a heterogeneous material composed of:

- cement (25 to 40%) and water on the one hand, the mixture of which forms a paste;
- Variable-diameter aggregates on the other hand, bound by the cement paste. Its complex behaviour, induced by its different constituents, leads us to present some experimental laws in addition to the conventional laws.

3.2Concrete

The Eurocode 2 – Part 1-2 [29] determines that the specific heat of dry concrete , using either siliceous or calcareous aggregates, is temperature dependent and shall be determined according to the following equations

$$c_p(\theta) = 900 \text{For} 20°C \leq \theta \leq 100°C \quad \text{(3.1 a)}$$

$$c_p(\theta) = 900 + (\theta - 100) 100°C \leq \theta \leq 200°C \text{ (3.1b)}$$

$$c_p(\theta) = 1000 + (\theta - 100)/2200°C \leq \theta \leq 400°C \text{ (3.1c)}$$

$$c_p(\theta) = 1100 400°C \leq \theta \leq 1200°C \text{ (3.1d)}$$

In the equations above, c_p is the specific heat of dry concrete (J/kgK), and θ is the concrete temperature (°C).

Still with regard to EN 1992 –1-2, whether the moisture content of the concrete is not considered explicitly in the calculation method, the function for the specific heat of concrete should be modelled using a constant value ($c_{p,peak}$), situated between 100 °C and 115 °C,

presenting a linear decrease between 115 °C and 200 °C. The following equations present the values specified by this standard for $c_{p,peak}$ as function of different moisture contents of concrete (u).

$$C_{p,peak} = 900\ j/kgk \quad \text{For u=0\%} \qquad (3.2a)$$

$$C_{p,peak} = 1470\ j/kgk \quad \text{For u=1.5\%} \qquad (3.2b)$$

$$C_{p,peak} = 2020 j/kgk \quad \text{For u=3 \%} \qquad (3.2c)$$

For other values of moisture contents, linear interpolation is acceptable. Figure 3.1 presents the specific heat of concrete as function of temperature at 5 different moisture contents by weight.

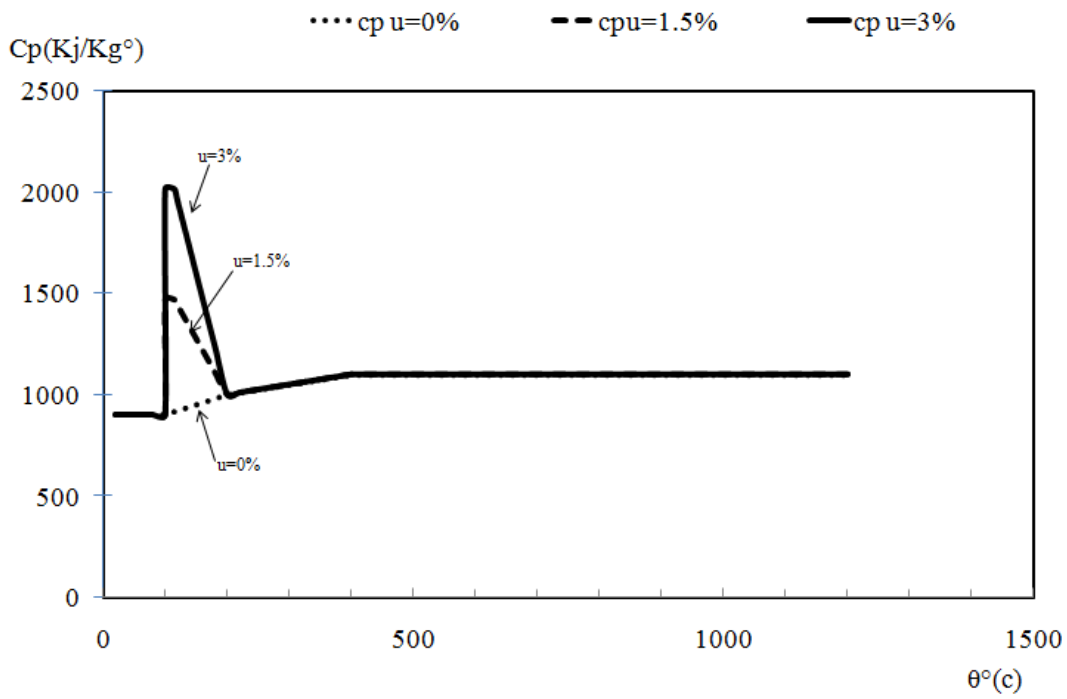

Figure3.1: Specific heat of concrete as function of temperature.

It can be observed that the specific heat of concrete is increased for temperatures between 100°C and 200°C. This is due to the influence of moisture evaporation in the early stage of heating. This investigation applies the models for the specific heat of concrete considering moisture contents of 3.0% for the parametric studies.

The EN 1992 – 1-2 also states that the thermal conductivity of concrete λ_c depends on the temperature of the concrete and should be determined between lower and upper limit values.
The lower limit of thermal conductivity λ_c [W/mK] of normal weight concrete should be calculated according to Eq. 3.3.

$$\lambda_c = 1.36 - 0.136\left(\frac{\theta}{100}\right) + 0.0057.\left(\frac{\theta}{100}\right)^2 \text{For} 20°C \leq \theta \leq 1200°C \quad (3.3)$$

In the equation above, θ is the concrete temperature (°C).
On the other hand, the upper limit of thermal conductivity λ_c(W/mK) of normal weight concrete shall be calculated according to Eq. 3.4.

$$\lambda_c = 2 - 0.2451\left(\frac{\theta}{100}\right) + 0.0107.\left(\frac{\theta}{100}\right)^2 \qquad \text{For } 20°C \leq \theta \leq 1200° (3.4)$$

In the equation above, θ is the concrete temperature (°C). Figure 3.2 illustrates the variation of the thermal conductivity of concrete with temperature for both lower and upper limits.

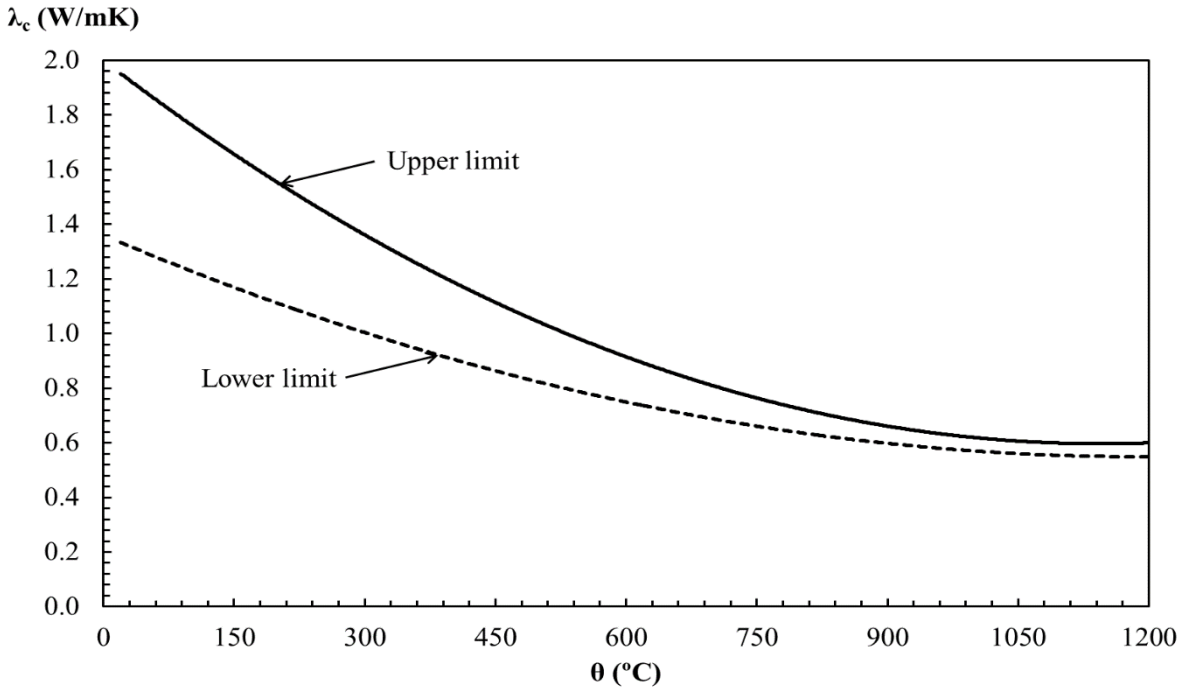

Figure3.2: Thermal conductivity of concrete: lower and upper limits.

The upper limit model for the thermal conductivity of concrete is used in this study, which is indicated for numerical analyses. Jan Jiang et al[9]. concluded that the thermal conductivity of concrete has larger influence on the temperature at the unexposed surface than the exposed surface.

According to the EN 1992 – 1-2, the density of concrete varies with temperature and is influenced by water loss. This variation with temperature is defined in Eqs. 3.5. The density of normal weight concrete at room temperature ρ_c (20 °C) is equal to 2300 kg/m^3.

For 20°C $\leq \theta \leq$ 115°C

$$\rho_c(\theta) = \rho_c(20°C) \qquad (3.5a)$$

For 115°C $\leq \theta \leq$ 200°C

$$\rho_c(\theta) = \rho_c(20°C)\left(1 - \frac{0.02(\theta-115)}{85}\right) \qquad (3.5b)$$

For 200°C $\leq \theta \leq$ 400°C

$$\rho_c(\theta) = \rho_c(20°C)\left(0.98 - \frac{0.03(\theta-200)}{200}\right) \qquad (3.5c)$$

For 400°C $\leq \theta \leq$ 1200°C

$$\rho_c(\theta) = \rho_c(20°C)\left(0.95 - \frac{0.07(\theta-400)}{800}\right) \qquad (3.5d)$$

In the equations above, ρ_c (θ) is the density of concrete (kg/m^3) and θ is the concrete temperature (°C). The relationship between the temperature and the density of concrete is graphically represented in Figure 3.3.

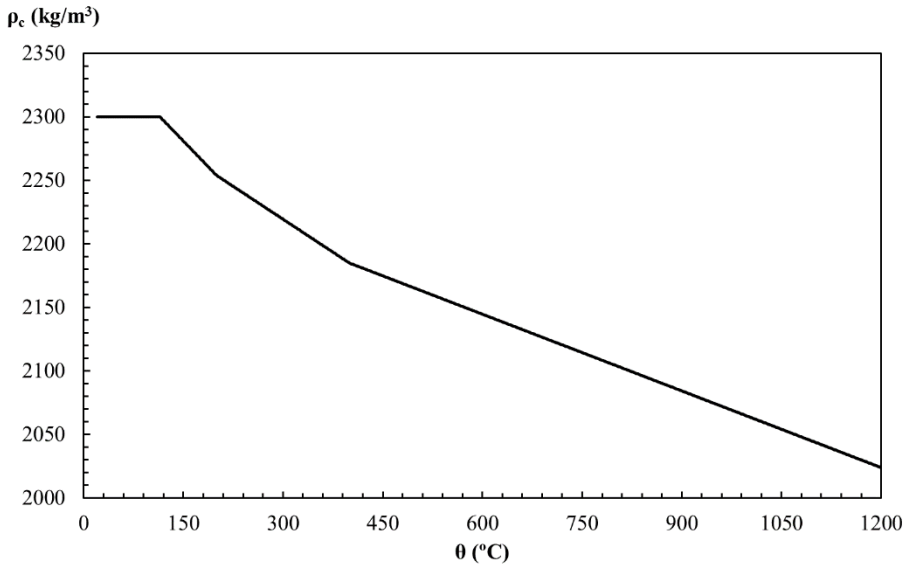

Figure3.3: Density of concrete as function of temperature.

3.3 Carbon steel

According to the Eurocode 3 – Part 1-2[37], the specific heat of carbon steel

c_a (J/kgK)is temperature dependent and shall be determined from the following equations.

For 20°C $\leq \theta \leq$ 600°C

$$c_a = 425 + 7.73 \times 10^{-1}.\theta_a - 1.69 \times 10^{-3}.\theta^2{}_a + 2.22.10^{-6}.\theta_a{}^3 \text{(3.6a)}$$

For 600°C $\leq \theta \leq$ 735°C

$$c_a = 666 + 13002/(738 - \theta_a) \text{(3.6b)}$$

For 735°C $\leq \theta \leq$ 900°C

$$c_a = 545 + 17820/(\theta_a - 731) \text{(3.6c)}$$

For 900°C $\leq \theta \leq$ 1200°C

$$c_a = 650 \text{(3.6d)}$$

In the equations above, θ_a is the steel temperature (°C). The variation of the specific heat of carbon steel with temperature is presented in Figure 3.4.

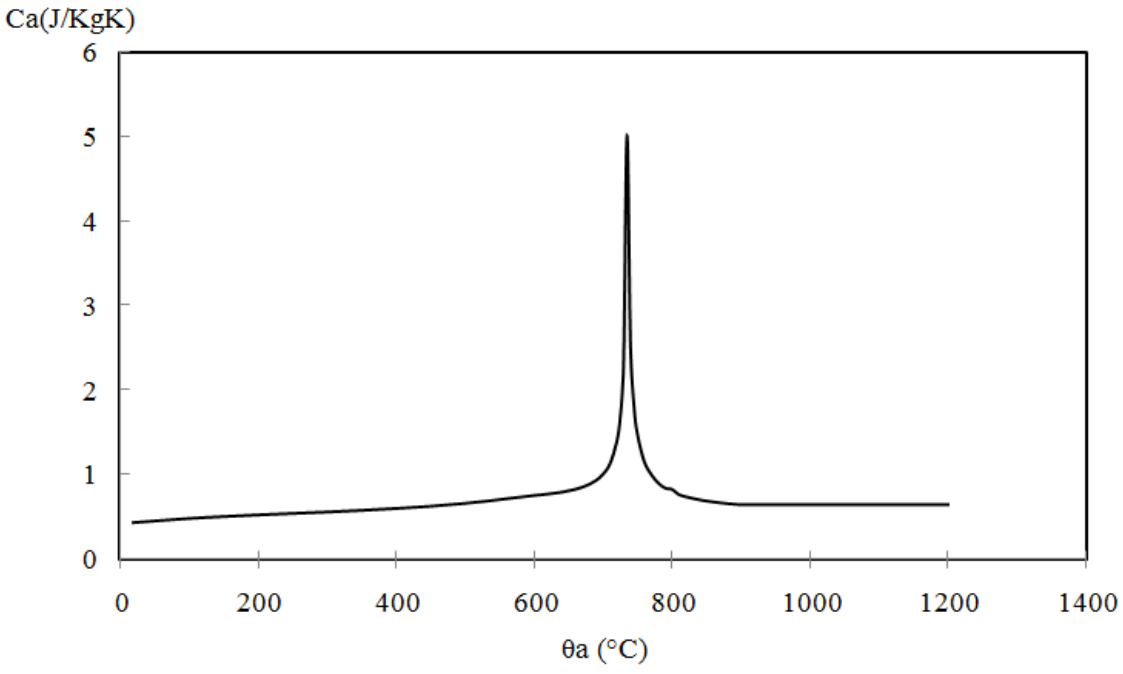

Figure3.4: Variation of the specific heat of carbon steel with temperature.

It can be noticed that the specific heat of steel has an abrupt variation for temperatures between 700 °C and 800 °C. This is due to the allotropic phase transformation, which can affect the temperature development on steel components.

The EN 1993 – 1-2 states that the thermal conductivity of carbon steel λ_a (W/mK) varies with temperature and should be calculated according to the following equations.

$$\lambda_a = 54 - 3.33 \times 10^{-2}\theta_a \text{For } 20°C \leq \theta \leq 800°C \qquad (3.7a)$$

$$\lambda_a = 27.3 \text{For } 800°C \leq \theta \leq 1200°C \qquad (3.7b)$$

In the equations above, θ_a is the steel temperature (°C). Figure 3.5 represents the variation of this thermal property with temperature.

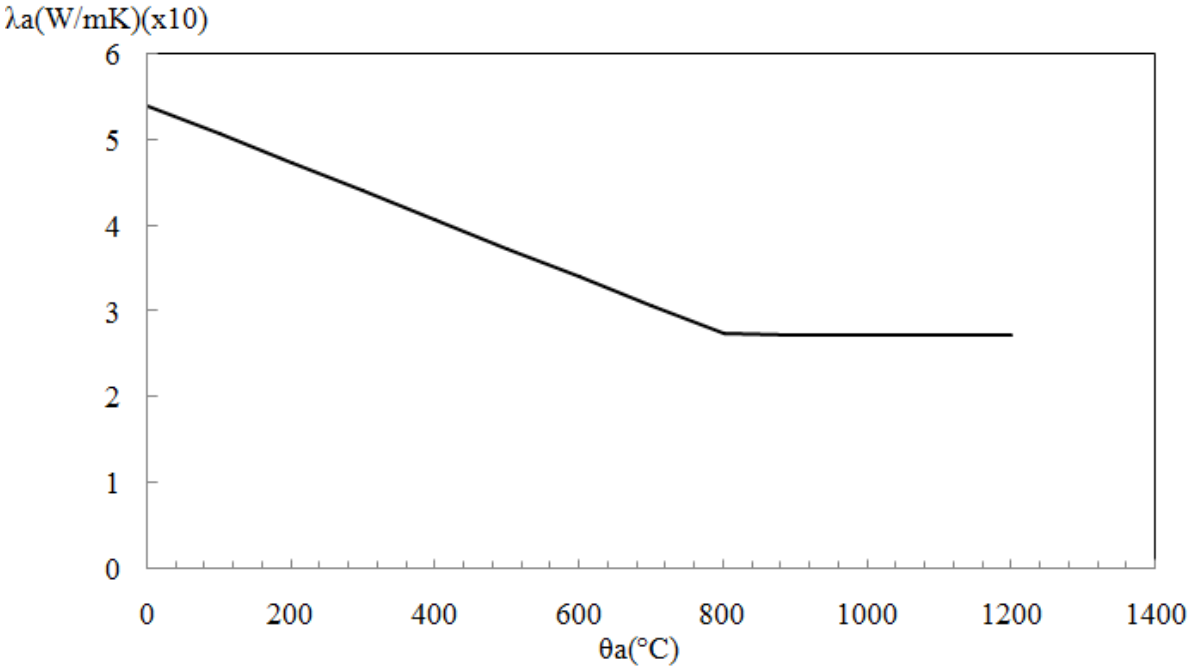

Figure3.5: Thermal conductivity of carbon steel as function of temperature.

Analysing the graph above, it can be observed that this thermal property has a linear decrease until 800 °C, and after that, assumes a constant value. The development of the thermal conductivity of steel is reversible after the cooling stage of fire[24].

According to the EN 1993 – 1-2, the unit mass of carbon steel ρ_a (kg/m^3)may be considered to be independent of the steel temperature. In this regard, a constant value of ρ_a = 7850 kg/m^3 should be taken.

3.4 Air

The thermal properties of air are temperature dependent and should be used to simulate the interface between the steel deck and the bottom surface of the concrete topping. In addition, these thermal properties vary with the air pressure. This work considers the thermal properties of air at 1 atm pressure[25].

Presently, there is no standard which specifies the thermal properties of air. However, computer programs and experimental tests provide reliable data for numerical analyses.

Table 3.1presents the variation of the main thermal properties of air with temperature θair (°C), namely the specific heat C_{air} (J/kgK), the thermal conductivity λair(W/mK) and the density ρair (kg/m3). These thermal properties are graphically represented in Figure 3.6.

Table3.1: Thermal properties of air at 1 atm pressure (adapted from Çengel**[**25]).

θ_{air} (°C)	c_{air} (J/kgK)	λ_{air} (W/mK)	ρ_{air} (kg/m^3)
20	1007	0,02514	1,20400
30	1007	0,02588	1,16400
60	1007	0,02808	1,05900
100	1009	0,03095	0,94580
200	1023	0,03779	0,74590
300	1044	0,04418	0,61580
400	1069	0,05015	0,52430
500	1093	0,05572	0,45650
600	1115	0,06093	0,40420
700	1135	0,06581	0,36270
800	1153	0,07037	0,32890
900	1169	0,07465	0,30080
1000	1184	0,07868	0,27720
15000	1234	0,09599	0,19900

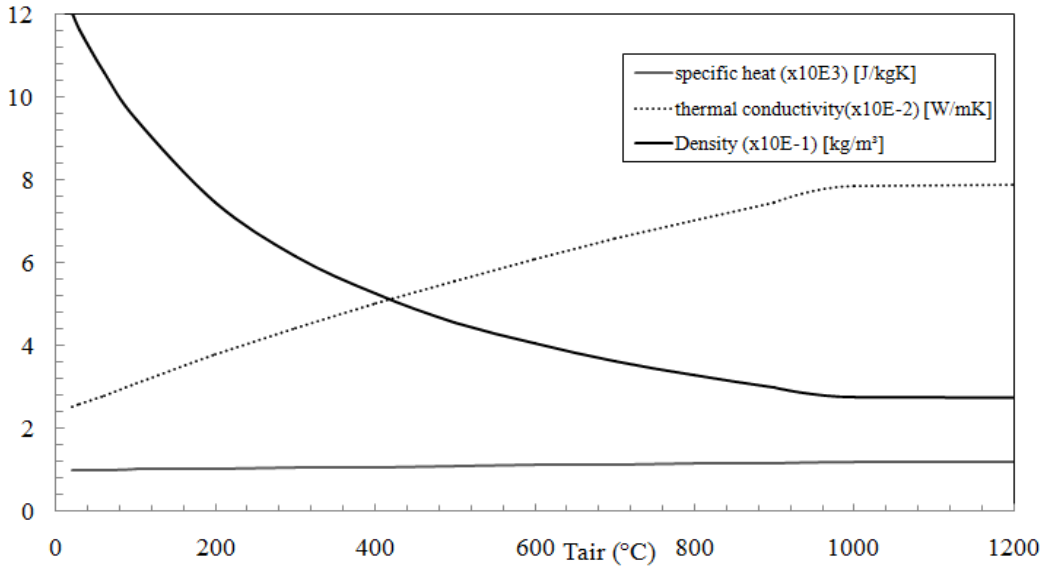

Figure3.6: Thermal properties of air as function of temperature at 1 atm pressure.

3.5 Simplified calculation methods:

The simplified calculation models for these standards generally come from experimental fire tests and numerical analyzes. These models allow the use of simple analytical expressions to calculate important parameters related to the fire resistance of composite panels (such as the fire resistance and temperature of steel components).

In the sub-specification, the simplified calculation method for the composite steel strip deck plate proposed in Annex D of Eurocode 4-part 1-2 [13].

3.6 Eurocode 4 – Part 1-2

The analytical expressions for composite slabs given in the current version of the EN 1994 – 1-2 are based on the study conducted by Both[1], in 1998. As stated before, no revisions were made to these methods during the last years.

The fire resistance of the composite panel against the thermal insulation standard tfi (min) depends on various parameters and should be determined according to the equation. 3.8

$$t_{fi} = a_0 + a_1.h_1 + a_2.\emptyset_{up} + a_3.\frac{A}{l_r} + a_4.\frac{1}{l_3} + a_5.\frac{A}{l_r}.\frac{1}{l_3} \qquad (3.8)$$

In the above formula, h1 is the thickness of the concrete (mm); Φup is the view factor of the top flange (dimensionless); A / Lr is the geometric coefficient of the ribs (mm); 13 is the width of the top rim (mm). The partial factor is a tabular coefficient, which is different for

normal weight concrete (NWC) and lightweight concrete (LWC). These coefficients are given in the table below.

Table3.2: Coefficients for the determination of the fire resistance of composite slabs with NWC and LWC (adapted from EN 1994 – 1-2[13]).

	a_0 (min)	a_1 (min/mm)	a_2 (min)	a_3 (min/mm)	a_4 (mm min)	a_5 (min)
Heating	-28.8	1.55	-12.6	0.33	-735.0	48.0
Cooling	-79.2	2.18	-2.44	0.56	-542.0	52.3

The scope of this investigation comprises only composite slabs with normal weight concrete. The geometric coefficient of ribs is defined as the ratio of the volume of rib concretes per meter of rib length A(mm3 / m) to the exposed area of the ribs per meter of rib length Lr (mm2/m). This factor can be calculated using the geometric parameters of the slab as follows.

$$A/L_r = h_2.((l_1 + l_2/2)/(l_2 + 2\sqrt{h^2{}_2 + \left(\frac{l_1 - l_2}{2}\right)^2}) \qquad (3.8)$$

The EN 1994 – 1-2 states that the effective thickness of a composite slab h_{eff} (mm) should be calculated according to Eqs. 2.32.

$$h_{eff} = h_1 + 0.5.h_2.(\frac{l_1+l_2}{l_1+l_3}) \quad For \frac{h_2}{h_1} \leq 1.5 \text{ and } h_1 > 40mm \qquad (3.9a)$$

$$h_{eff} = h_1.\left[1 + 0.75.(\frac{l_1+l_2}{l_1+l_3})\right] For \frac{h_2}{h_1} > 1.5 \text{ and } h_1 > 40mm \quad (3.9b)$$

The geometric parameters of the slab h_1, h_2, l_1, l_2 and l_3 are illustrated in Figures 1.2 and 1.3. The effective thickness may be adopted as h_1 if $l_3 > 2\ l_1$.

Table 3.3 presents the relation between the minimum effective slab thickness and the standard fire resistance (I). The parameter "h_3" represents the thickness of the screed layer, if any on top of the composite slab, see Figures 1.2 and 1.3.

4. ADVANCED CALCULATION METHOD

The advanced calculation model is based on numerical methods and can perform real analysis of structures exposed to fire. However, since these methods involves many calculations, a computer program is required. Compared to simple calculation models, advanced calculation metods can better estimate the actual structural performance under fire conditions. These models should be used in conjunction with time-temperature curves, and the thermal properties of the material should be known within the appropriate temperature range.

According to EN 1994-1-2[13], advanced calculation models must include different models (thermal models) to determine the temperature distribution in structural components. This research involves the development and application of a three-dimensional thermal model for the analysis of the fire behavior of composite panels. These models should be implemented through the Partial Differential Equation (PDE) Toobox in cluded in MATLAB R2018a [38]

4.2 MATLAB

4.2.1 General definition:

The MATLAB (Matrix LABoratory) software is a multi-paradigm programming environment developed by MathWorks. This software has been selected for the development of the new tool for nonlinear transient thermal analysis due to its flexibility and large number of functions for finite element analysis.

The MATLAB PDE Toolbox™[38] is a widely used tool for solving partial differential equations (PDEs) involving problems of heat transfer, structural mechanics, and electrostatics, among others. Its algorithm uses FEM principles for problems defined on bounded domains in 2-D or 3-D space, and allows the performance of steady-state and transient heat transfer analysis.

4.2.3 Finite element models for thermal analysis

Modelling complex 3D multi-domains as geometric figures in MATLAB PDE Toolbox is a challenge. Thermal analysis in MATLAB PDE Toolbox requires the definition of a thermal model object, which contains information about heat transfer issues, such as geometry, material properties, and boundary conditions. For simplicity's sake, rebar and crack resistant mesh are not included in the MATLAB digital model. The geometry is created by the function

geometry From Mesh. Figure 4.1 shows the geometric model of the composite plate created in MATLAB.

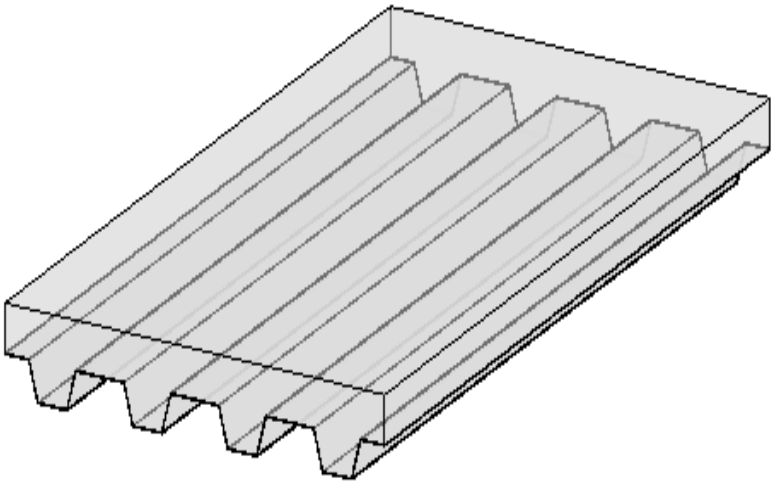

Figure4.1: Modelling of composite slabs in MATLAB[38]

4.2.3 Validation of the experimental and numerical result

The validation and the numerical result (Matlab) with the experimental result [31], for the slab F2 with different values of the air gap 0.5 , 1 and 2 mm is presented here.

In the experimental test, the slab was subjected to fire at the trough location (temperature locations T20, T21, T22, T16, T19 and T15) shown in Figure 4.2. We notice that in figure 4.3 the numerical and experimental results are almost equal but in figures 4.4 and fig 4.5 there is a big difference between the two results specially in the point T19(lower flange) and T22 (upper flange) because these points are in direct contact with the fire.

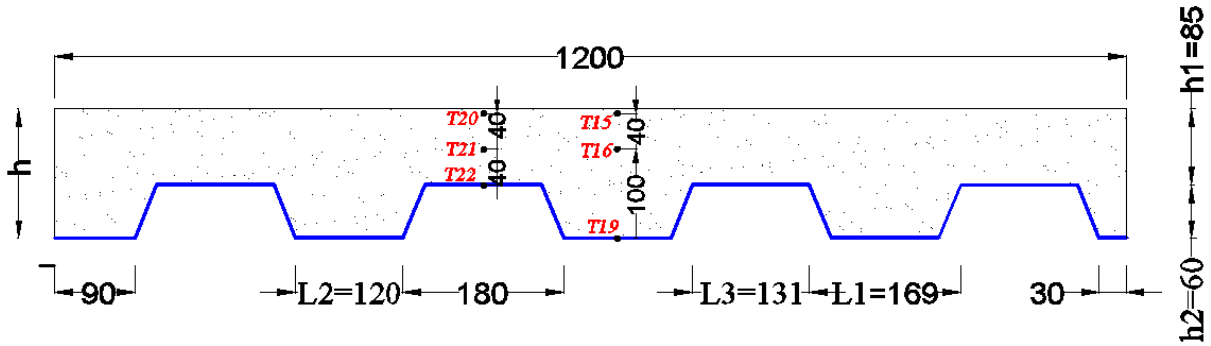

Figure4.2: Profile of the composite slab F2 with different points

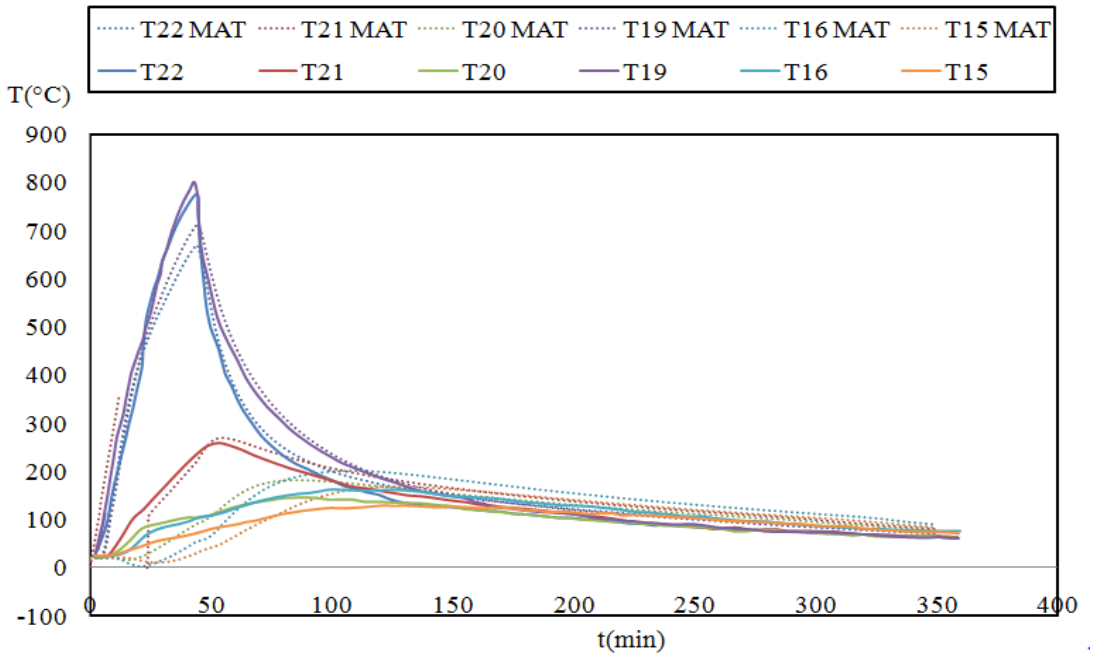

Figure 4.3: Comparison between the experimental and Numerical results with ta=0.5mm

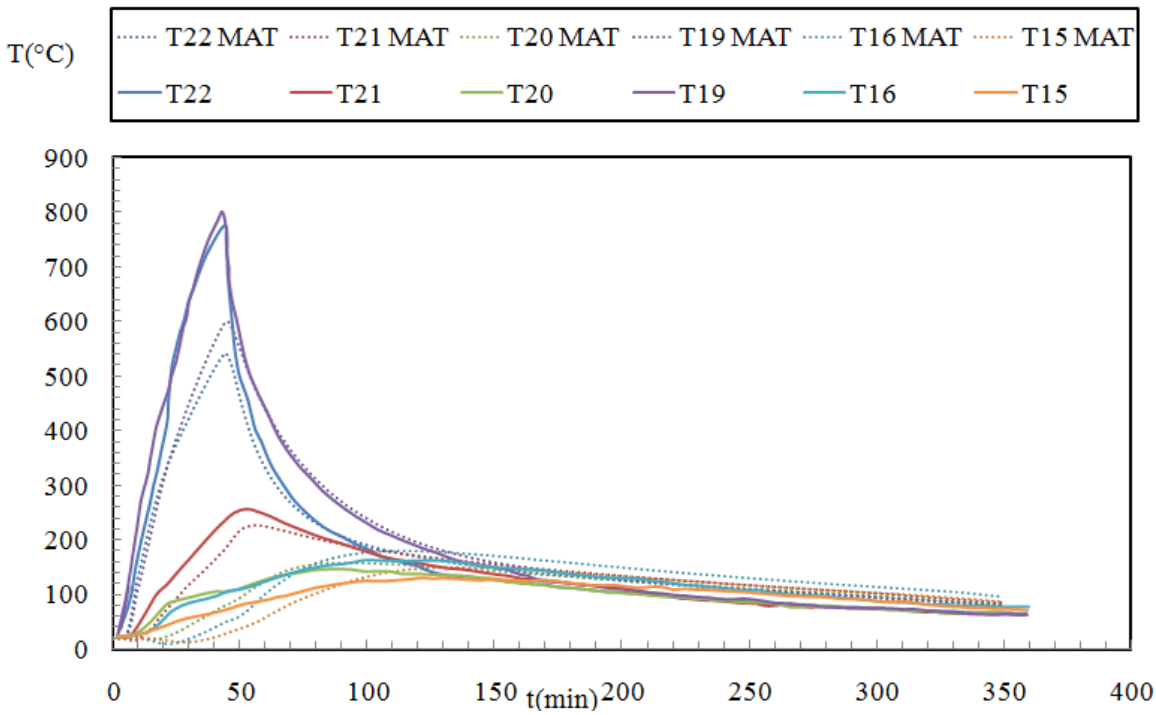

Figure 4.4: Comparison between the experimental and Numerical results with ta=1mm

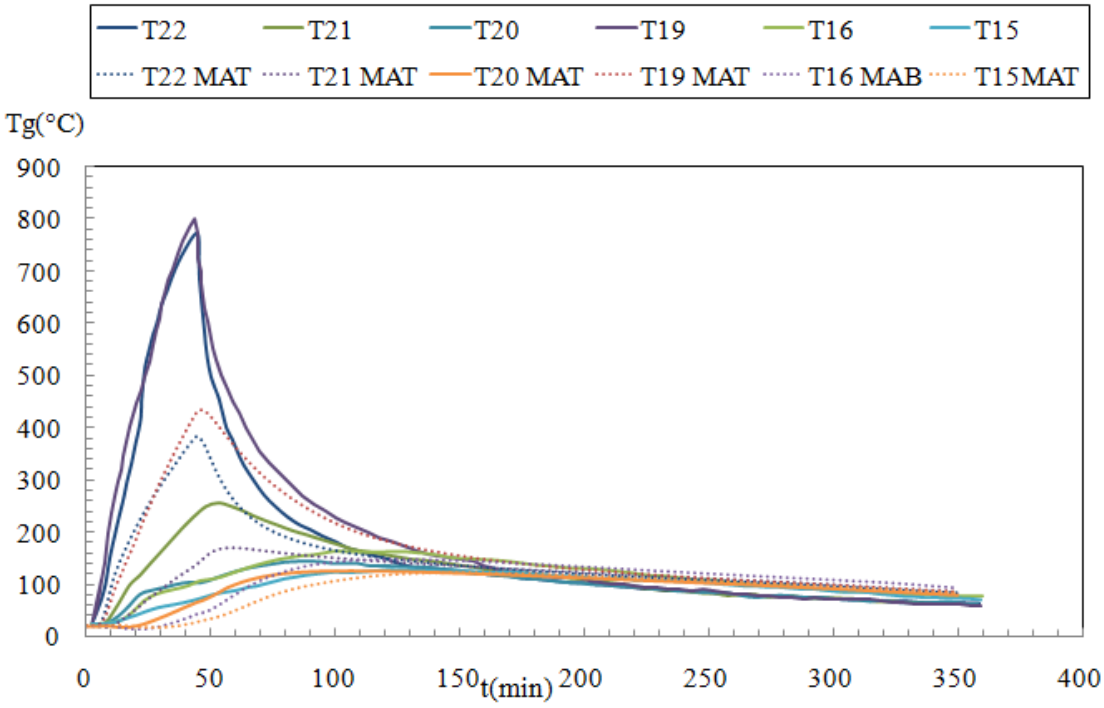

Figure 4.5: Comparison between the experimental and Numerical results with ta=2mm

Figures 4.3, 4.4 and 4.5 compare the experimental results obtained by Both [cite] with the numerical values obtained with different air gaps (*ta* equal to 0.5, 1 and 2mm). Based on the results obtained with the different values of ta and we observed that the results closest to the experimental results are the results with ta = 0.5 mm. So, from now on we will keep all the next simulations with a ta = 0.5 mm

5. PARAMETRIC ANALYSES

5.1 Description

A parametric study comprising six natural curves with different concrete heights h1 and different composite slabs with commercial steel deck profiles was carried out in this investigation. A representative portion of 1 m by 1 m of each slab is selected for performing thermal analyzes taking into account standard fire conditions. In addition, a moisture content of 3% of the weight of the concrete is considered.

All composite slabs are exposed to fire for 7200 seconds (2 hours). In cases where none or only one of the two fire resistance criteria (MAX_T crit and AVE_T crit) is reached, the numerical simulation must be performed again, considering the exposure to fire for 21600 seconds (6 hours).

In this parametric study, the focus is on the influence of the various parameters on the temperatures of the parts of the composite slab, namely the effective thickness and still deck thickness. In total, 96 numerical simulations were carried out in Matlab using an air gap of 0.5 mm. The Table 5.1 summarizes the ranges of the parameters studied, where td is the steel deck thickness. The steel deck profiles corresponding to current models available on the market.

Table5.1: Investigated parameters of the first parametric study

Steel deck profile	**h_1 (mm)**	**t_d (mm)**
Cofraplus (Trapezoidal)	50, 70, 90,110	1.25
Polydeck 59S (Trapezoidal)	50, 70, 90,110	1.25
Multideck (Re-entrant)	50, 70, 90,110	1.2
Bondek (Re-entrant)	50, 70, 90,110	1.2

The ranges of selected parameters comprise commonly used values. The diameters and spacing of the anti-crack meshes have been determined from technical catalogues.

For the determination of the fire resistance (I) of each composite slab, the average temperature on the unexposed side (AVE_T) is calculated from a weighted mean between 8 points located on the central section. The maximum temperature on the unexposed side (MAX_T) is obtained from these points as well. Figure 5.1 illustrates the geometry of the steel deck profiles, corresponding to current models available on the market.

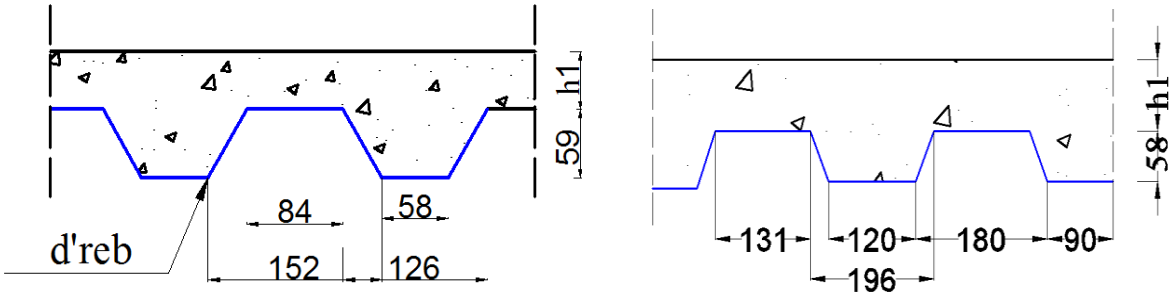

a) Slab 1: Polydeck 59S

b) Slab 2: Cofraplus H60

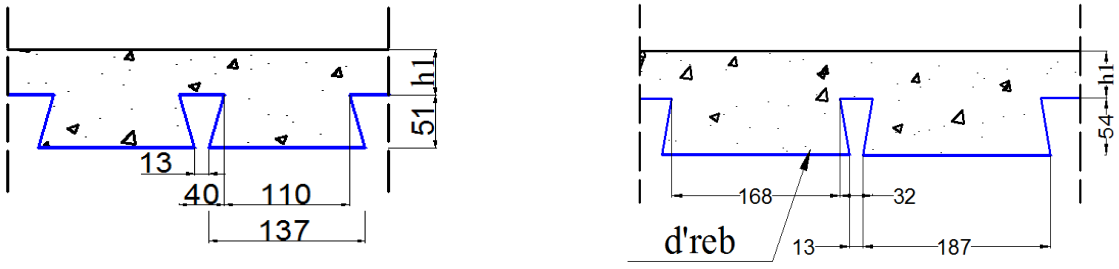

c) Slab 3: Multideck

d) Slab 4: Bondeck

Figure5.1: Steel deck geometries for the first parametric study (dimensions in millimeters)

Table 5.2: Calculated view factors.

Steel deck profile	**Φ_{up}**	**Φ_{web}**
Polydeck 59S (slab 1)	0.78	0.67
Cofraplus60 (slab 2)	0.72	0.56
Multideck (slab 3)	0.12	0.08
Bondeck (slab 4)	0.12	0.085

In Table 5.2, it can be seen that there is a significant difference between the view factors of the trapezoidal and re-entrant profiles. The lower values of the view factors are due to the large obstruction of the ribs.

The parametric study also examined the effect of concrete thickness (h1) and air gap (ta) on fire resistance according to the insulation standard, and 96 numerical simulations were performed in MATLAB, using the model of the air gap with 0.5 mm.

The view factors and the points for the calculation of the AVE_T and MAX_T are the same as those of the first parametric study see Table 5.2.

5.2 Numerical result

With respect to the first parametric study, the fire resistance (I) of the composite slabs is predominantly governed by the average temperature rise criterion. The results are given for slabs with the same parameters, however only for the thinnest concrete thickness for each steel deck family, which is the critical case (highest temperature).

The following subsection discusses the influence of each investigated parameter on the fire resistance of composite slabs according to thermal insulation criterion.

5.3 Influence of different parameters on fire resistance (I)

5.3.1 Steel deck geometry

Trapezoidal steel deck profiles have similar geometric parameters to each other, namely the height of the steel deck h2 and the width of the bottom flange l2, see figure 4.1. For similar concrete thicknesses, it is observed that slab 2 has a slightly higher fire resistance compared to slab 1, with small differences, because the higher inclination of the core results in the presence of a volume most important .of concrete on the ribs of the composite slab. The following Figure 5.3 shows the temperature distribution across slab 1 and slab 2 with similar concrete thicknesses after 120 minutes of fire exposure.

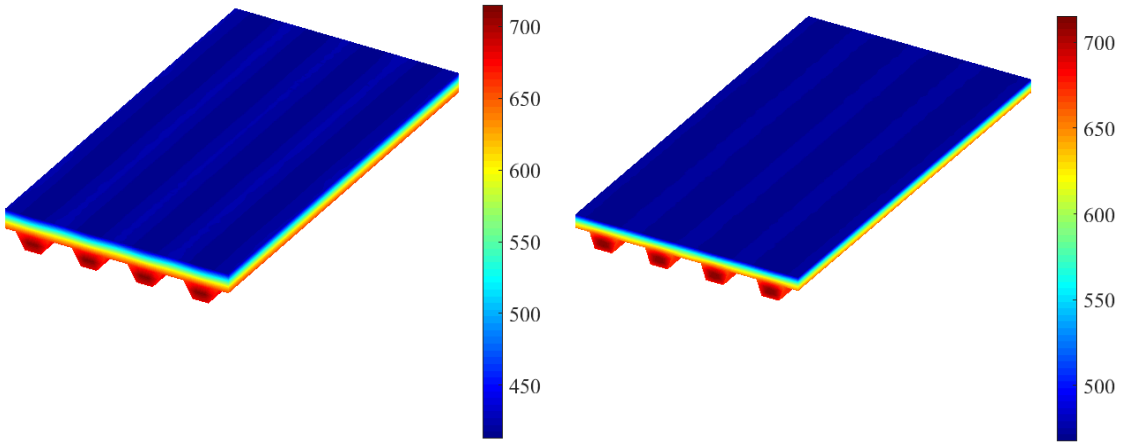

a) Slab 1: h_2 = 58 mm. b)Slab2:h_2 = 59 mm

Figure 5.3: the temperature distribution across slab 1 and slab 2 with similar concrete thicknesses after 120 minutes of fire exposure (Matlab, first parametric study).

From the above temperature limits, it can be seen that the temperatures on the unexposed surface of slab 1 and 2 are nearly equal.

According to Jian Jiang et al.[9], increasing the width at the top of the rib L1 should lead to a reduction of temperatures in the thick portion of the slab, however shall not present a considerable effect on the temperatures in the thin portion. In addition, decreasing the width of the upper flange l3, the temperatures in the thin portion also decrease, but this effect is very small.

The slabs with re-entrant steel deck profiles (slabs 3 and 4) cannot be directly compared to each other because they present very different geometric parameters which may influence on the fire resistance, such as the height of the steel deck profile and the width of the upper flange.

5.3.2 Concrete thickness

The thickness of the continuous upper part of the slab (concrete thickness h1) as the most significant geometric factor influencing the fire resistance (I).

For the first parametric study, four different concrete thicknesses were selected for each group of composite slabs, see Table 5.1. The following Figure 5.4 shows the relationship between fire resistance tfi and concrete thickness for all groups of slabs.

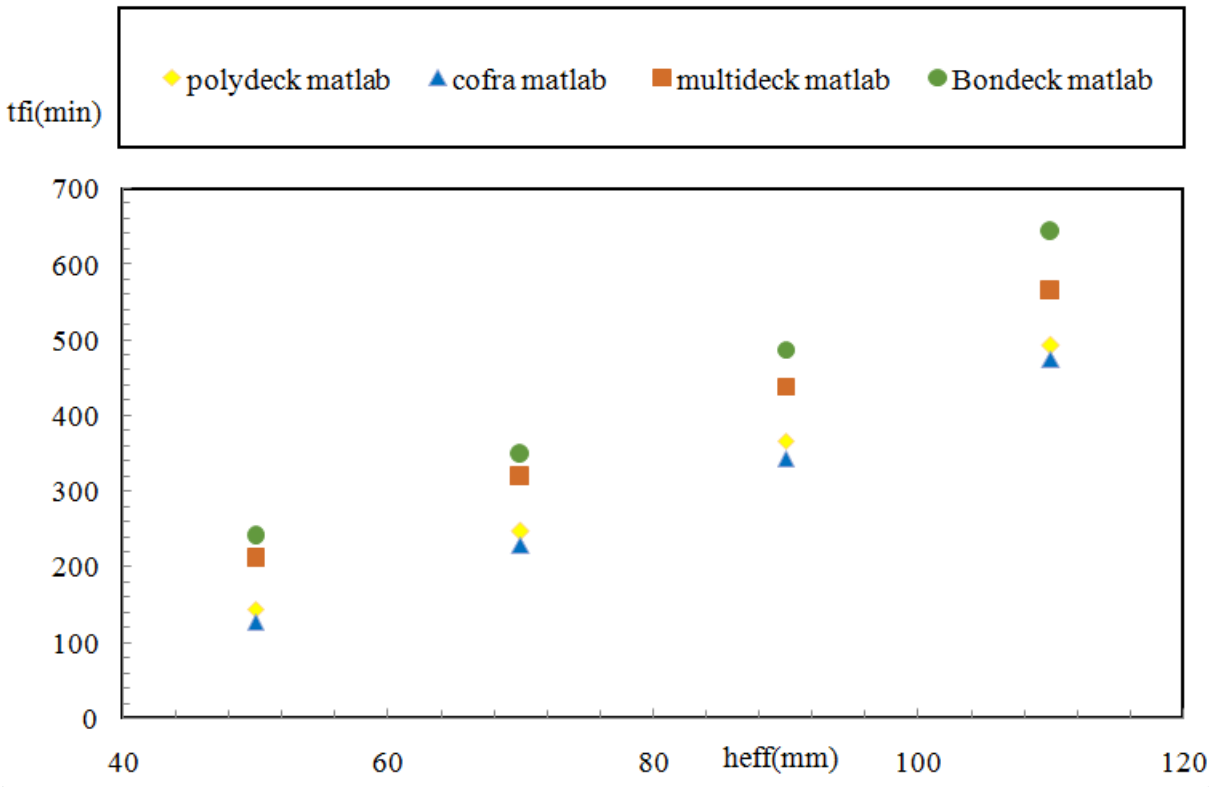

Figure5.4: Influence of concrete thickness on fire resistance (I) of all the slabs (Matlab , first parametric study).

According to the results above, it is observed that the fire resistance (I) considerably increases with the concrete thickness for all the groups of slabs. In addition, the results for the slabs with re-entrant steel deck profiles present an almost linear increase pattern. The same is observed for the slabs with trapezoidal steel deck profiles.

Comparing the results for simulations with the same concrete thickness, the slabs with re-entrant profiles present higher fire resistance in comparison to the slabs with trapezoidal profiles. These differences are situated between 24 min and 34 min, approximately. This is explained by the fact that the re-entrant profiles allow the employment of more uniform volume of concrete along the cross section, resulting in more homogeneous temperature distributions.

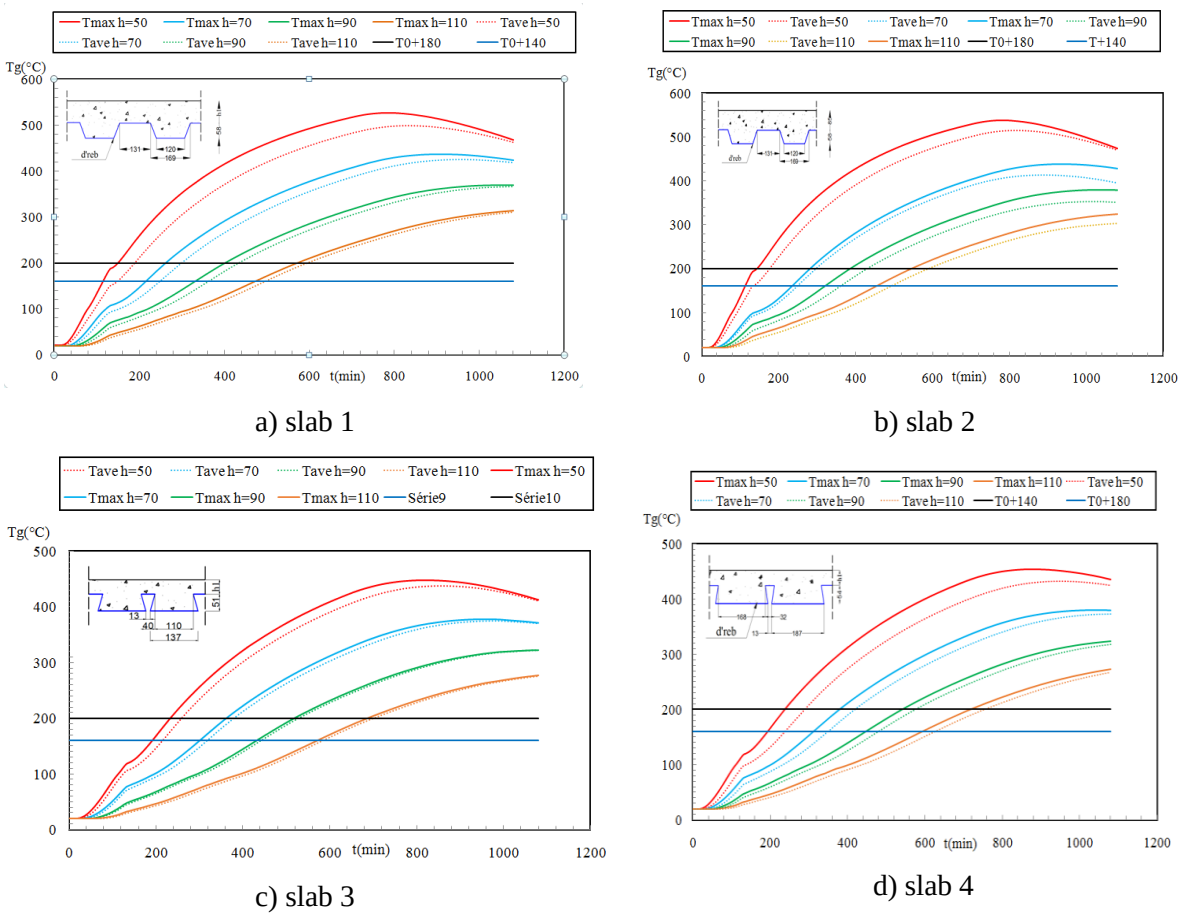

Figure 5.5: Average and maximum temperature development on the unexposed side of the slabs.

According to the results above, it is observed that whereas the concrete thickness is increased, both average and maximum temperature curves are horizontally translated, hence increasing the fire resistance time. In addition, a slight plateau at about 100 °C is evident for all the curves due to moisture evaporation. It is noticeable that the slabs with re-entrant profile present less accentuated temperature development in comparison to the slabs with trapezoidal profile. For slab 4, the curves of the average and maximum temperature are closer to each other in comparison to the other slabs.

With respect to the second parametric study, eight different concrete thicknesses have been selected for the numerical analyses, see Table 4.3. The following figure presents a comparison between the fire resistance t_{fi} and the concrete thickness h_1 for different air gap thicknesses t_a

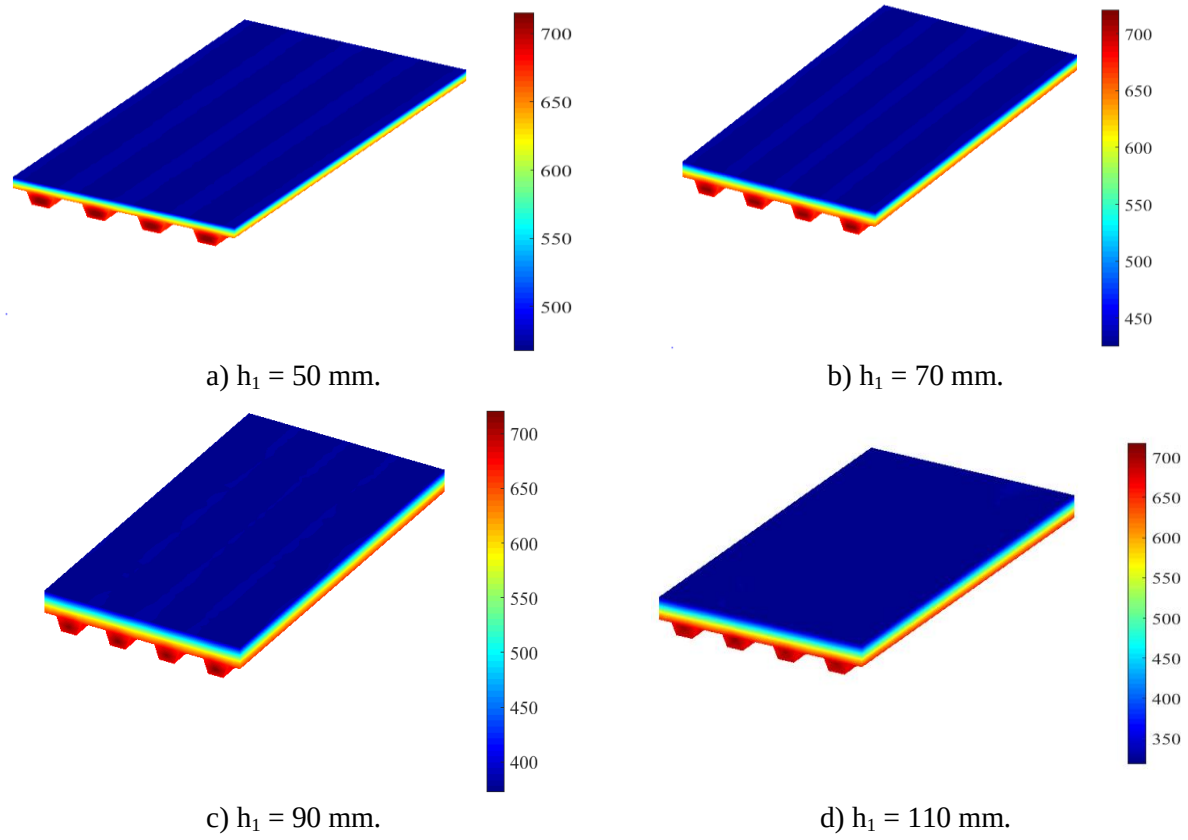

a) h_1 = 50 mm. b) h_1 = 70 mm.

c) h_1 = 90 mm. d) h_1 = 110 mm.

Figure5.6: Temperature distribution in slab1 of fire exposure for different concrete thicknesses.

From the above Figure 5.6, it is observed that the temperatures of the unexposed side of the slab with the smallest height h1 are considerably higher compared to the slab with the highest h1. For slabs with h1 = 50 mm and h1 = 70 mm, the segment with higher temperatures on the unexposed side (above the top flange) should be highlighted. These segments are not noticed in slabs with a higher concrete thickness because the concrete layer allows a more even distribution of temperatures over the cross section.

Therefore, for considerably large concrete thicknesses, the temperature distribution of the unexposed side of composite slabs is quite similar to the temperature distribution of flat concrete slabs. Therefore, when the concrete height of the slab increases, the fire resistance increases.

5.3.3 Numerical results and Eurocode 4 – Part 1-2

Figure 5.7 present the comparation between numerical results and results obtained with the simplified calculation method of Eurocode 4 - Part 1-2 (EC4) for fire resistance (I), as a

function of the effective thickness of the composite panels and of the different natural curves using four types of steel deck.

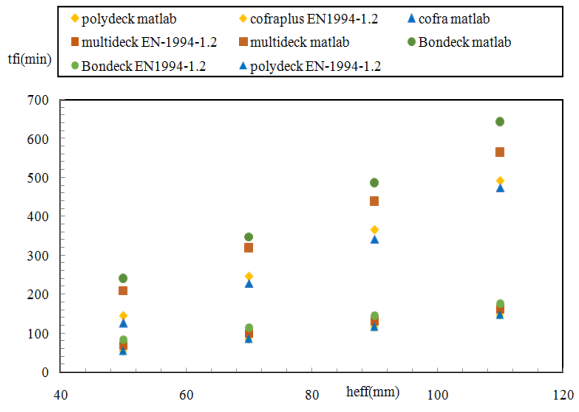

a) Natural curve 1

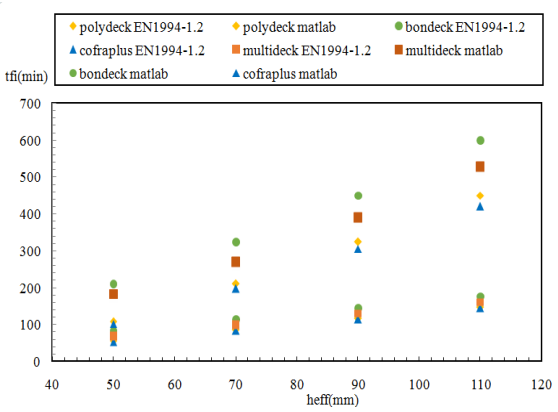

b) Natural curve 2

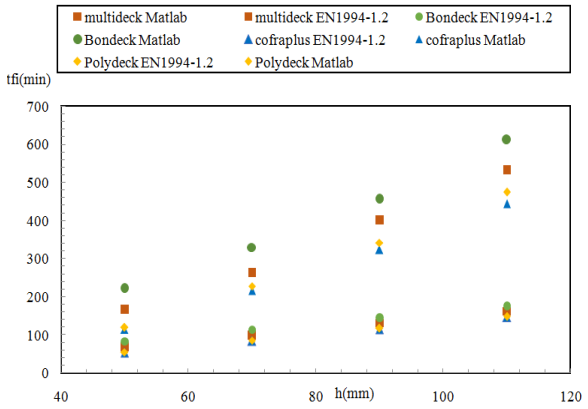

c) Natural curve 3

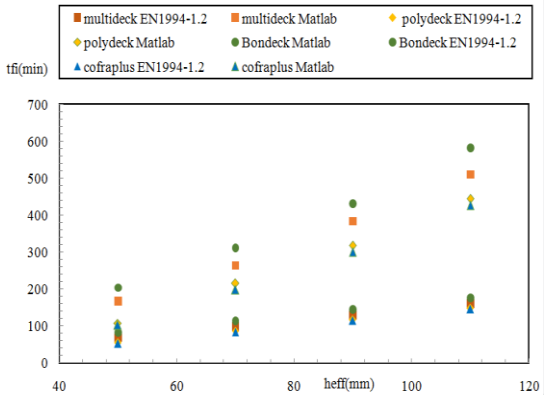

d) Natural curve 4

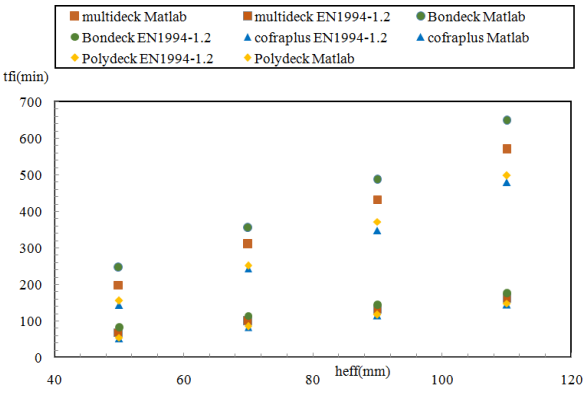

e)Natural curve 5

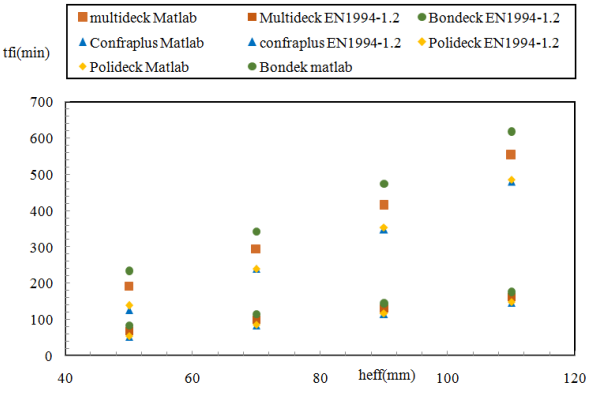

f)Natural curve 6

Figure 5.7: Comparison between the numericalresults from Matlab and Eurocode 4 – Part 1-2 for the fire resistance (I).

For the parametric study, we observe that all the results obtained with Matlab in dicates fire resistance superior to the provisions of Eurocode 4.
According to the numerical results, there is a linear dependence between the fire resistance tfi and the effective thickness heff which is taken into account in the simplified calculation methods of European standards.

5.3.4 New proposal

A model between the fire resistance t_{fi} and the effective thickness h_{eff} is chosen to fit the results of the numerical simulations. A linear relationship between the effective thickness and the thickness of the air gap *ta* is considered in order to take into account the increase in fire resistance. The new coefficient proposed for the fire resistance of composite slabs is given in Table 5.3 for Eq. 3.8.

Table 5.3: new coefficients for the determination of the fire resistance of composite slabs with (solver of excel)for natural curve 1.

a0	a1	a2	a3	a4	a5
-243,043	6,059	57,084	-2,595	6380,267	64,563

Where t_{fi} is given in minutes, and h_{eff} and t_a are given in millimetres; with the following limits: $70 \leq h_{eff} \leq 150$ mm and $0 \leq t_a \leq 3$ mm. Figure 5.8: illustrates the results obtained with the application of these coefficients in Eq (3.8).

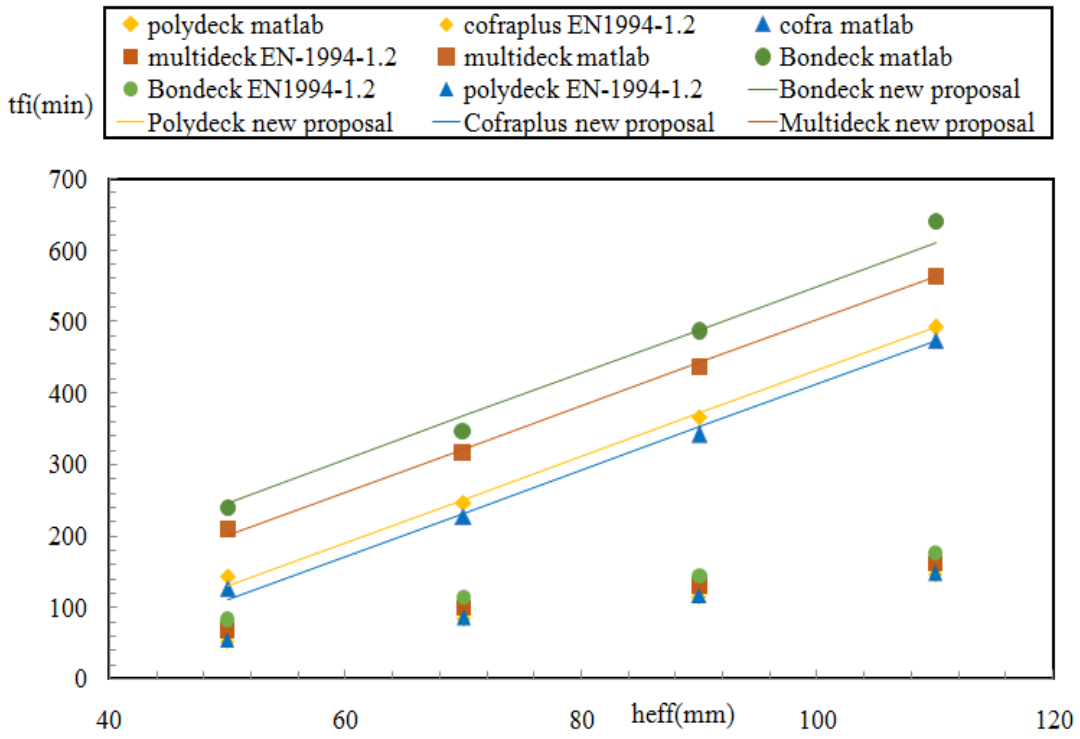

Figure 5.8: Results of the new proposal for the fire resistance (I) under natural fire curve 1

Table 5.4: new coefficients for the determination of the fire resistance of composite slabs with (solver of excel) for natural curve 2.

a0	a1	a2	a3	a4	a5
-602,650	5,819	-174,484	20,873	7357,702	-347,905

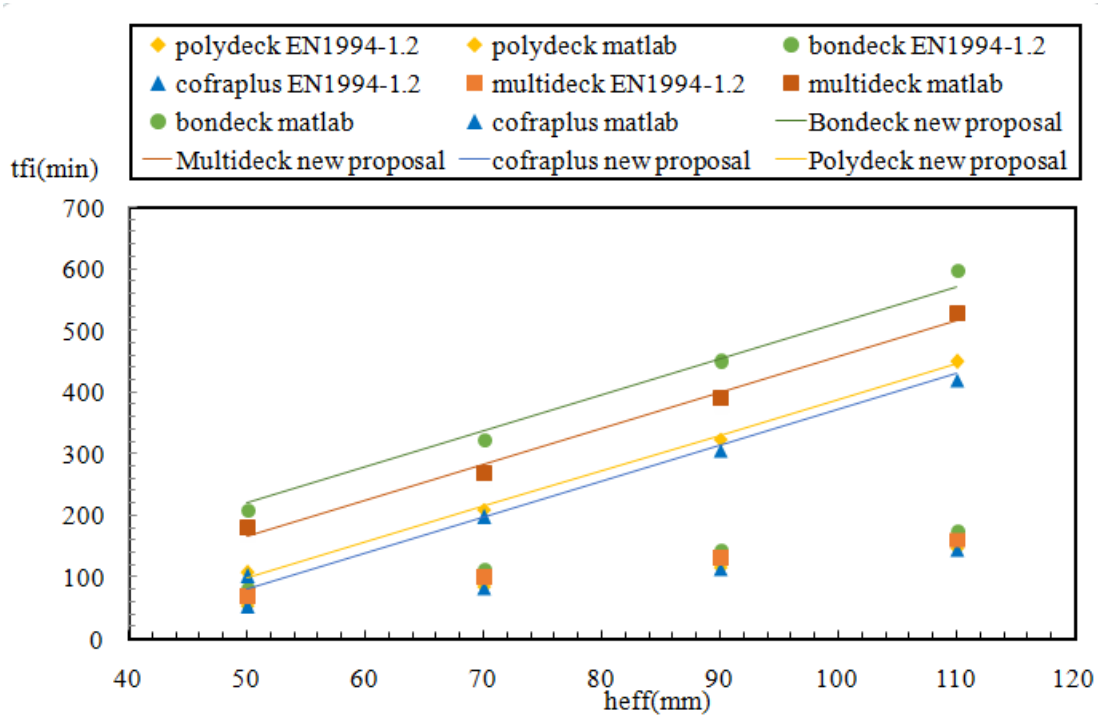

Figure5.9: Results of the new proposed for the fire resistance (I) under natural fire curve 2

Table 5.5: new coefficients for the determination of the fire resistance of composite slabs with (solver of excel) for natural curve 3

a0	a1	a2	a3	a4	a5
-828,500	6,007	-288,375	35,172	7301,840	-573,046

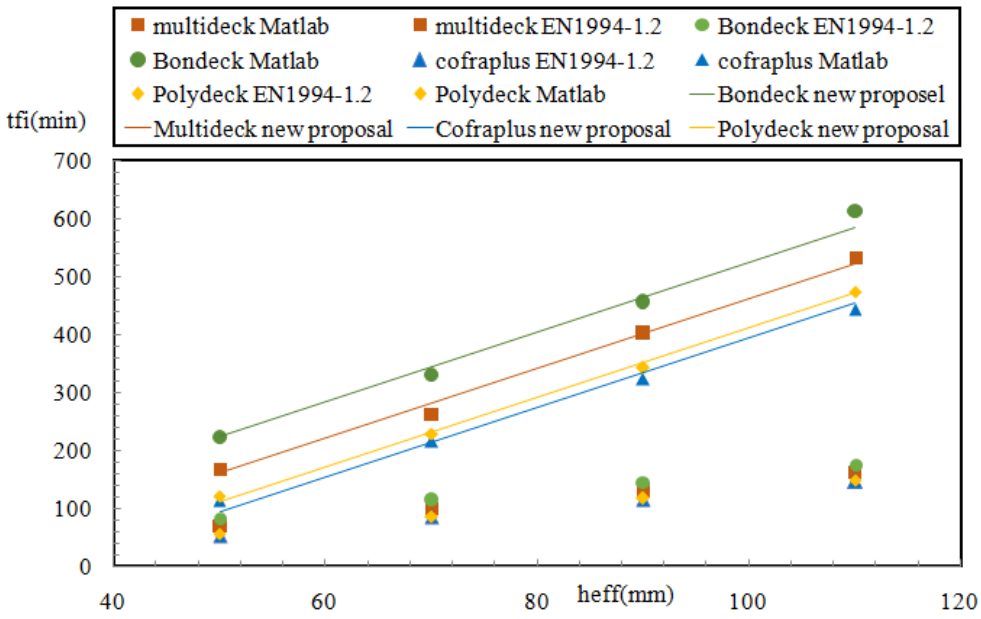

Figure5.10: Results of the proposed new equation for the fire resistance (I) under natural fire curve 3

Table 5.6: new coefficients for the determination of the fire resistance of composite slabs with (solver of excel) for natural curve 4.

a0	a1	a2	a3	a4	a5
-733,451	5,737	-272,805	30,738	7315,449	-528,417

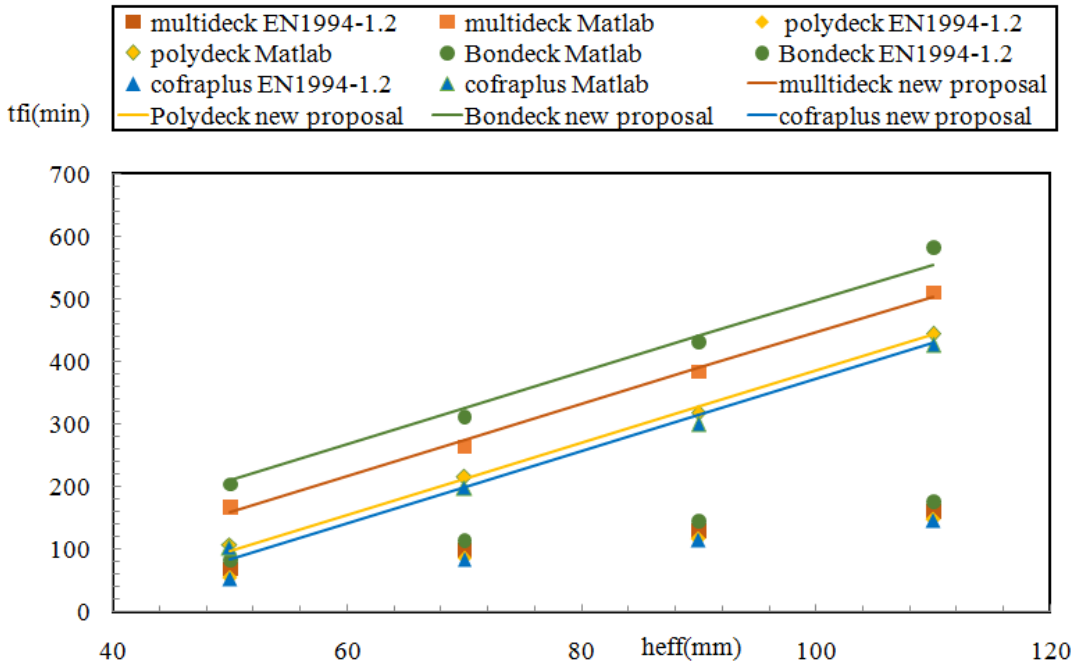

Figure5.11: Results of the proposed new equation for the fire resistance (I) under natural fire curve 4

Table 5.7: new coefficients for the determination of the fire resistance of composite slabs with (solver of excel) for natural curve5

a0	a1	a2	a3	a4	a5
-706,823	6,042	-248,263	29,582	7303,712	-493,878

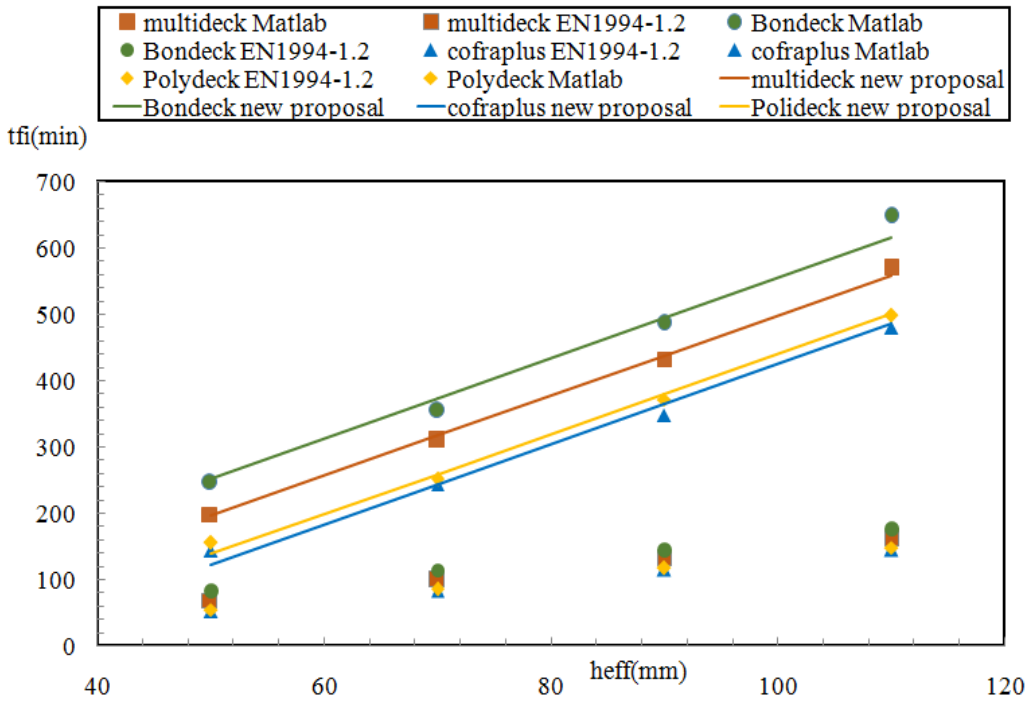

Figure5.12: Results of the proposed new equation for the fire resistance (I) under natural fire curve 5

a0	a1	a2	a3	a4	a5
-1091,050	6,112	-566,988	57,973	7173,163	-1003,483

Table 5.8: new coefficients for the determination of the fire resistance of composite slabs with (solver of excel) for natural curve6

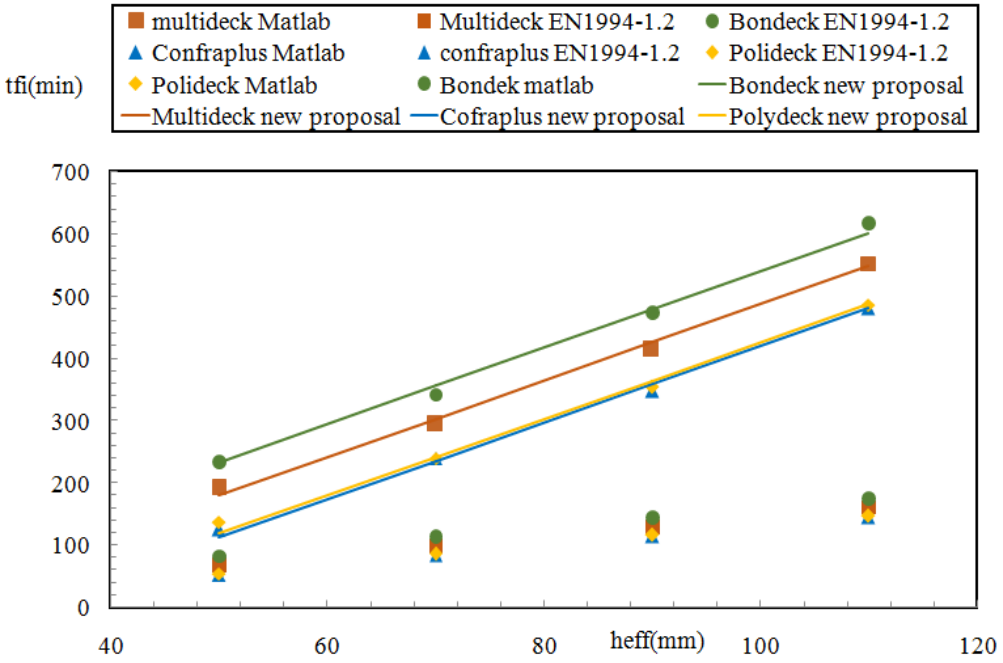

Figure 5.13: Results of the proposed new equation for the fire resistance (I) under natural fire curve 6

it can be seen in this results we used the solver of excel to found all this result for each natural fire scenario there is a big difference between the result with Eurocode and the numerical result because the calculation with eurocode is parametric for ISO 834 but the numerical result with the natural fire that’s why we found the result of the new proposal is nearly the result of the simulation

6. CONCLUSIONS

The work is based on 3D numerical simulations of the thermal behavior of composite slabs under fire conditions, using MATLAB software.

The first part of the work consists of making numerical models to build for a composite slab with different thicknesses of the insulating layer (air gap) between the concrete layer and the steel surface to simulate the deboning effects. We have chosen the numerical result closest to the experimental result and from these results we will continue the work with the value of

ta = 0.5 mm

The second part of the work was carried out parametric studies with 94 composite slabs containing 6 different types of natural fire with 4 types of steel deck of 4 different heights on concrete in order to assess the influence of different parameters on the fire resistance according to thermal insulation criterion (I).

Concerning the normative recommendations, the fire resistance t_{fi} and the temperature of the steel components obtained thanks to the calculation rules of EN 1994-1-2, they are not similar in all the simulations. The numerical values of t_{fi} are high compared to the calculation of EN 1994-1-2. For considerably high concrete thicknesses, the composite slab has an unexposed side similar to a flat concrete slab.

The parameters that most affected the fire resistance of composite slabs according to the thermal insulation criterion were the thickness of the air gap and the thickness of the concrete screed above the steel deck. Considerably tall, the composite slab has an unexposed face similar to a flat concrete slab.

On the basis of the numerical results, new coefficients have been proposed for the calculation of the fire resistance tfi, depending on the effective thickness of the composite slab and the thickness of the air gap. In addition, new calculation methods have been proposed for the determination of the temperature of the steel components of the slab. These equations show good agreement with the numerical results.

The research related to the fire behaviour of structures is of great importance and complexity in the field of civil and construction engineering. Additional research shall be carried out in the future in order to complement the results of this work:

a) Influence of the thickness of the concrete of the ISO834 fire resistance of composite slabs
b) Conduct experimental fire tests with composite slabs with trapezoidal and re-entrant steel deck profile.
c) Experimentally verify the thermal material properties.

7.REFERENCES

[1]Fernando Freire Ribeiro"numerical simulation of composite slabs with steel deck under fire conditions"Polytechnic Institute of Bragança – IPB**,** july ,2019

[2] L. Calado and J. Santos, Steel-concrete composite structures [in portuguese]. Lisbon: IST press, 2010.

[3] X. Yu, Z. Huang, I. Burgess, and R. Plank, "Nonlinear analysis of orthotropic composite slabs in fire," Eng. Struct., vol. 30, pp. 67–80, 2008.

[4] M. A. H. Abdel-Halim, M. R. Hakmi, and D. C. O'Leary, "Fire resistance of composite floor slabs using a model fire test facility," Eng. Struct., vol. 21, no. 2, pp. 176–182, 1999.

[5] M. Gillie, A. Usmani, M. Rotter, and M. O'Connor, "Modelling of heated composite floor slabs with reference to the Cardington experiments," Fire Saf. J., vol. 36, no. 8, pp. 745–767, 2001.

[6] R. Hamerlinck, "The behaviour of fire-exposed composite steel/concrete slabs," Eindhoven University of Technology, 1991.

[7] J. Jiang, J. A. Main, J. M. Weigand, and F. H. Sadek, "Thermal performance of composite slabs with profiled steel decking exposed to fire effects," Fire Saf. J., vol. 95, no. May 2017, pp. 25–41, 2018.

[8] G. M. E. Cooke, R. M. Lawson, and G. M. Newman, "Fire resistance of composite deck slabs," Struct. Eng., vol. 66, no. 16, pp. 253–267, 1988.

[9] J. Jiang, J. A. Main, F. Sadek, and J. M. Weigand, "Numerical modeling and analysis of heat transfer in composite slabs with profiled steel decking," 2017.

[10] M. Crisinel and D. O'Leary, "Composite floor slab design and construction," Struct. Eng. Int., vol. 6, no. Special Issue 1, pp. 41–46, 1996.

[11] D. Pantousa and E. Mistakidis, "Advanced modeling of composite slabs with thin-walled steel sheeting submitted to fire," Fire Technol., vol. 49, no. 2, pp. 293–327, 2013.

[12] J. M. Davies and H. B. Wang, "Numerical temperature calculation for composite deck slabs exposed to fire," Trans. Eng. Sci., vol. 5, pp. 331–338, 1994.

[13] CEN - European Committee for Standardization, EN 1994-1-2: Design of composite steel and concrete structures - Part 1-2: General rules - Structural fire design. Brussels, 2005.

[14] ABNT NBR 14323: Structural fire design of steel and composite steel and concrete structures for buildings: ABNT/CB-002, 2013, p. 66.

[15] C. Both, J. H. H. Fellinger, and L. Twilt, “Shallow floor construction with deep composite deck: from fire tests to simple calculation rules,” Heron, vol. 42, no. 3, pp. 145–158, 1997.

[16] D. L. Logan, A first course in the Finite Element Method, 4th ed. Platteville: Thomson, 2007.

[17] PURKISS, J. Fire safety engineering, design of structures. Great Britain: Butterworth-Heinemann, 2007.

[18]CEN - European Committee for Standardization, EN 1993-1-2: Design of steel structures - Part 1-2: General rules - Structural fire design. Brussels, 2005.

[19] European Convention for Constructional Steelwork - Committee T3 - Fire Safety of Steel Structures, “Calculation of the fire resistance of composite concrete slabs with profiled steel sheet exposed to the standard fire,” Brussels, 1983.

[20] R. Hamerlinck and L. Twilt, “Fire resistance of composite slabs,” J. Constr. Steel Res., vol. 33, no. 94, pp. 71–85, 1995.

[21] CEN- European Committee for Standardization, EN 1994-1-1: Design of composite steel and concrete structures - Part 1-1: General rules and rules for buildings. Brussels: CEN - European Committee for Standardization, 2004.

[22] J.-M. Franssen, “Analysis of the fire behaviour of composite steel-concrete structures [in french],” University of Liège, 1987.

[23] CEN - European Committee for Standardization, EN 1991-1-2: Actions on structures - Part 1-2: General actions - Actions on structures exposed to fire. Brussels, 2002.

[24] P. A. G. Piloto, “Experimental and numerical analisys of metalic structures behaviour under fire conditions [in portuguese],” University of Porto, 2000.

[25] Y. A. Çengel and A. J. Ghajar, Heat and mass transfer: fundamentals & applications, Fifth edit. New York: McGraw-Hill Education, 2015.

[26] R. Regobello, “Numerical analysis of steel and composite steel-concrete cross sections and structural elements in fire situation [in portuguese],” University of São Paulo, 2007.

[27] J. P. Holman, Heat transfer, Tenth edit. New York: McGraw-Hill Education, 2010.J. P.

[28] Y. Wang, Steel and composite structures: behaviour and design for fire safety, vol. 1. London: Spon Press, 2002.

[29] CEN - European Committee for Standardization, EN 1992-1-2: Design of concrete structures - Part 1-2: General rules - Structural fire design. Brussels, 2004.

[30] S. Guo and C. G. Bailey, “Experimental behaviour of composite slabs during the heating and cooling fire stages,” Eng. Struct., vol. 33, pp. 563–571(2011)

[31] S. Lamont, A. S. Usmani, and D. D. Drysdale, “Heat transfer analysis of the composite slab in the Cardington frame fire tests,” Fire Saf. J., vol. 36, no. 8, pp. 815–839, 2001.

[32] A. K. Abu, “Behaviour of Composite Floor Systems in Fire,” The University of Sheffield, 2008.

[33] R. Hamerlinck and L. Twilt, “Fire resistance of composite slabs,” J. Constr. Steel Res., vol. 33, no. 94, pp. 71–85, 1995.

[34] A. H. Buchanan and A. K. Abu, Structural design for fire safety, Second Ed. Chichester, UK: John Wiley & Sons Ltd, 2017.

[35] C. Both, J. W. B. Stark, and L. Twilt, “Partial fire protection of composite slabs,” J. Constr. Steel Res., vol. 27, no. 1–3, pp. 143–158, 1993.

[36] G. M. Newman, J. T. Robinson, and C. G. Bailey, “Fire safe design: A new approach to multi-storey steel framed buildings,” Ascot, 2000.

[37]R. Hamerlinck and L. Twilt, “Fire resistance of composite slabs,” J. Constr. Steel Res., vol. 33, no. 94, pp. 71–85, 1995.

[38] MathWorks, “Partial Differential Equation Toolbox ™ User’s Guide R2019a,” Natick, MA, 2019.

[39] P. E. Gill and W. Murray, “Algorithms for the solution of the nonlinear least-squares problem,” SIAM J. Numer. Anal., vol. 15, no. 5, pp. 977–992, 1978.

[40] G. M. Newman, J. T. Robinson, and C. G. Bailey, “Fire safe design: A new approach to multi-storey steel framed buildings,” Ascot, 2000.

APPENDIXA:

TECHNICAL FILES FOR THE FIRST PARAMETRIC ANALYSES

Steel deck: Trapezoidal –Polydeck	**Natural Fire curve 1**
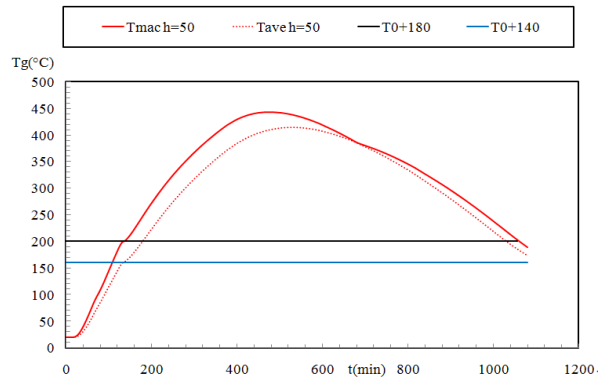	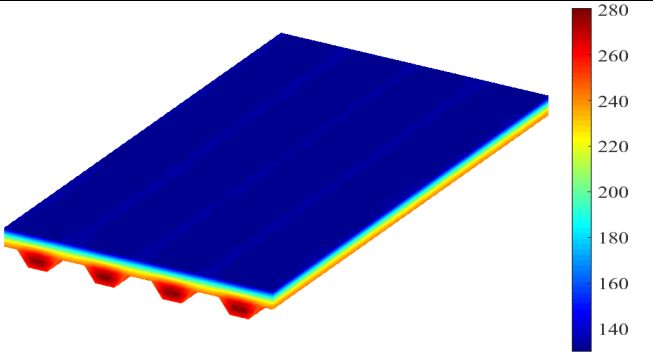 Slab1 h1=50mm Tmax=144 Tave=150
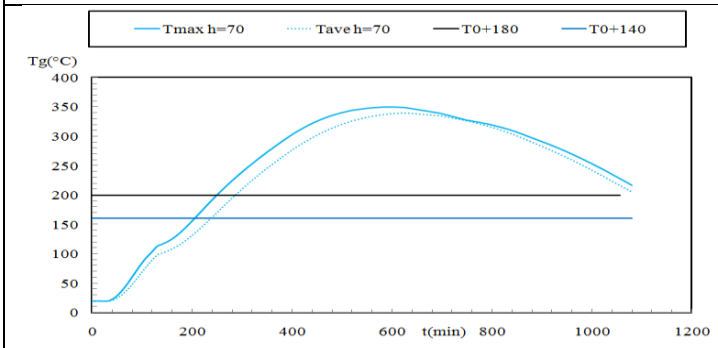	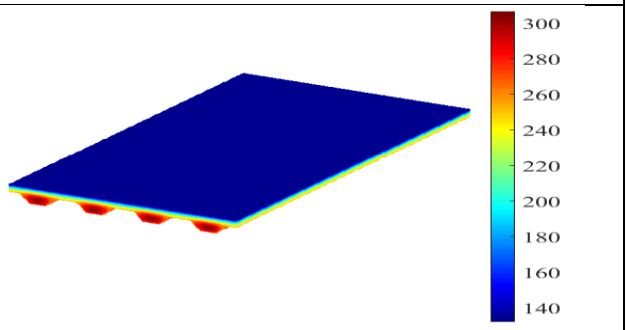 Slab2: h1=70mm Tmax=264 Tave=246min
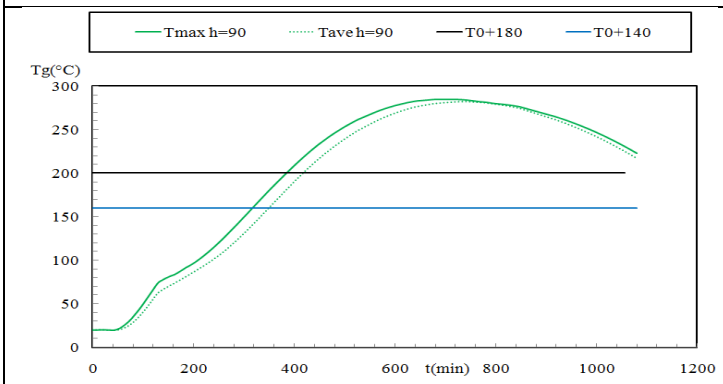	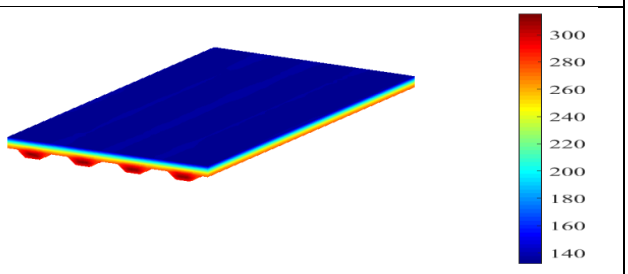 Slab3: h1=90mm Tmax=396Tave=366min
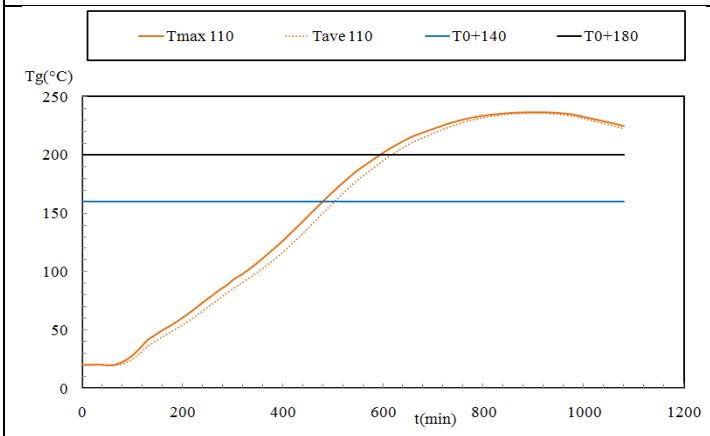	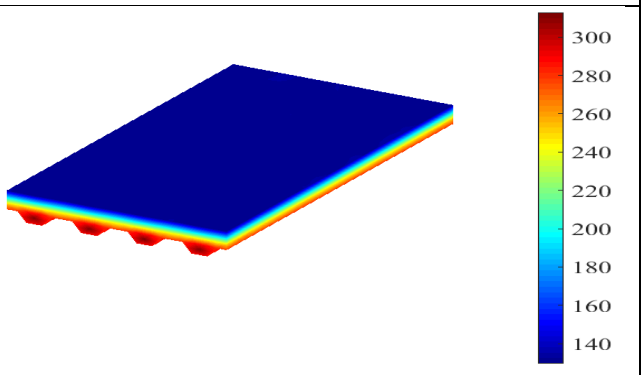 Slab4:h1=110mm Tmax=576 Tave=492min

Steel deck: Trapezoidal –Polydeck	**Natural Fire curve 1**
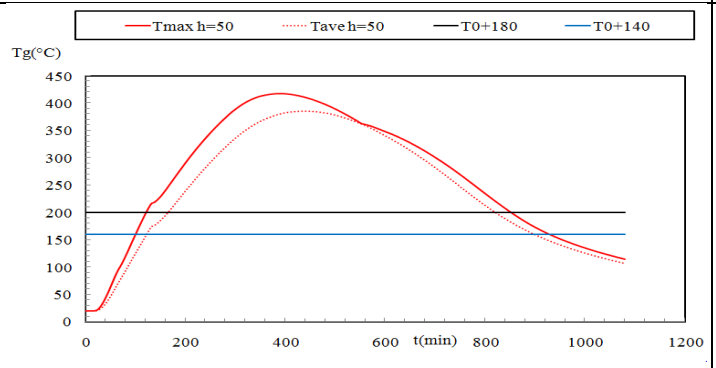	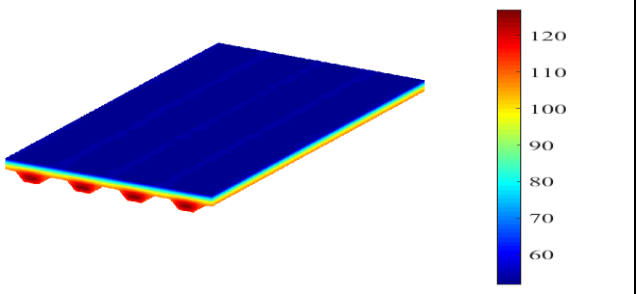 Slab 5:h1=50mm Tmax=108 Tave=108
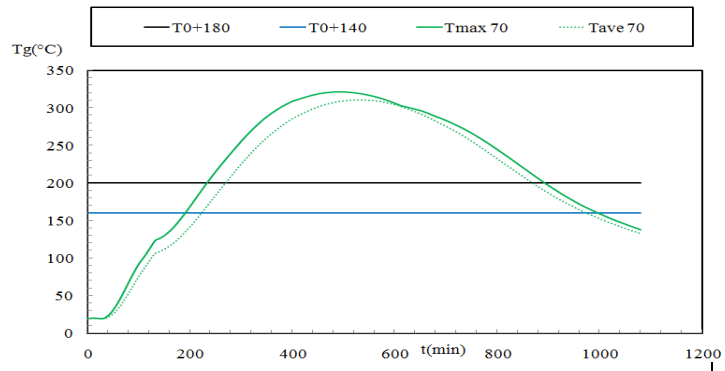	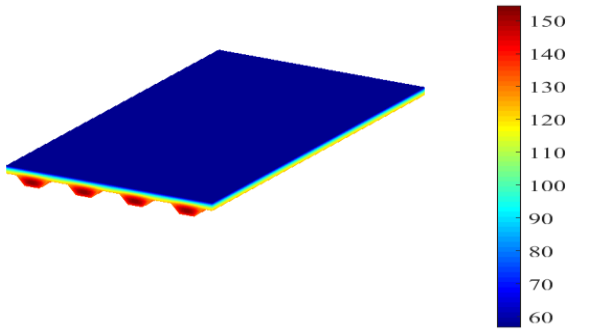 Slab6:h1=70mm Tmax=222 Tave=210min
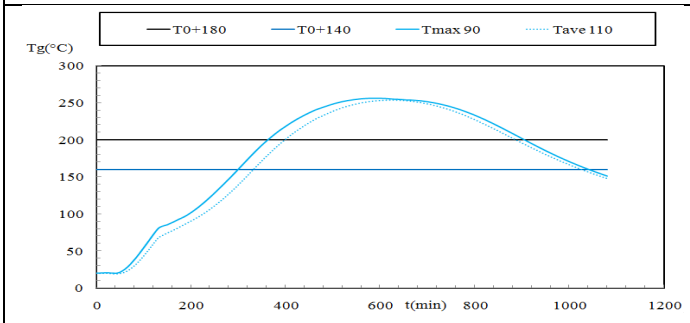	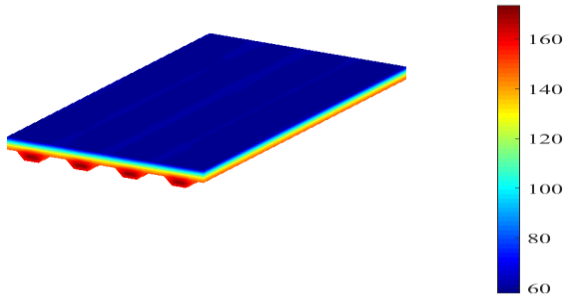 Slab7:h1=90mm Tmax=360 Tave=324min
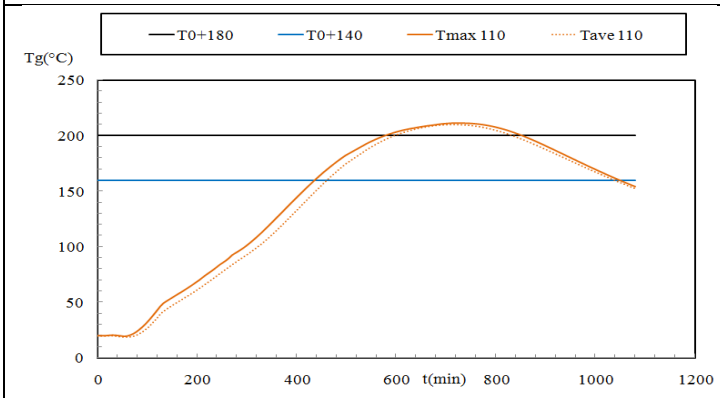	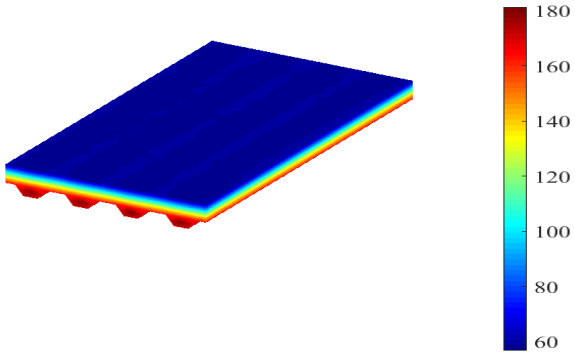 Slab8:h1=110mm Tmax=564 Tave=450min

Steel deck: Trapezoidal – ¨Polydeck	**Natural Fire curve 3**
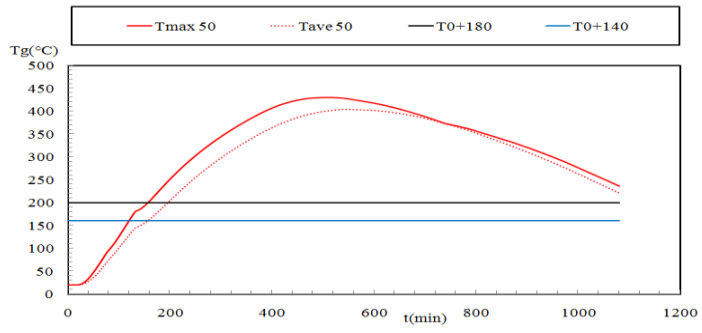	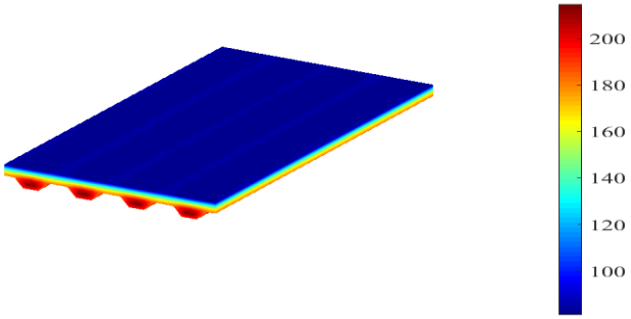 Slab 9:h1=50mm Tmax=120 Tave=120
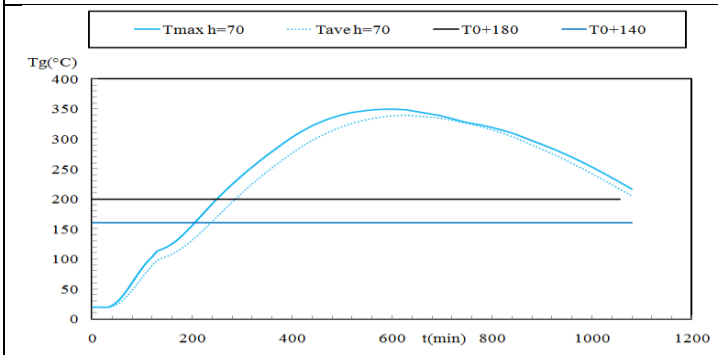	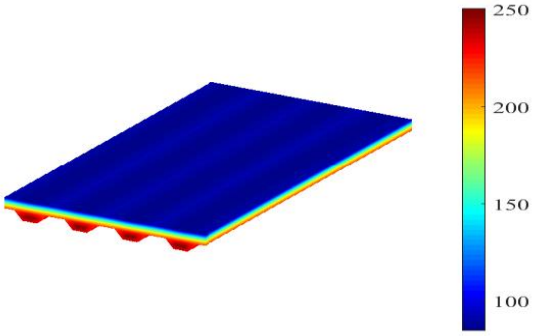 Slab10:h1=70mm Tmax=240 Tave=228 min
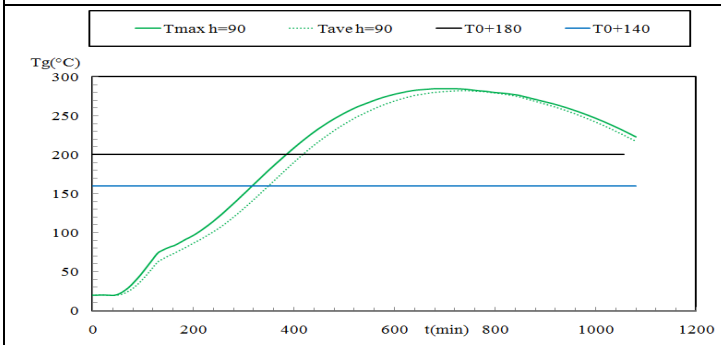	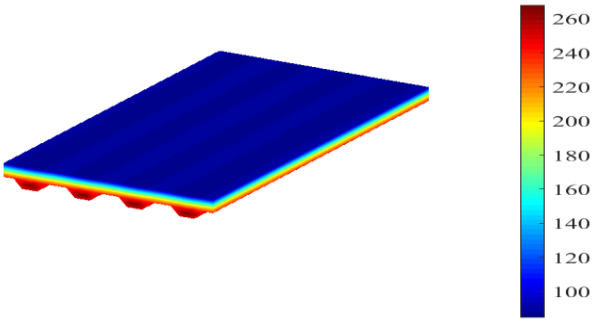 Slab11:h1=90mm Tmax=378Tave=342 min
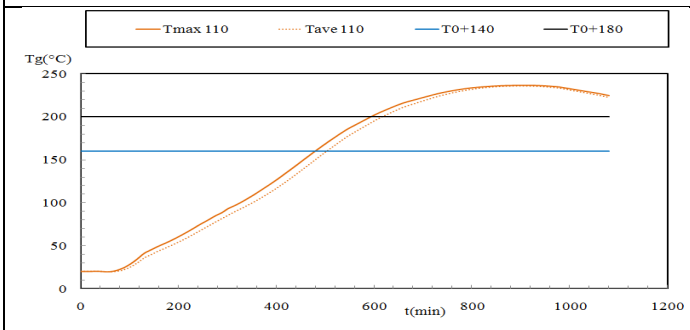	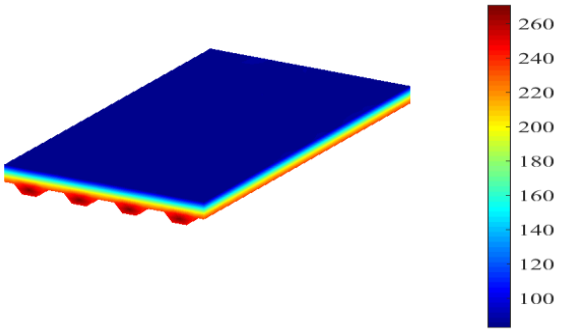 Slab12:h1=110mm Tmax=552 Tave=474 min

Steel deck: Trapezoidal – Polydeck	**Natural Fire curve 4**
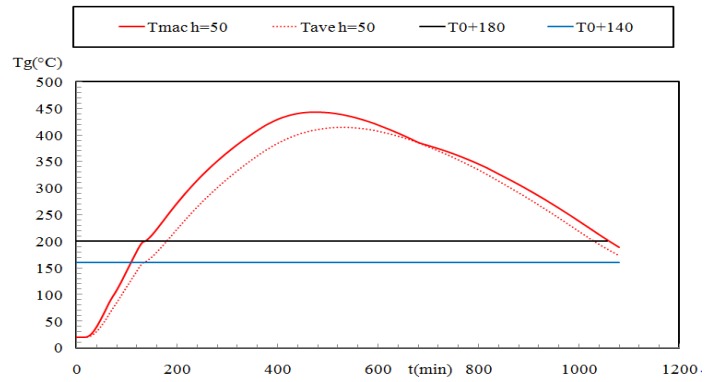	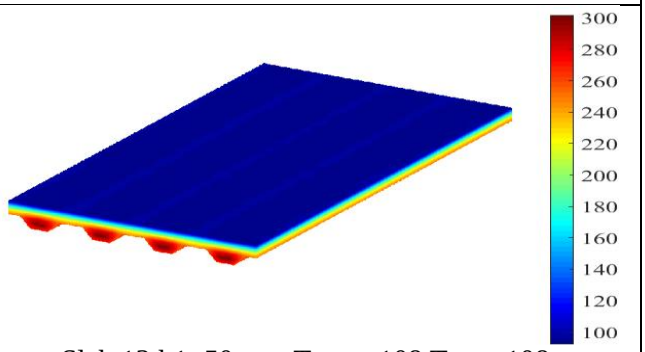 Slab 13:h1=50mm Tmax=108 Tave=108
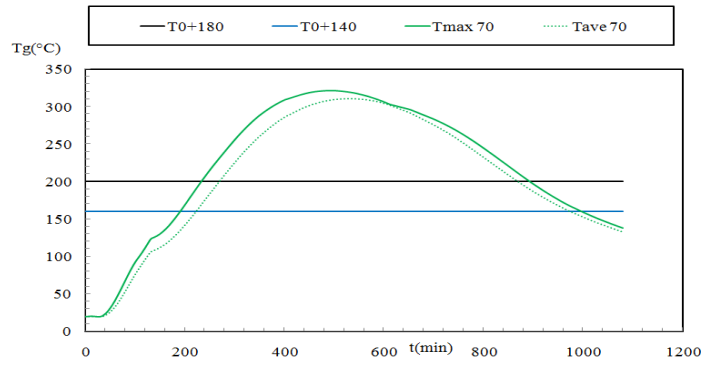	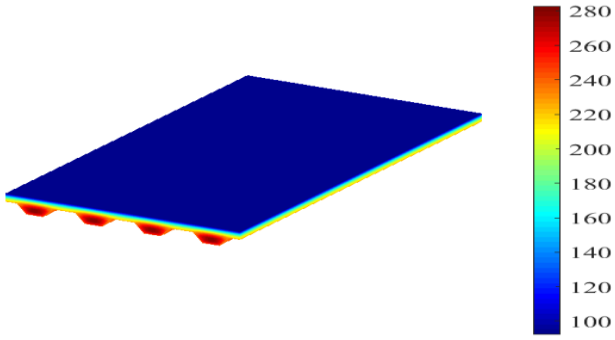 Slab14:h1=70mm Tmax=222 Tave=210min
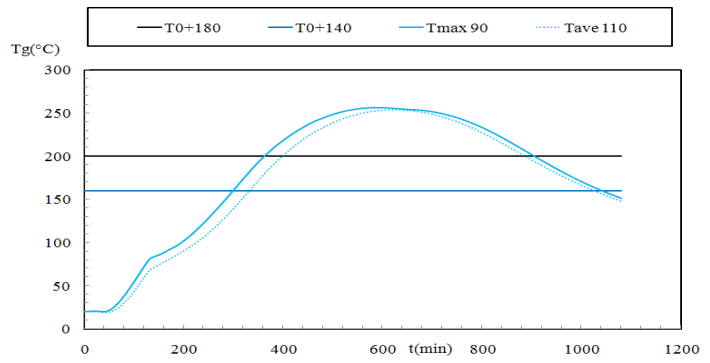	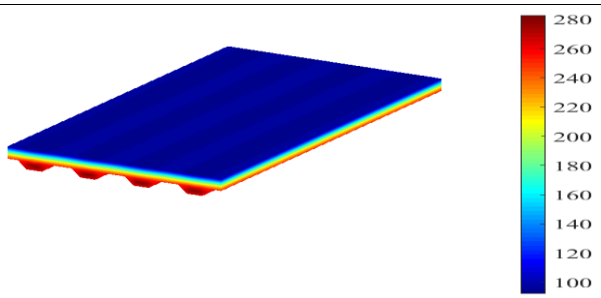 Slab15:h1=90mm Tmax=348Tave=318min
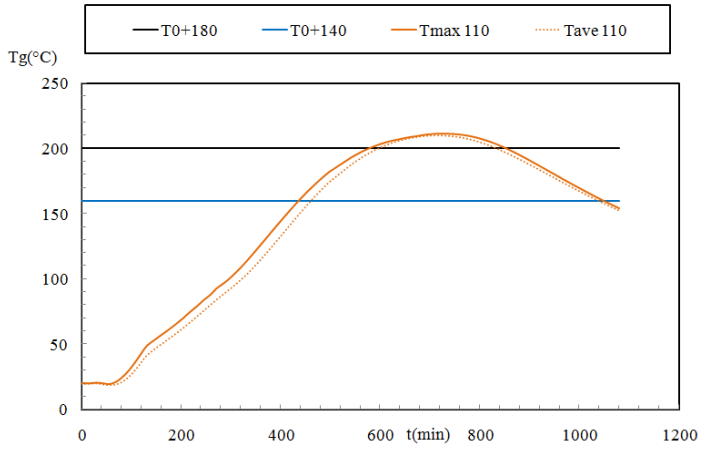	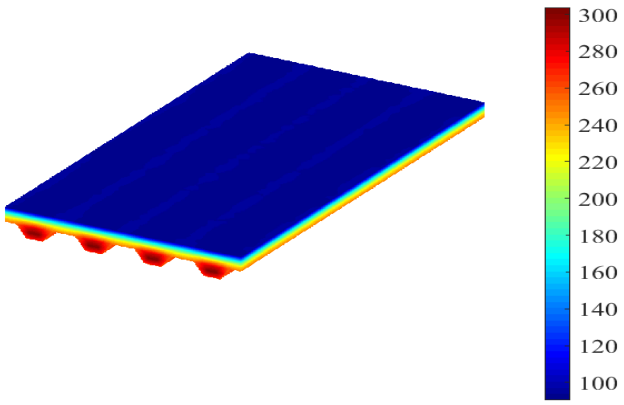 Slab16:h1=110mm Tmax=510 Tave=444min

Steel deck: Trapezoidal – ¨Polydeck	**Natural Fire curve 5**
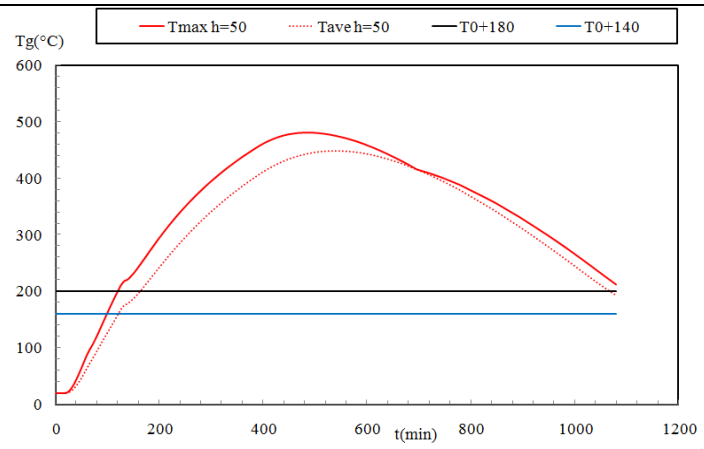	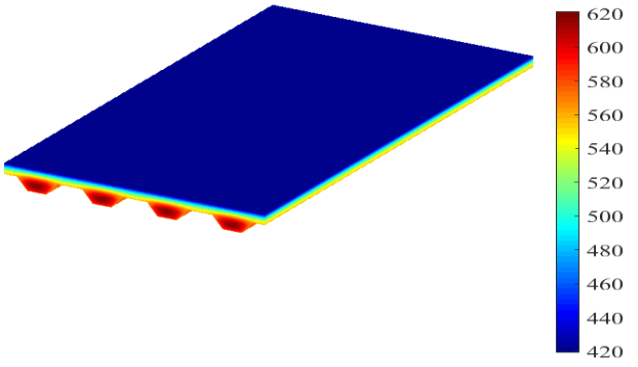 Slab 17:h1=50mm Tmax=156 Tave=156
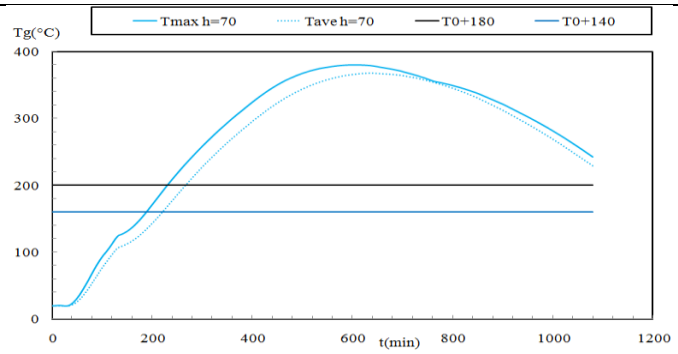	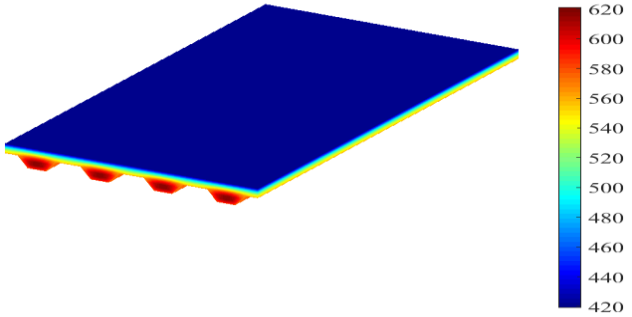 Slab18:h1=70mm Tmax=270 Tave=252min
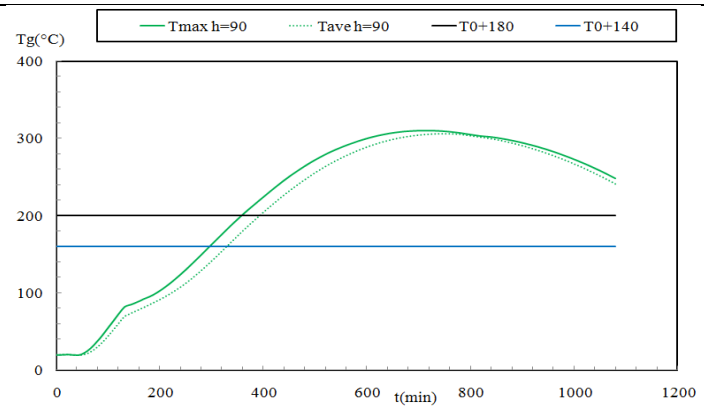	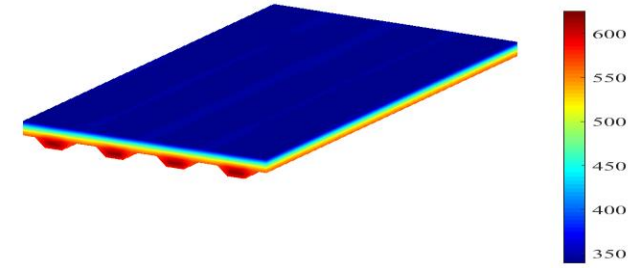 Slab19:h1=90mm Tmax=414 Tave=372min
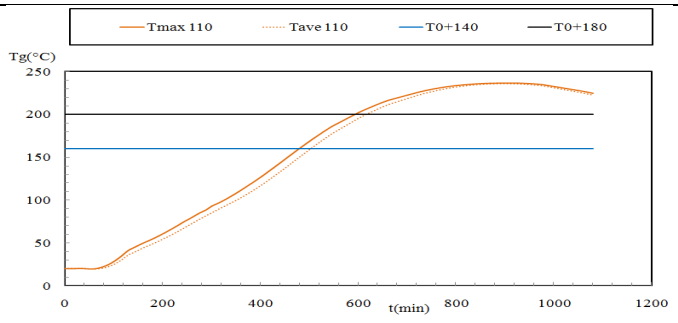	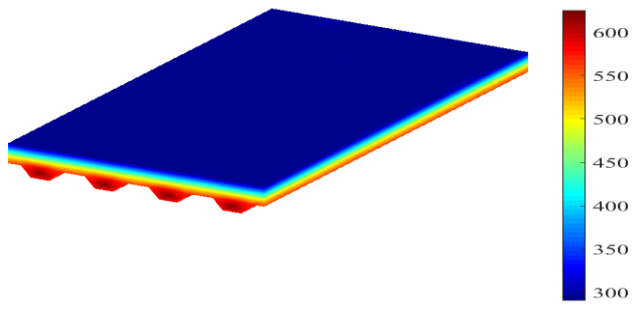 Slab20:h1=110mm Tmax=594 Tave=498min

Steel deck: Trapezoidal –Polydeck	**Natural Fire curve 6**
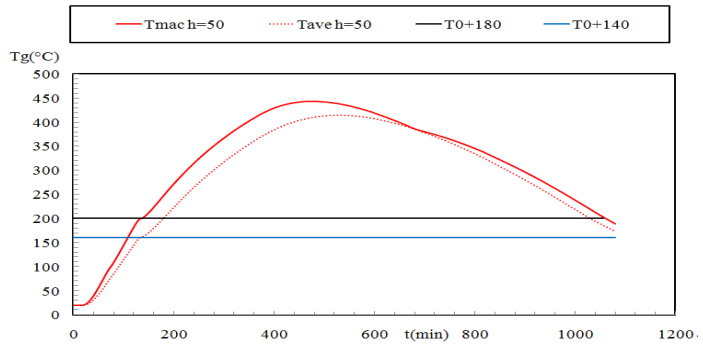	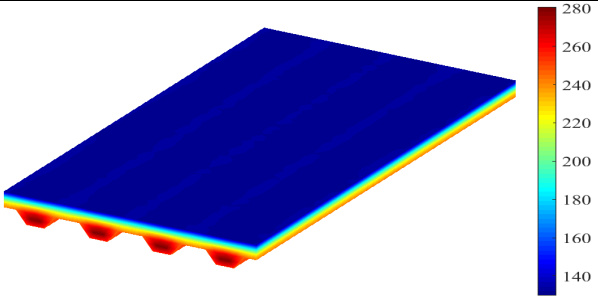 Slab 21:h1=50mm Tmax=120 Tave=148
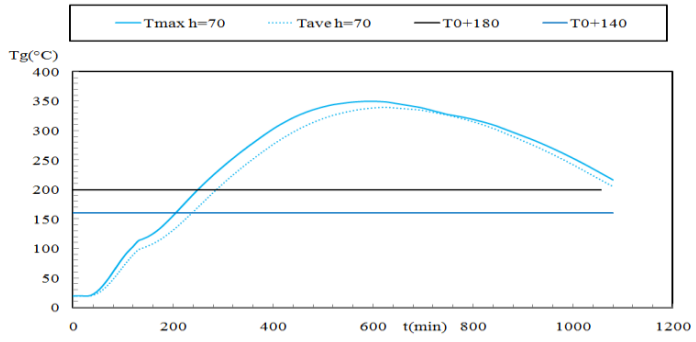	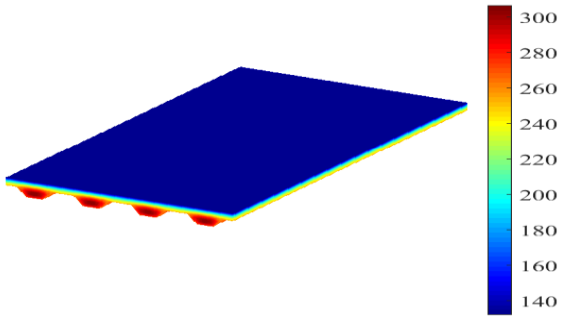 Slab22:h1=70mm Tmax=258 Tave=246min
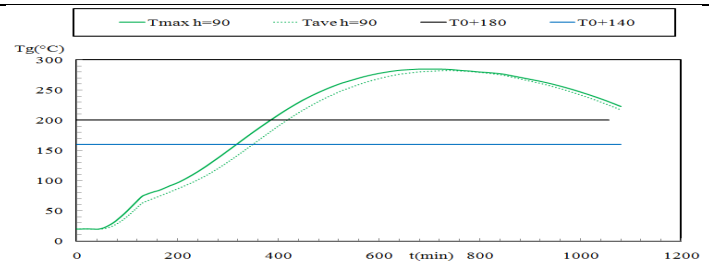	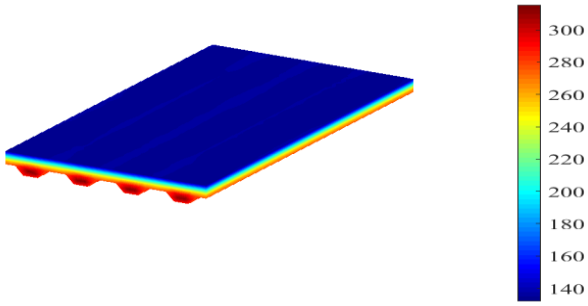 Slab23=90mm Tmax=396Tave=360min
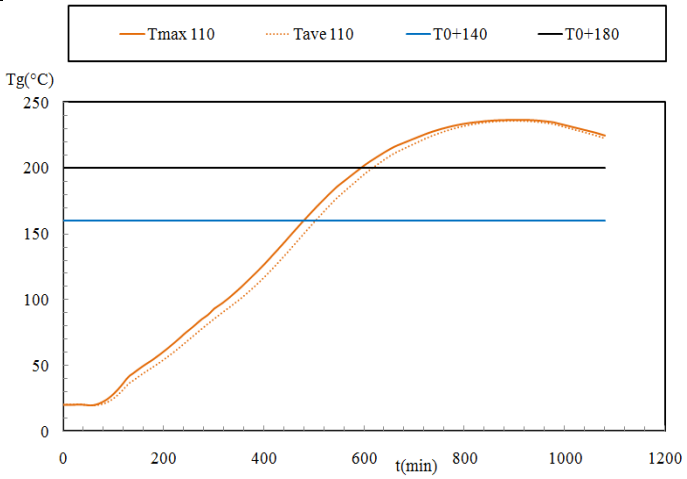	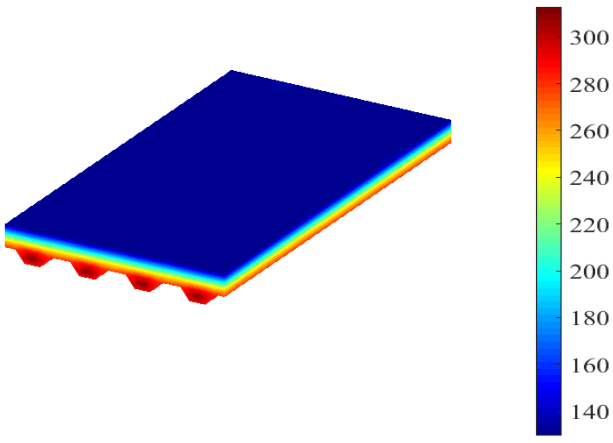 Slab24:h1=110mm Tmax=582 Tave=486min

Steel deck: Trapezoidal – cofraplus	**Natural Fire curve 1**
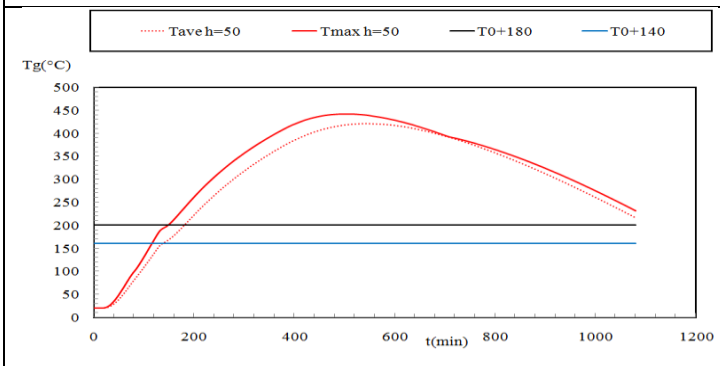	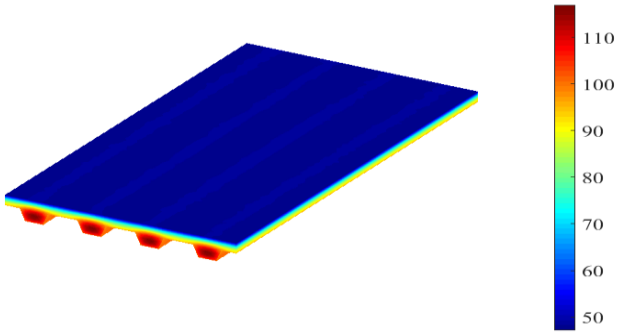 Slab25:h1=50mm Tmax=144Tave=126min
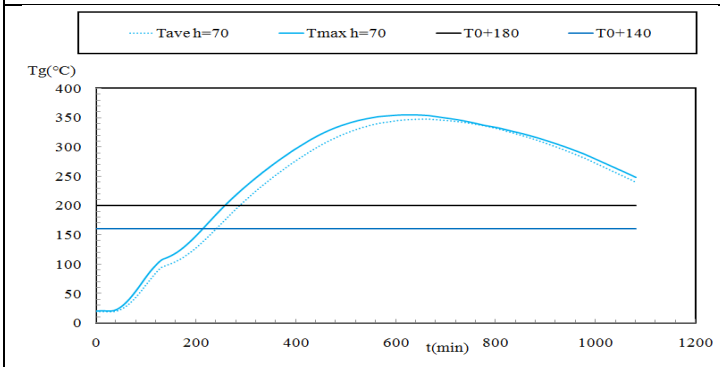	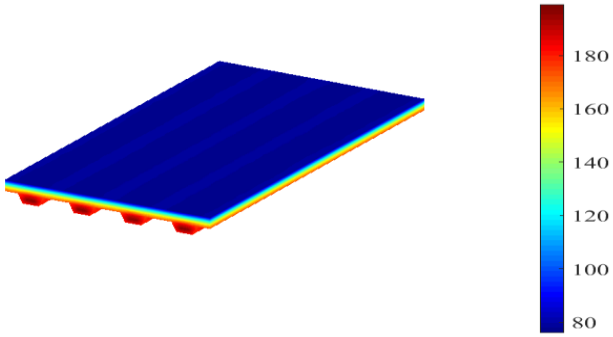 Slab26:h1=70mm Tmax=252Tave=228min
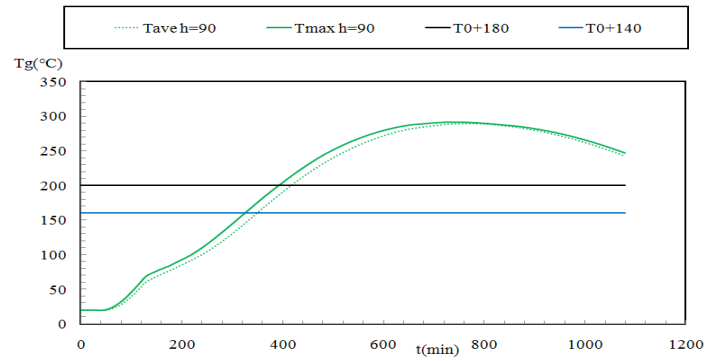	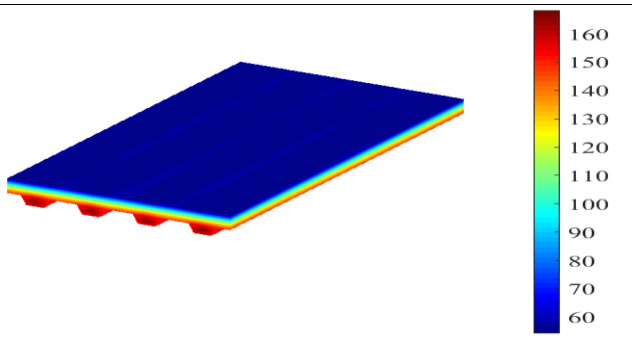 Slab27:h1=90mm Tmax=390Tave=342min
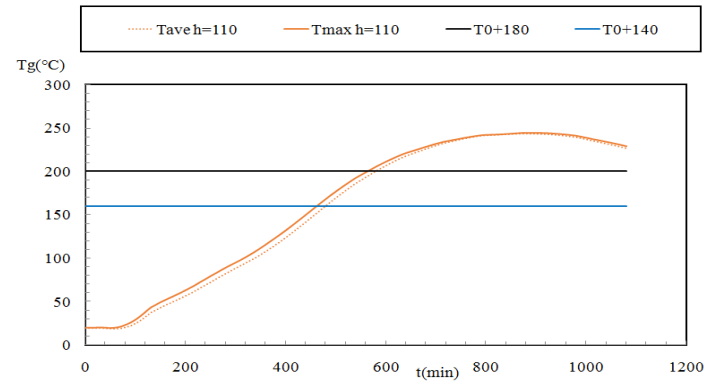	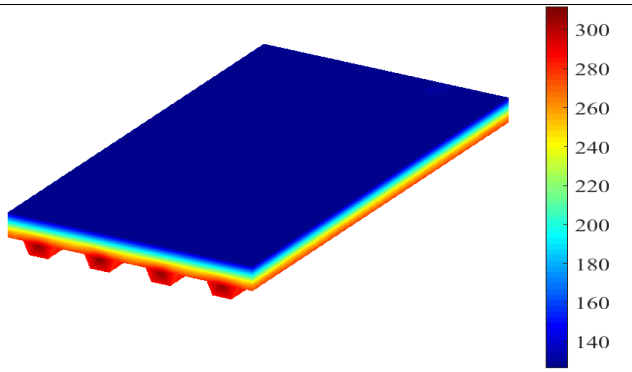 Slab 28:h1=110mm Tmax=558Tave=474

Steel deck: Trapezoidal – cofraplus	**Natural Fire curve 2**
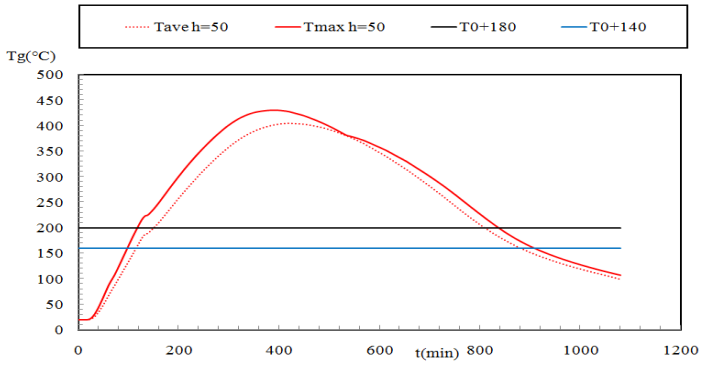	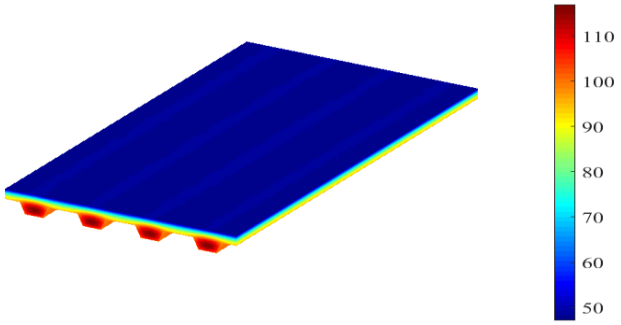 Slab29:h1=50mm Tmax=108 Tave=102min
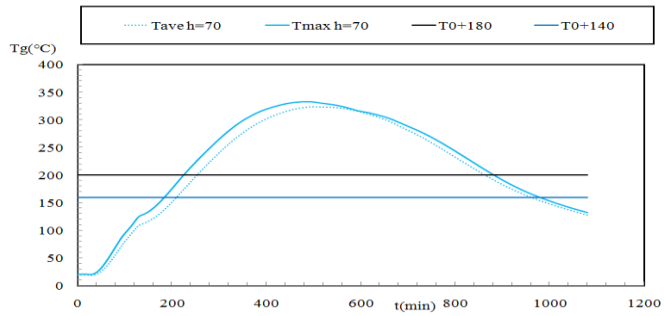	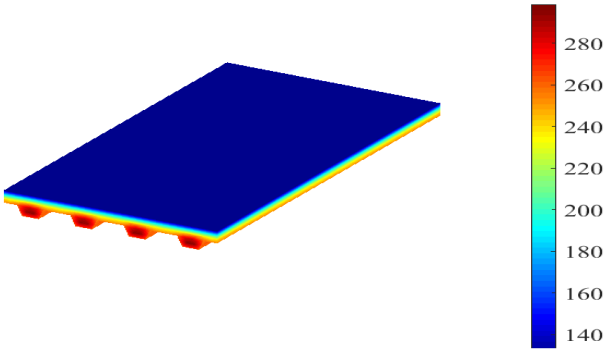 Slab30:h1=70mm Tmax=210 Tave=198 min
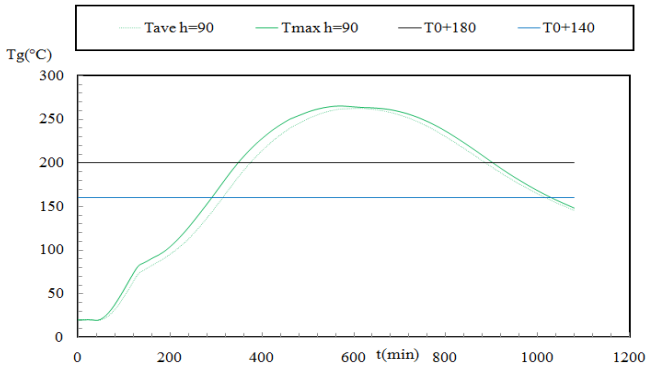	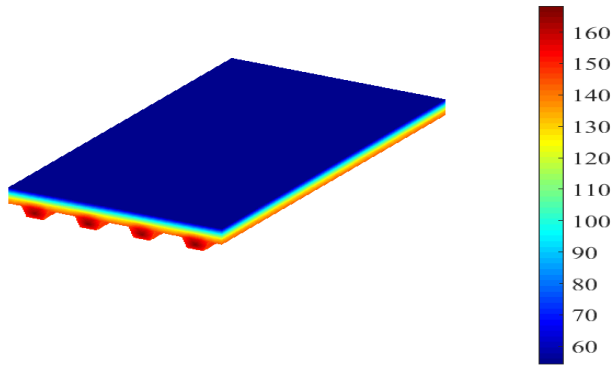 Slab31:h1=90mm Tmax=336 Tave=306
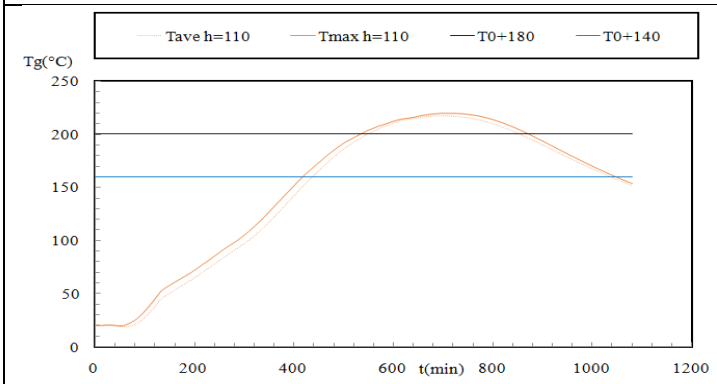	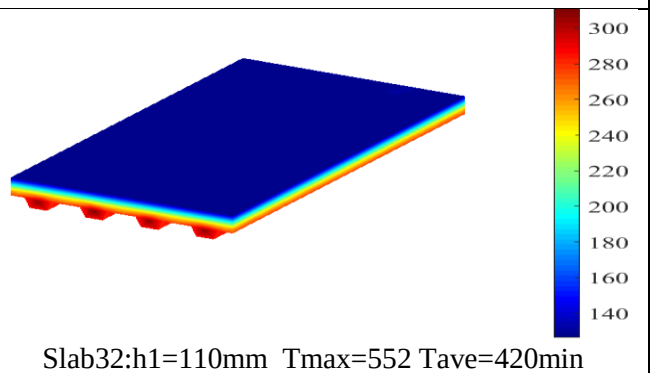 Slab32:h1=110mm Tmax=552 Tave=420min

Steel deck: Trapezoidal – cofraplus	**Natural Fire curve 3**
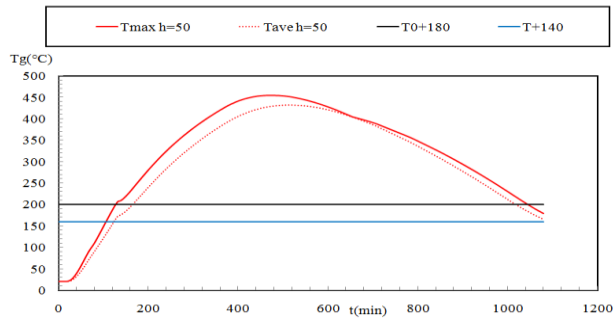	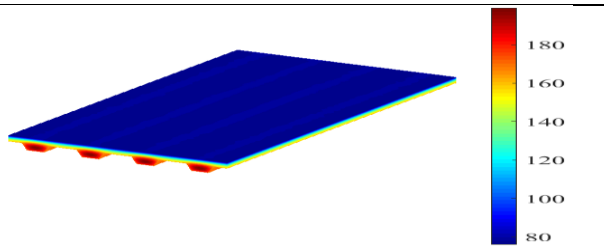 Slab33:h1=50mm Tmax=120 Tave=114 min
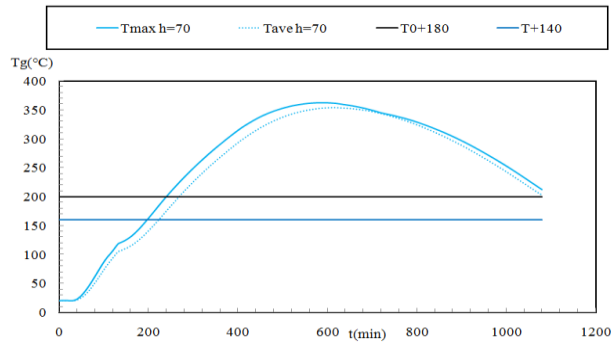	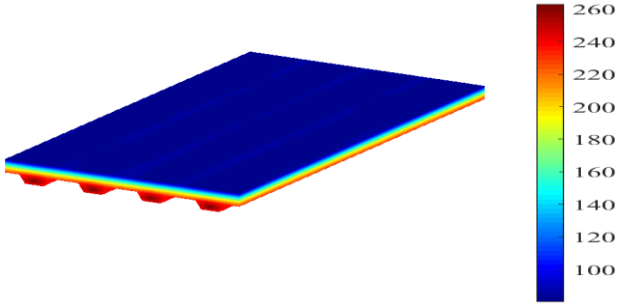 Slab34:h1=70mm Tmax=234Tave=216 min
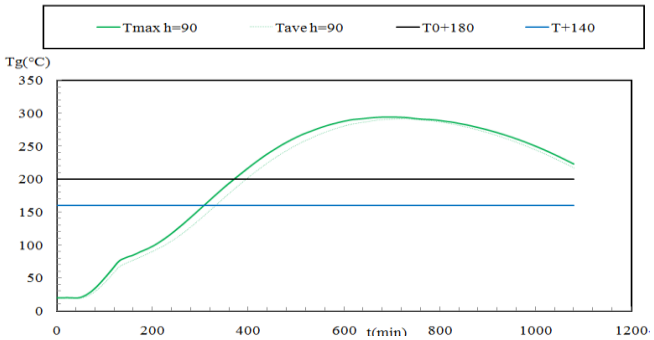	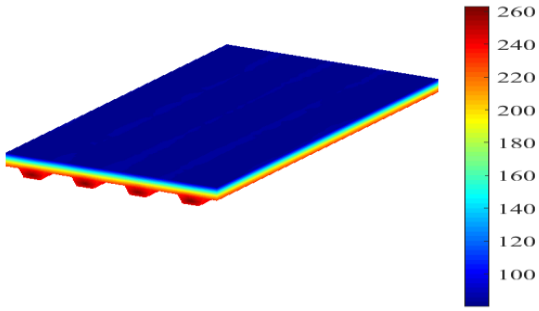 Slab 35:h1=90mm Tmax=360 Tave=324min
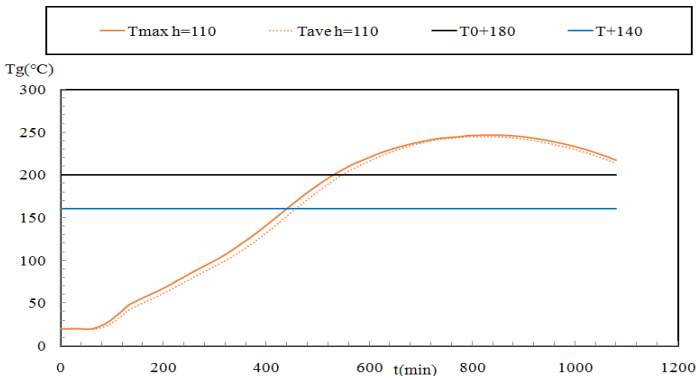	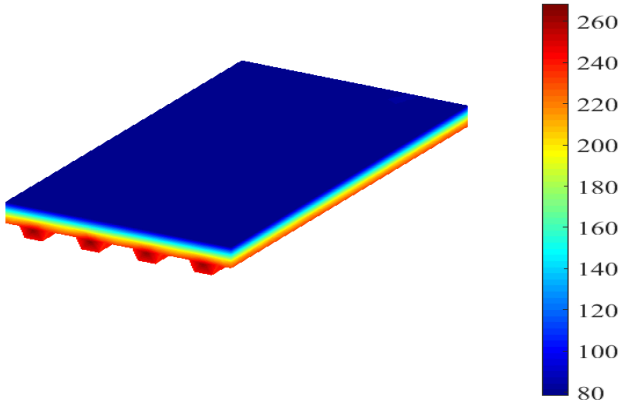 Slab 36:h1=90mm Tmax=522 Tave=444min

Steel deck: Trapezoidal – cofraplus	**Natural Fire curve 4**
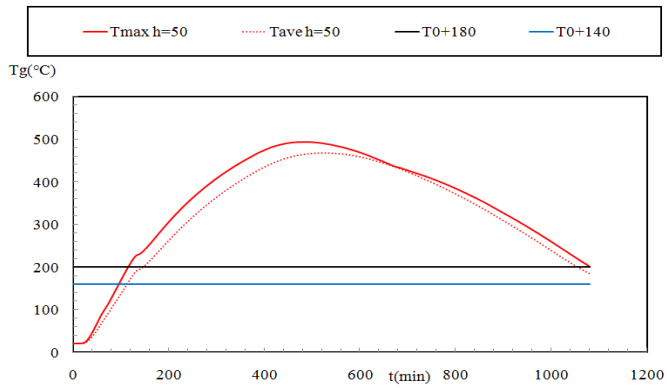	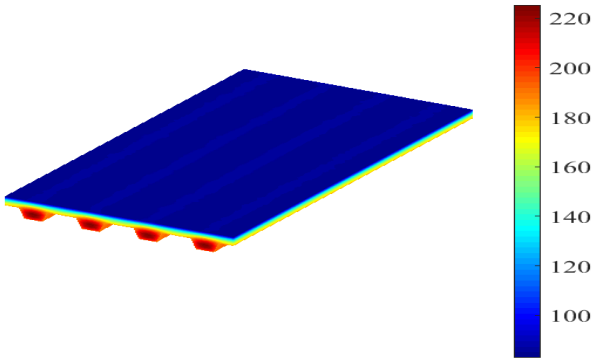 Slab37:h1=50mm Tmax=108Tave=102min
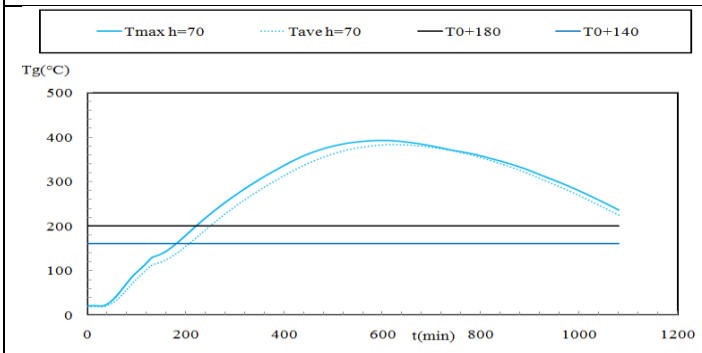	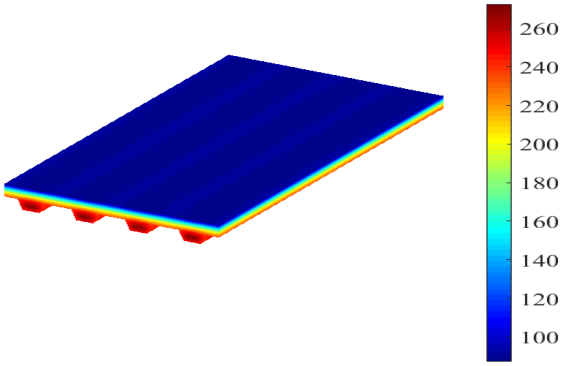 Slab38:h1=70mm Tmax=210 Tave=198 min
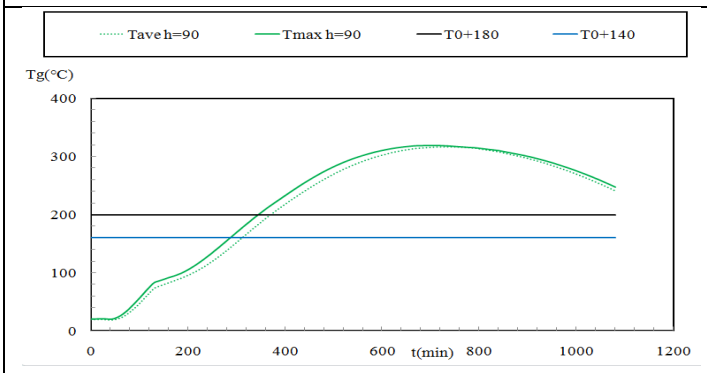	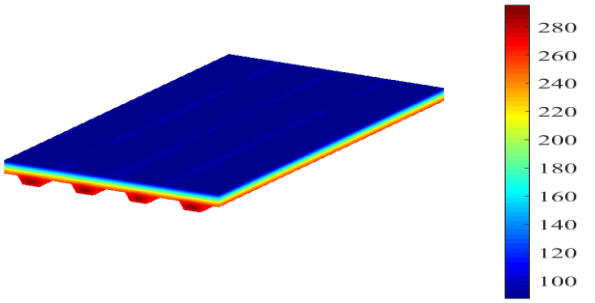 Slab39:h1=90mm Tmax=336 Tave=300 min
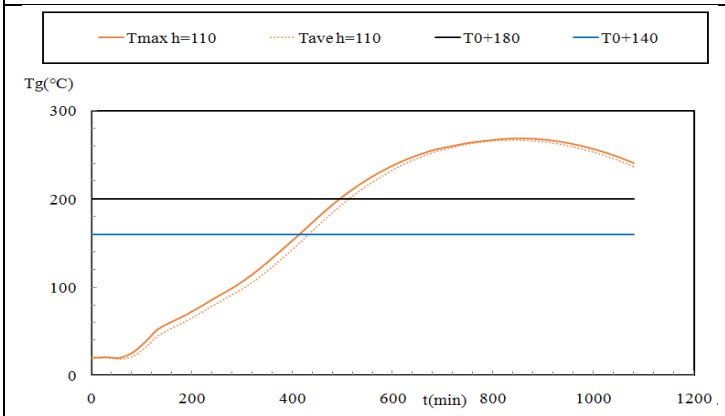	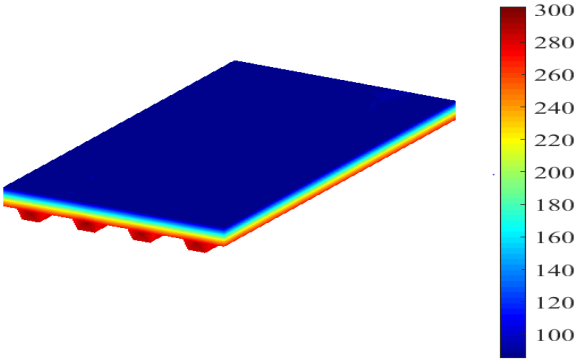 Slab40:h1=110mm Tmax=486 Tave=426 min

Steel deck: Trapezoidal – cofraplus	**Natural Fire curve 5**
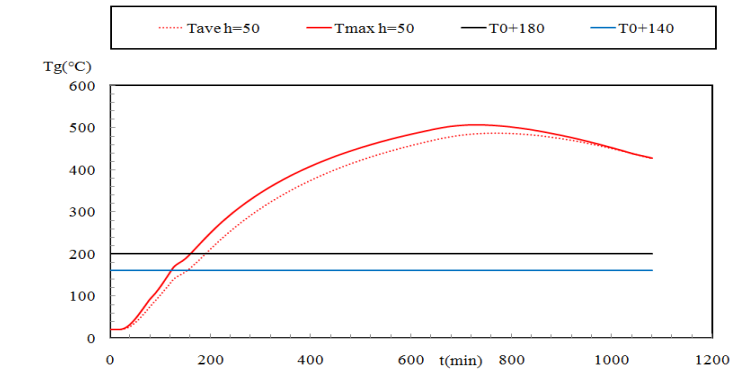	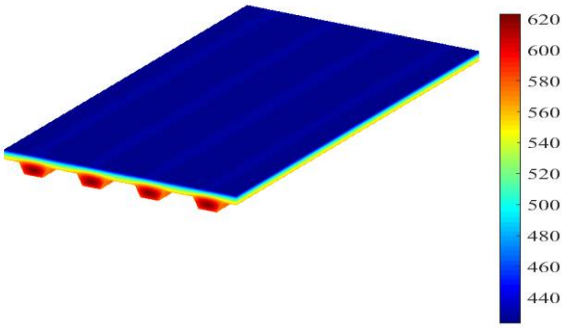 Slab41:h1=50mm Tmax=150Tave=144min
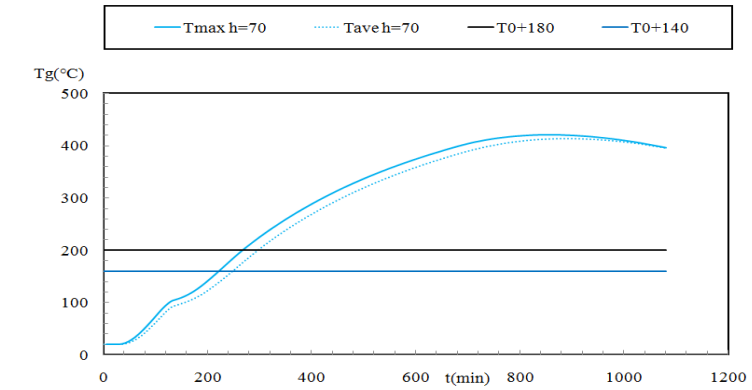	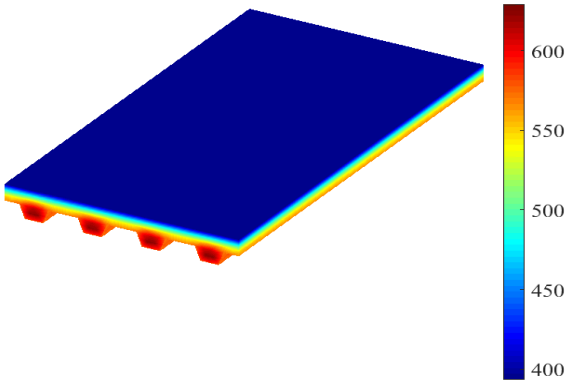 Slab42:h1=70mm Tmax=258Tave=244min
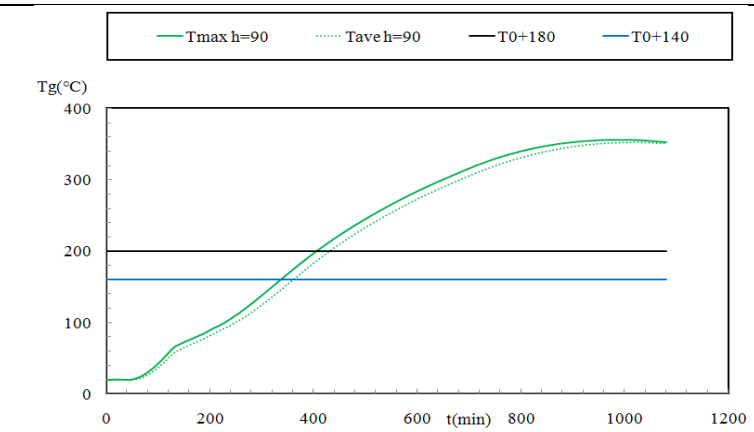	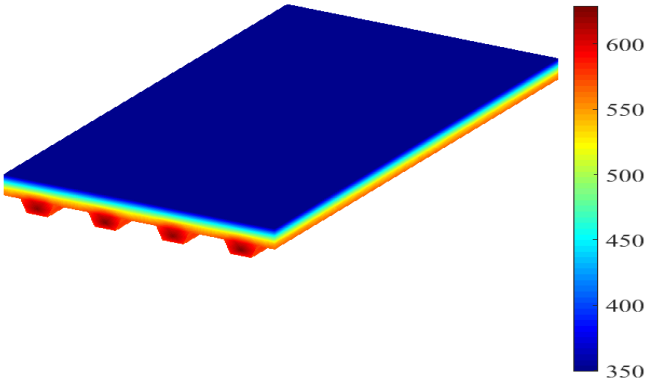 Slab43:h1=90mm Tmax=396 Tave=348min
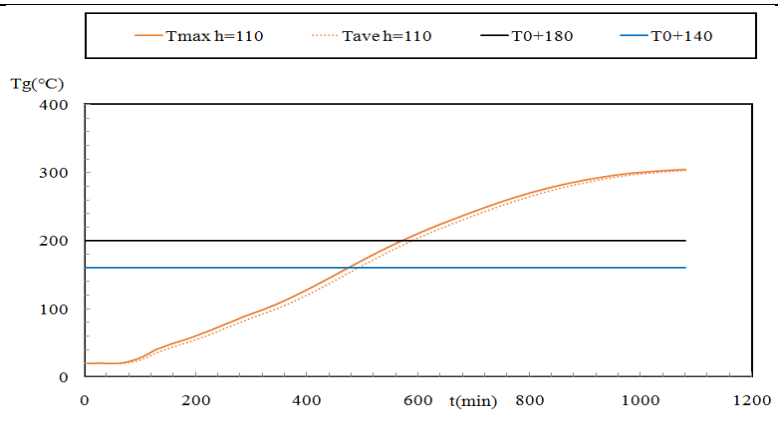	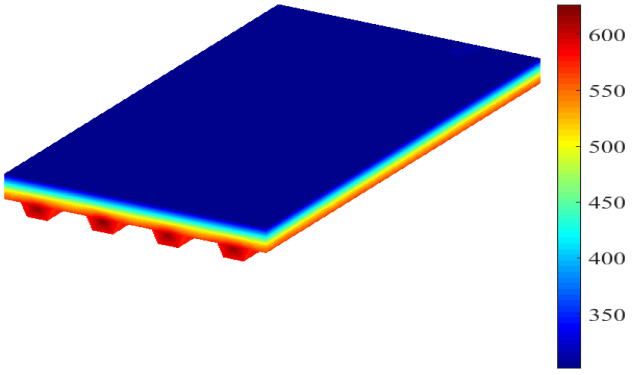 Slab44:h1=110mm Tmax=558Tave=480min

Steel deck: Trapezoidal – cofraplus	**Natural Fire curve 6**
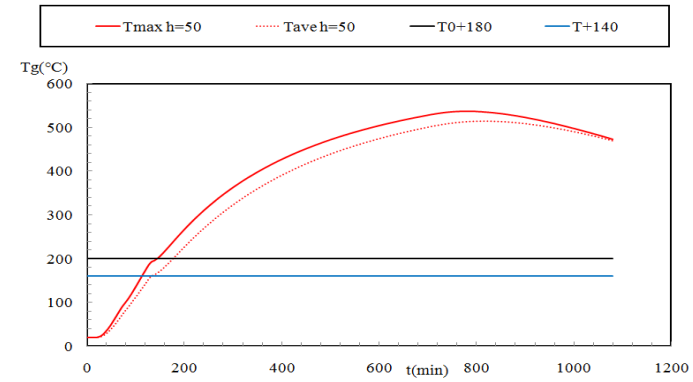	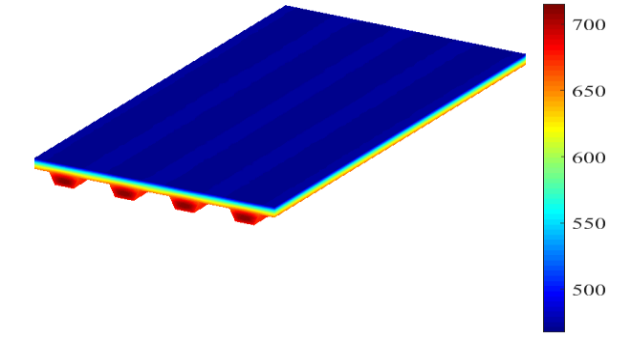 Slab45:h1=50mm Tmax=138 Tave=120min
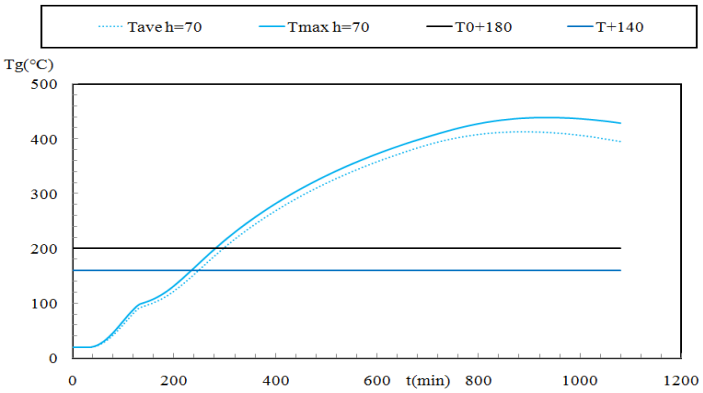	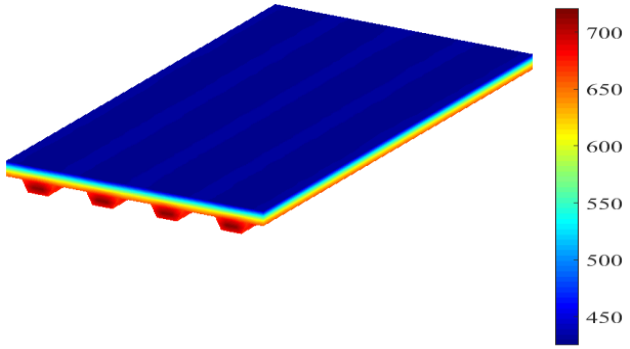 Slab46:h1=70mm Tmax=276 Tave=240min
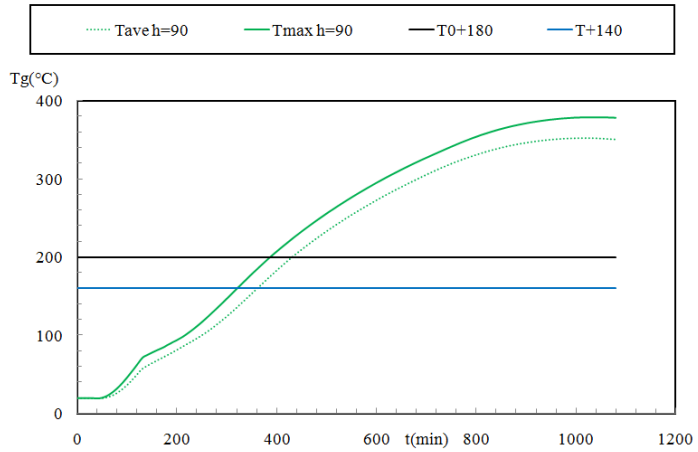	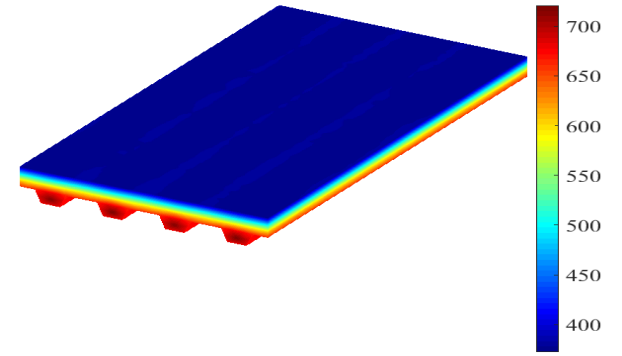 Slab47:h1=90mm Tmax=378 Tave=348min
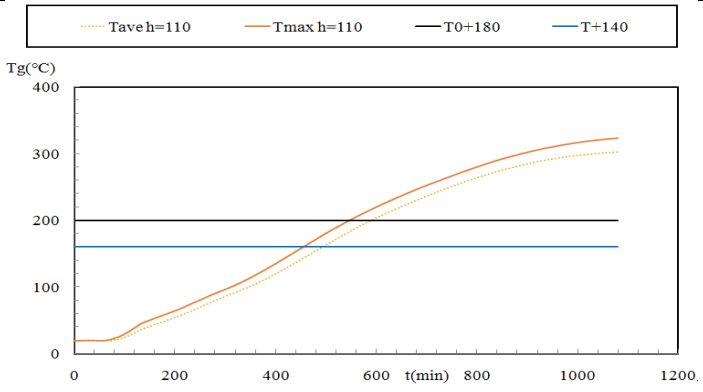	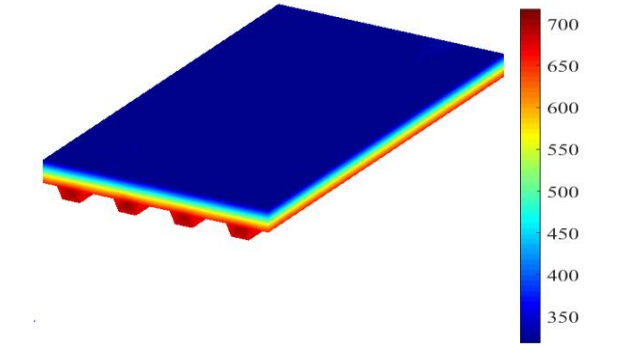 Slab48:h1=110mm Tmax=534 Tave=480min

Steel deck: -multideck	**Natural Fire curve 1**
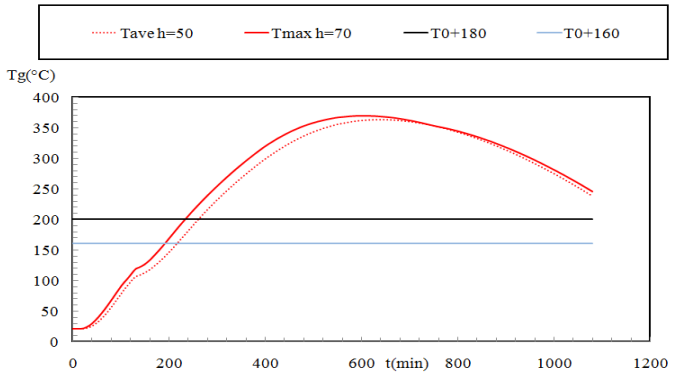	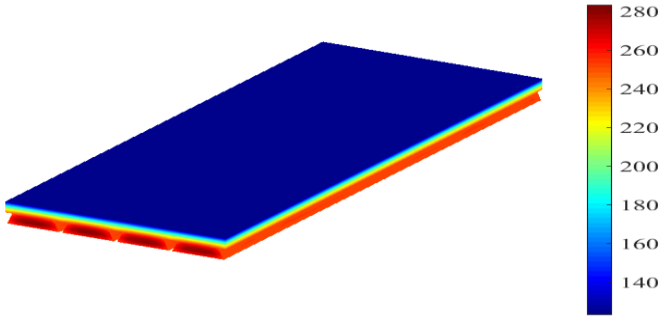 Slab49:h1=50mm Tmax=228 Tave=210min
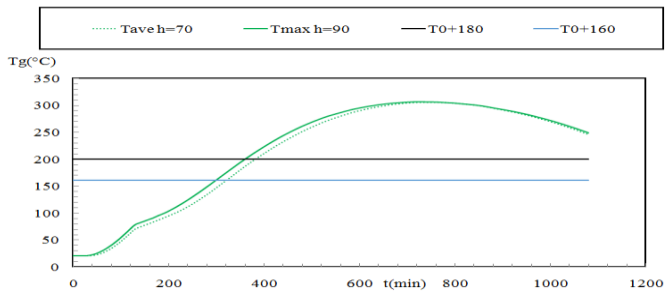	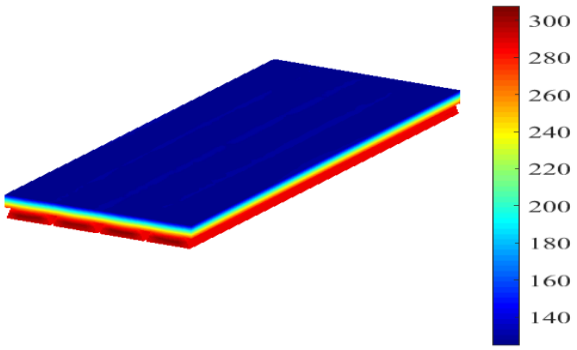 Slab50:h1=70mm Tmax=354 Tave=312min
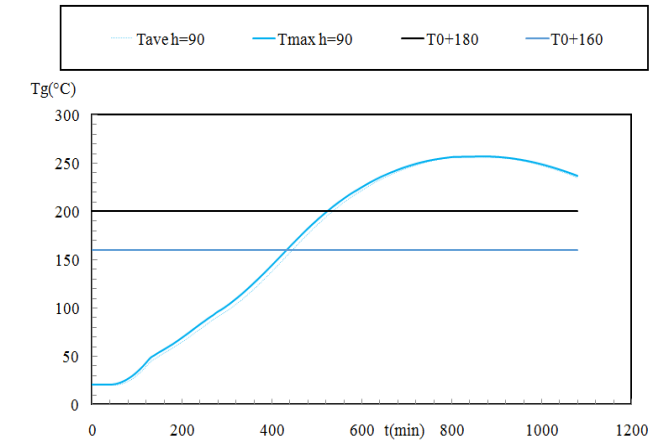	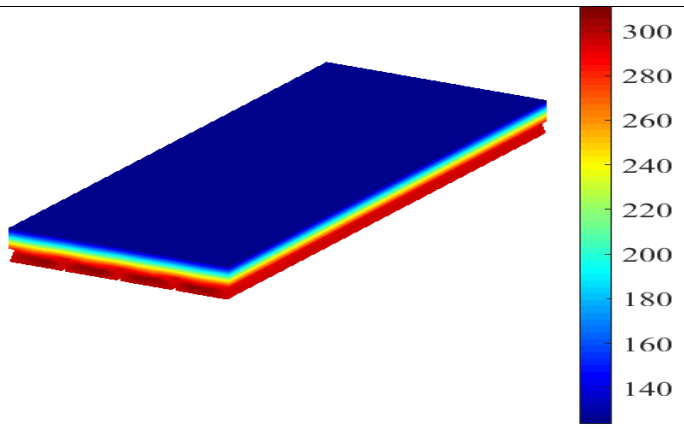 Slab51:h1=90mm Tmax=516 Tave=438min
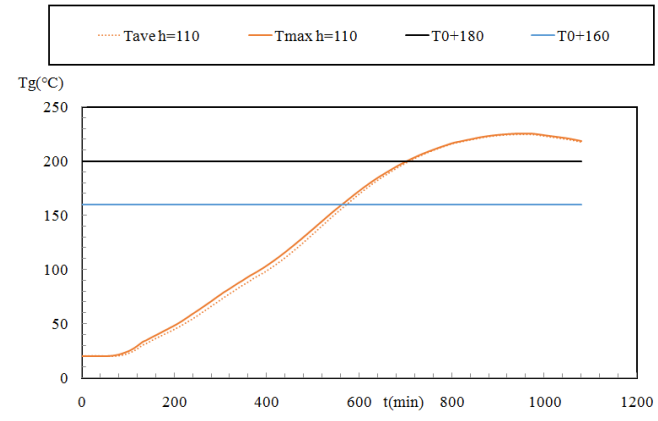	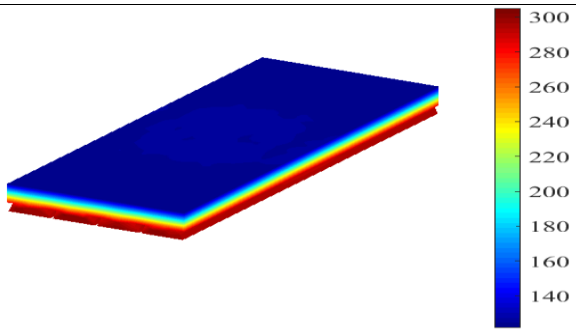 Slab52:h1=90mm Tmax=690 Tave=564min

Steel deck: -multideck	**Natural Fire curve 2**
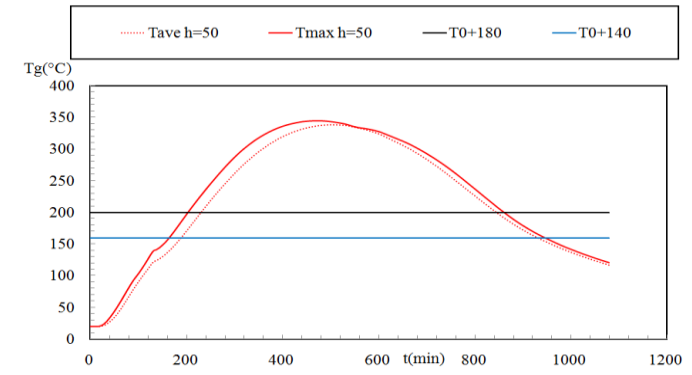	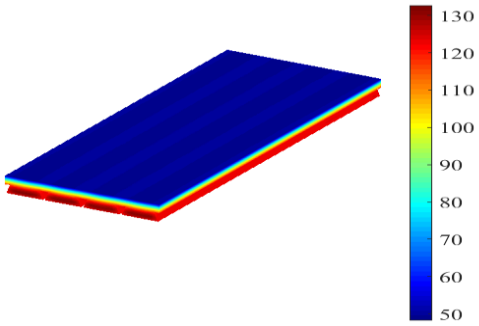 Slab53:h1=50mm Tmax=192 Tave=182min
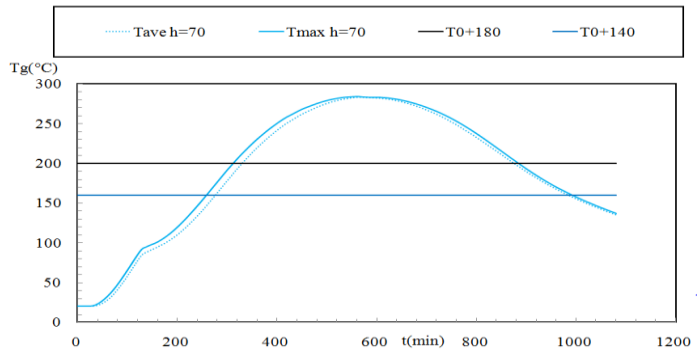	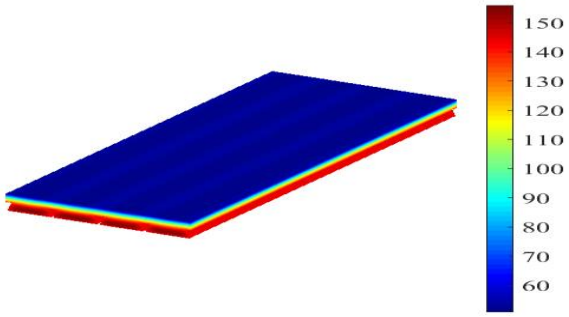 Slab54:h1=70mm Tmax=306 Tave=270min
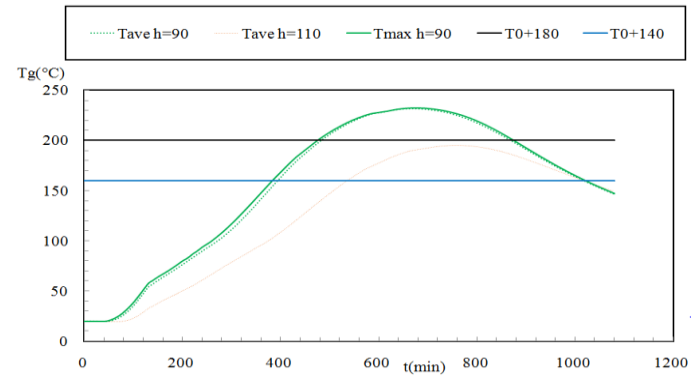	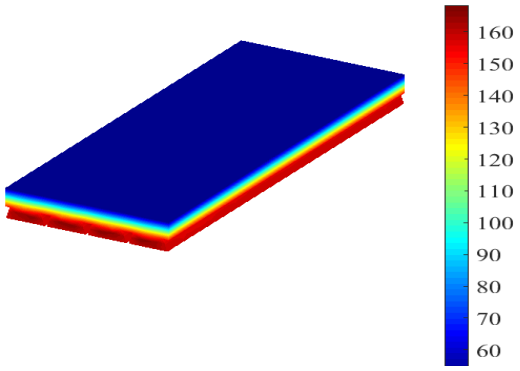 Slab55:h1=90mm Tmax=468 Tave=390min
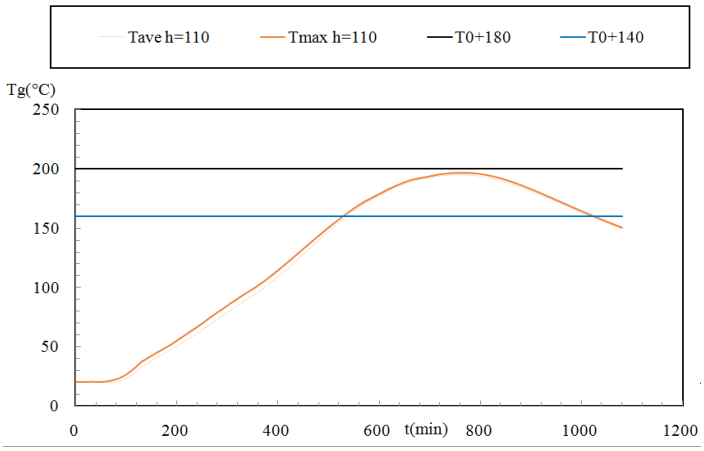	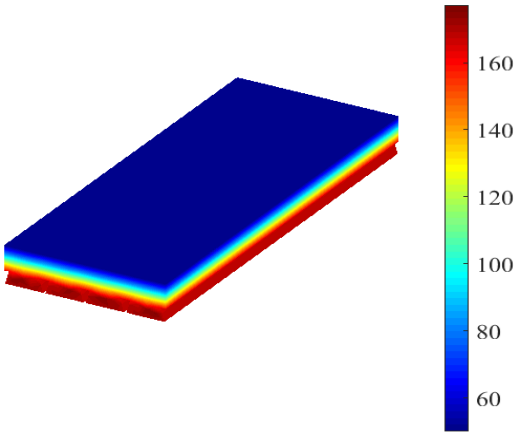 Slab56:h1=110mm Tave=528min

Steel deck: multideck	**Natural Fire curve 3**
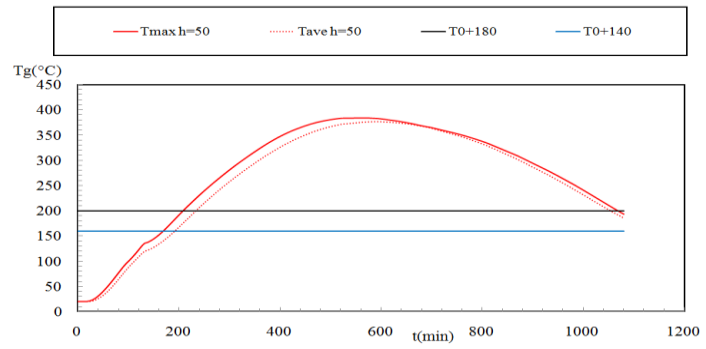	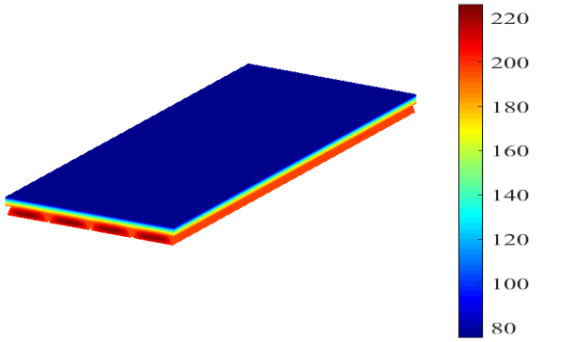 Slab57:h1=50mm Tmax=198 Tave=168min
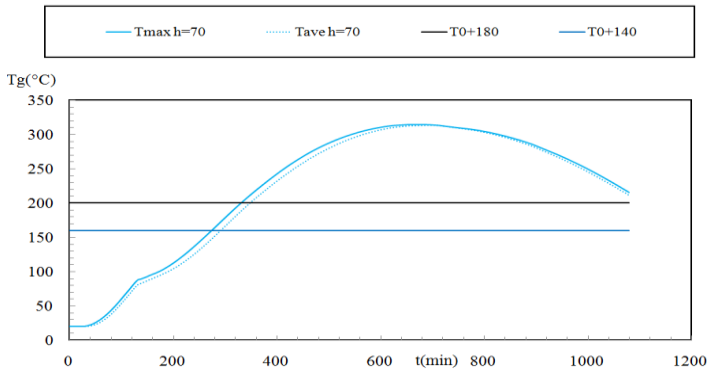	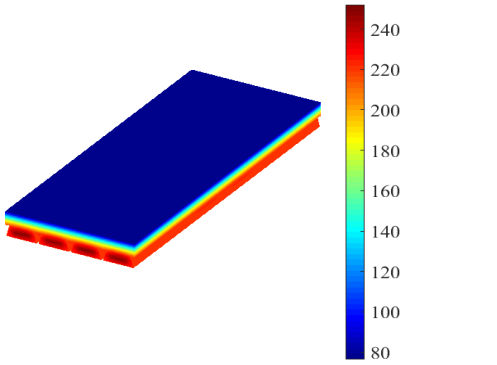 Slab58:h1=70mm Tmax=324 Tave=264min
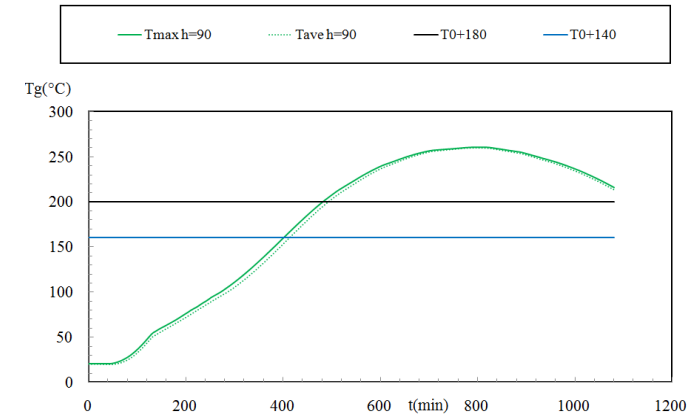	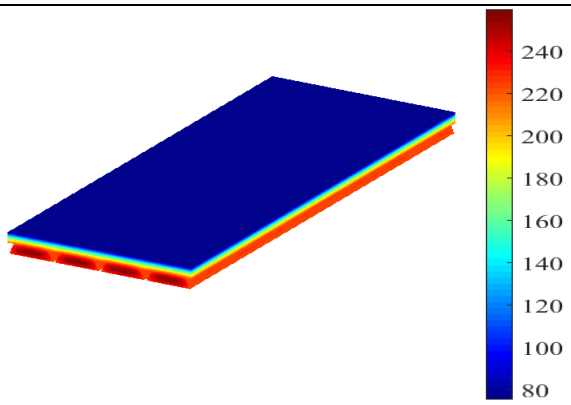 Slab59:h1=90mm Tmax=474Tave=402min
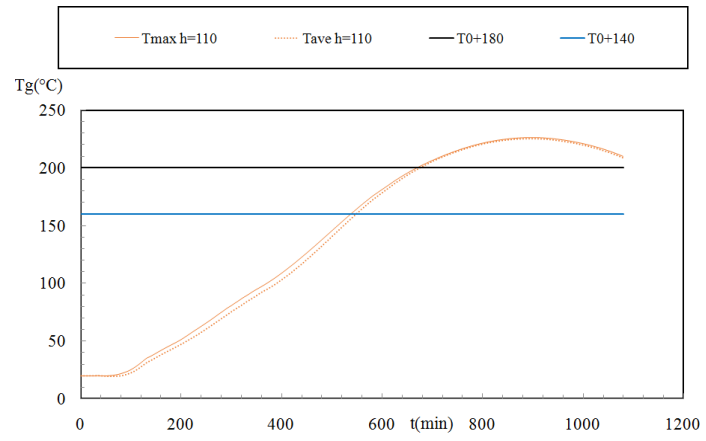	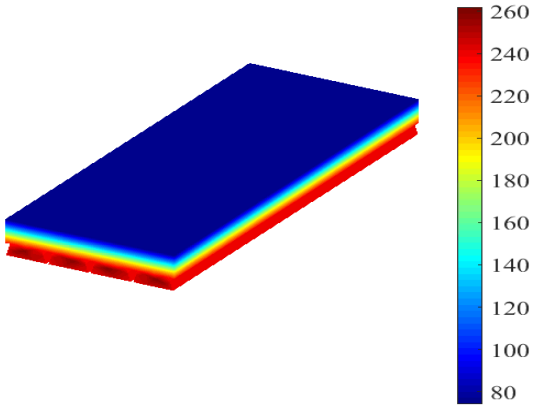 Slab60:h1=110mm Tmax=660 Tave=534min

Steel deck: -multideck	**Natural Fire curve 4**
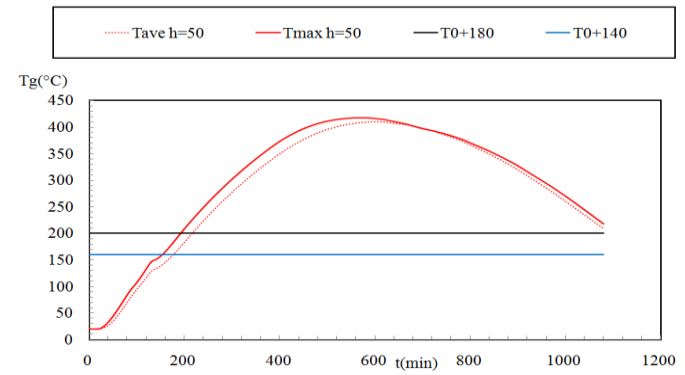	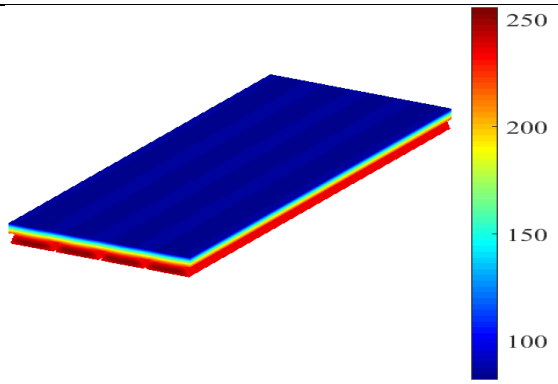 Slab61:h1=50mm Tmax=180 Tave=168min
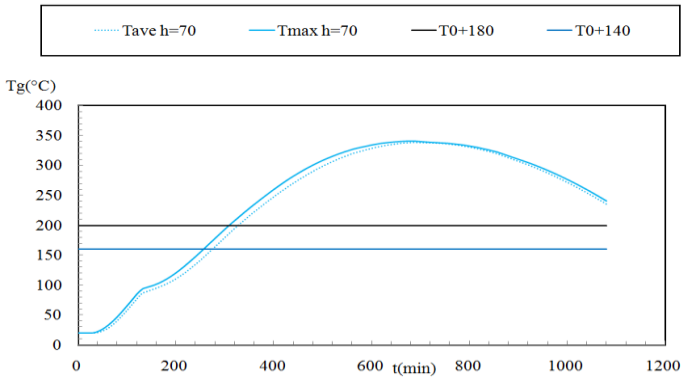	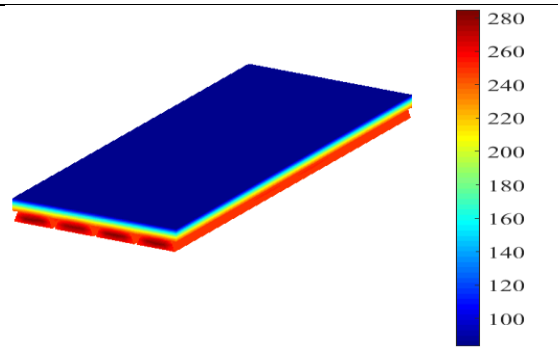 Slab62:h1=70mm Tmax=300 Tave=264 min
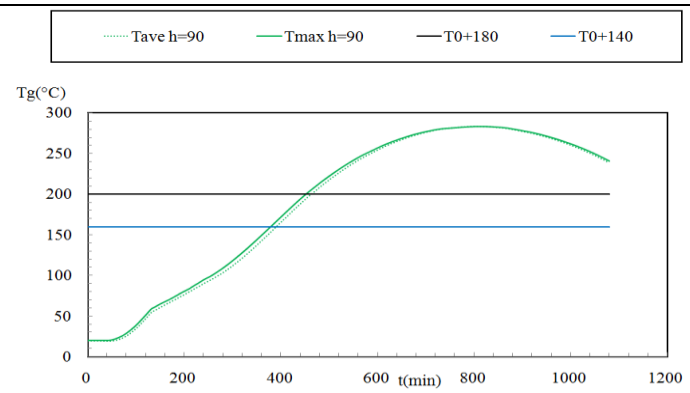	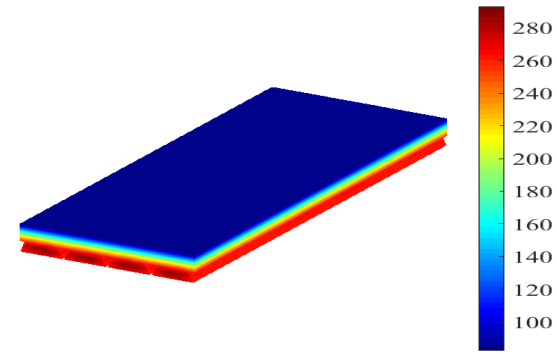 Slab63:h1=90mm Tmax=444Tave=378min
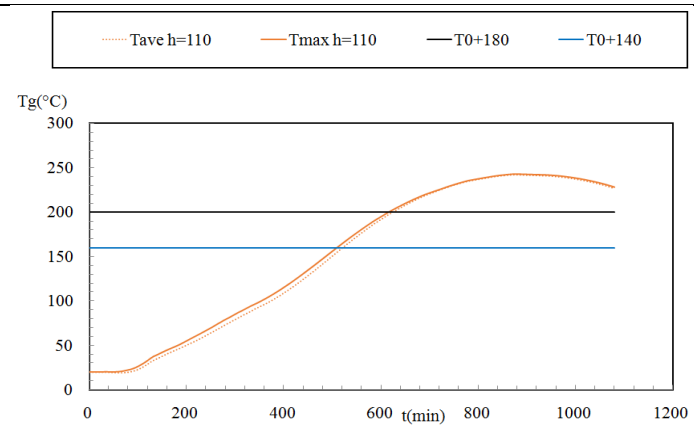	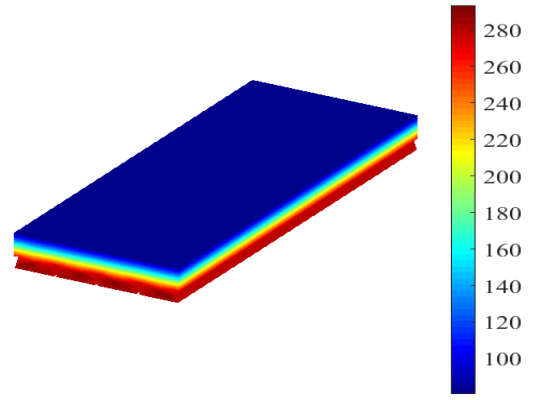 Slab64:h1=90mm Tmax=606 Tave=510min

Steel deck: -multideck	**Natural Fire curve 5**
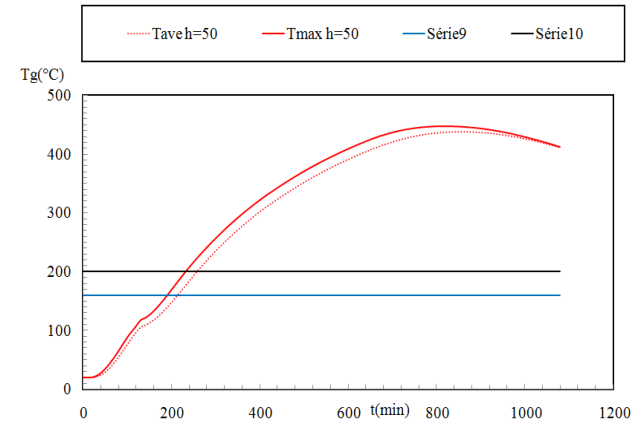	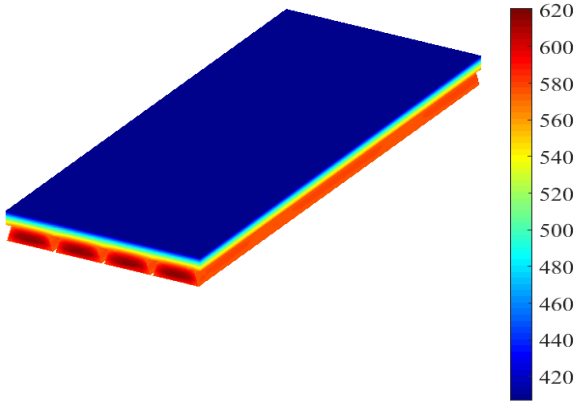 Slab65:h1=50mm Tmax=222 Tave=198min
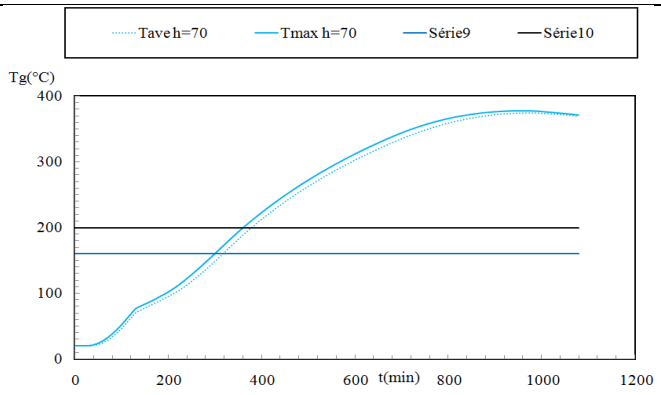	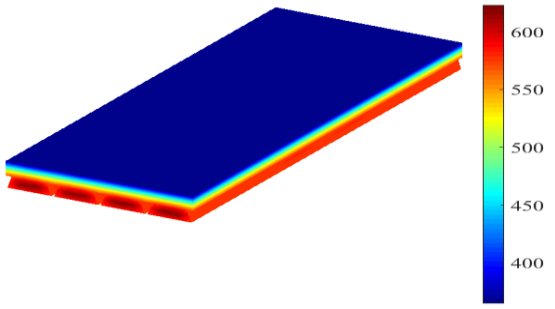 Slab66:h1=70mm Tmax=354 Tave=310min
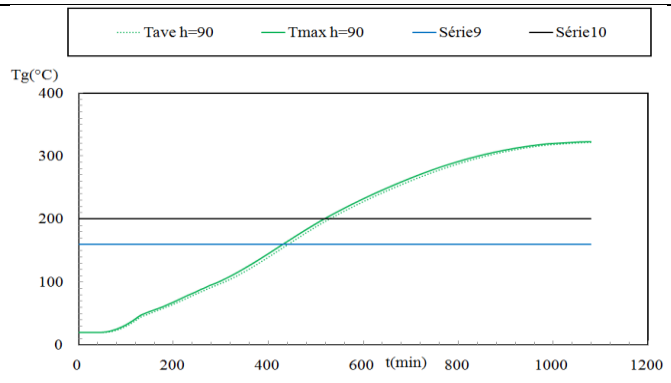	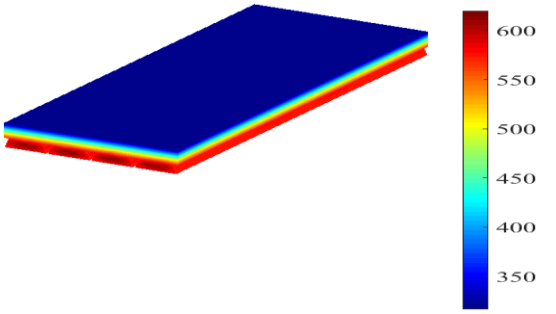 Slab67:h1=90mm Tmax=510 Tave=432min
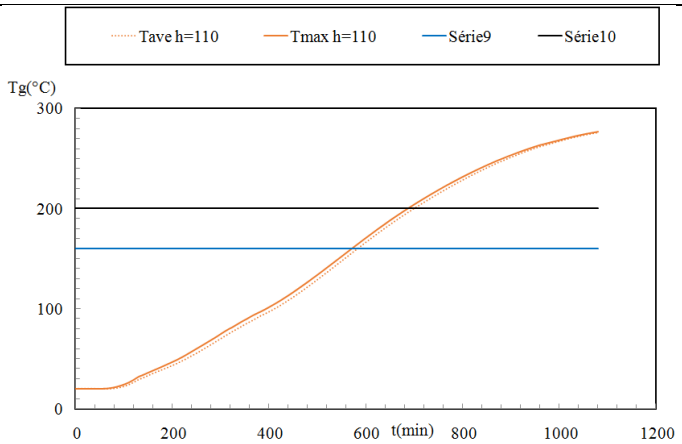	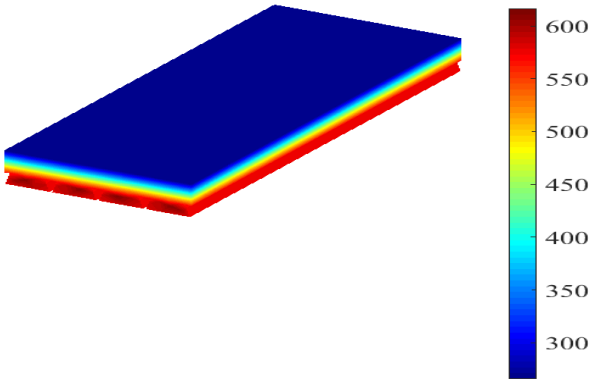 Slab68:h1=110mm Tmax=678 Tave=570min

Steel deck: -multideck	**Natural Fire curve 6**
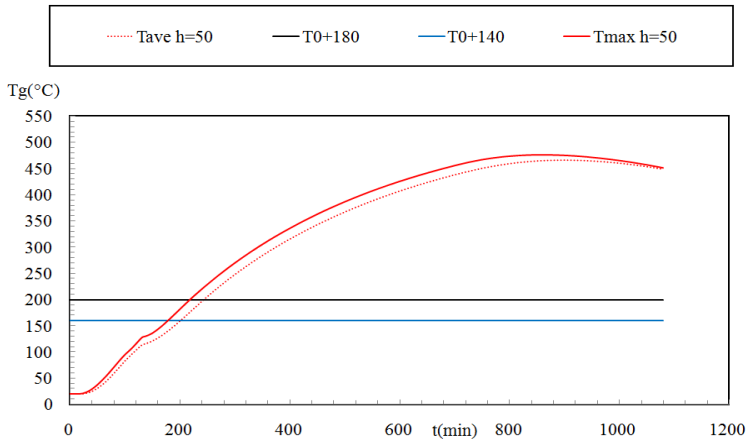	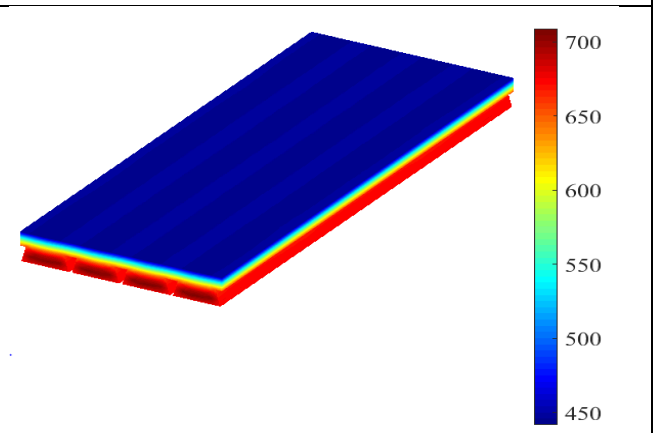 Slab69:h1=50mm Tmax=212 Tave=192min
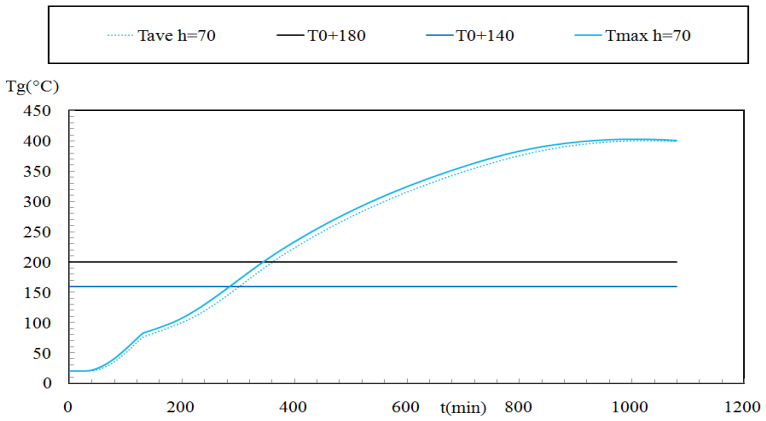	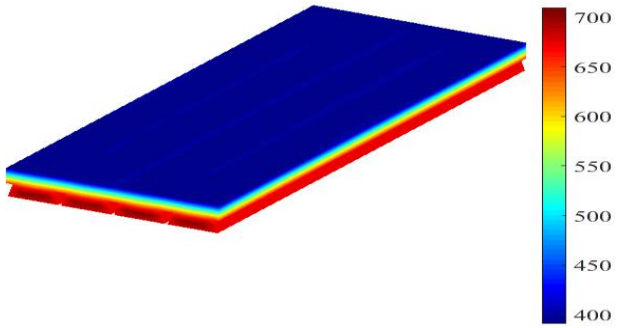 Slab70:h1=70mm Tmax=342 Tave=294min
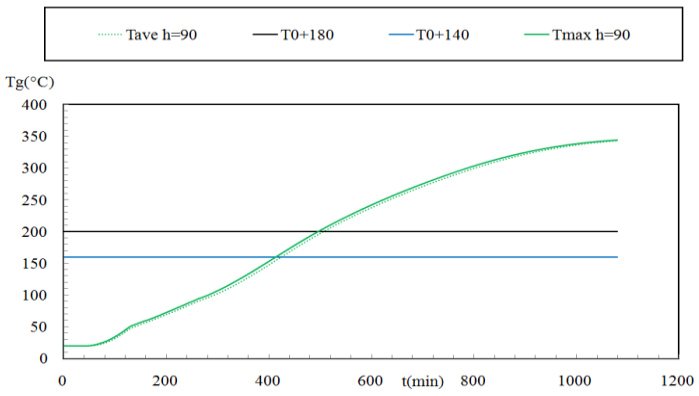	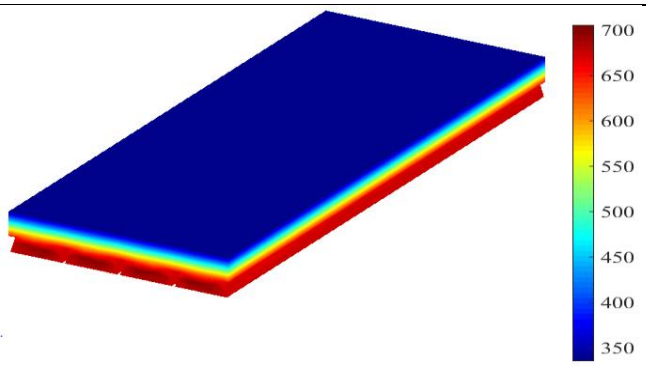 Slab71:h1=90mm Tmax=492 Tave=420min
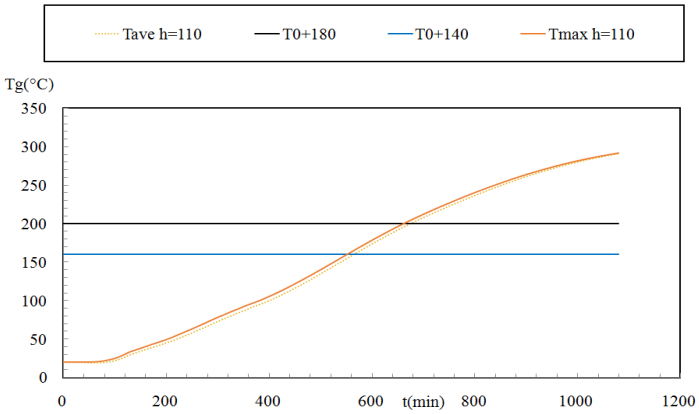	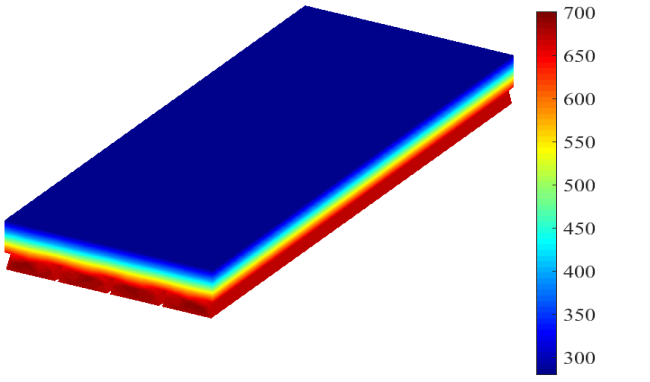 Slab72:h1=110mm Tmax=654 Tave=552min

Steel deck: Bondeck	**Natural Fire curve 1**
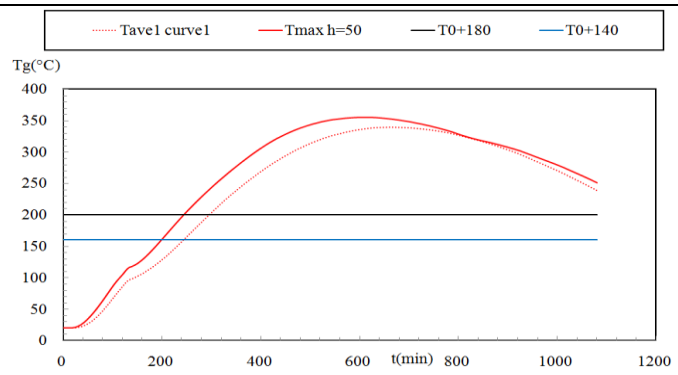	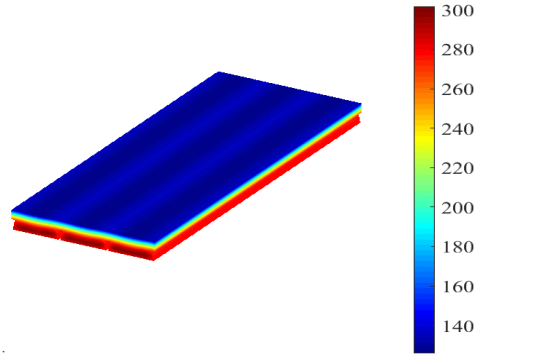 Slab73:h1=50mm Tmax=240Tave=228min
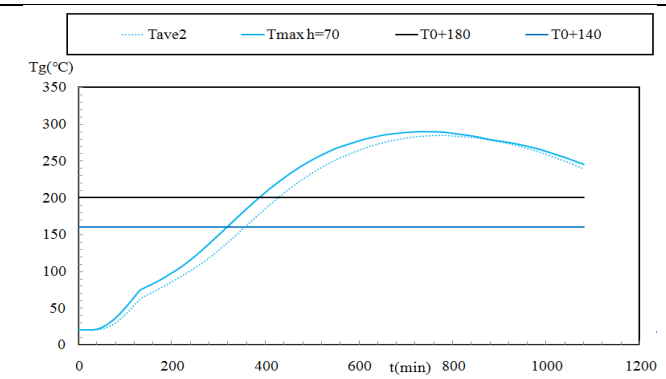	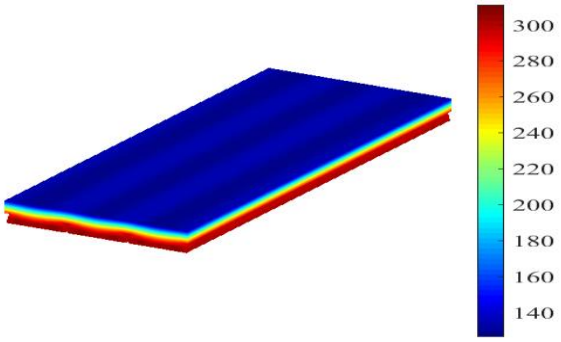 Slab74:h1=70mm Tmax=378Tave=354min
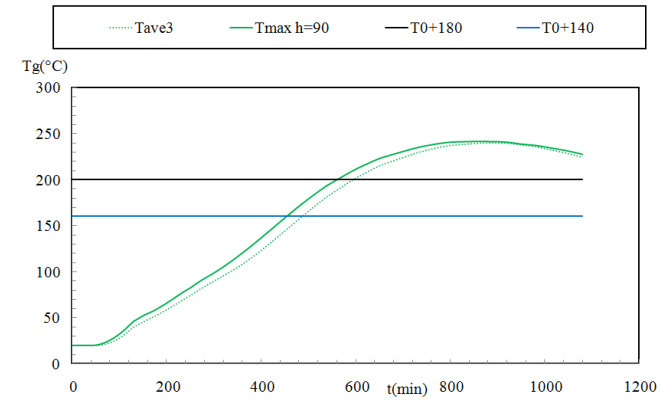	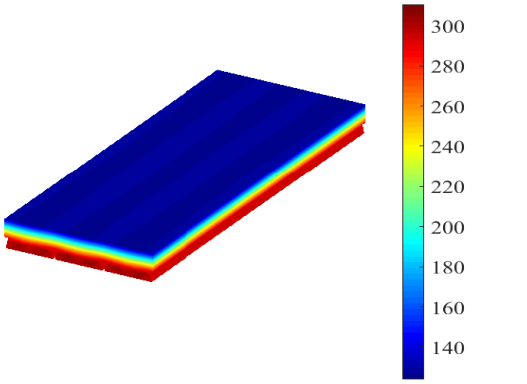 Slab75:h1=90mm Tmax=552Tave=486min
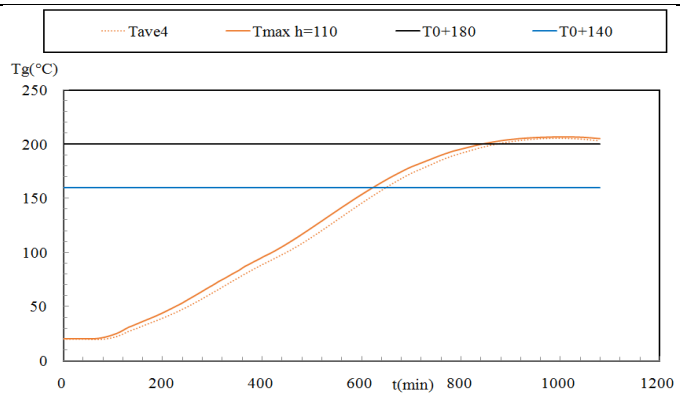	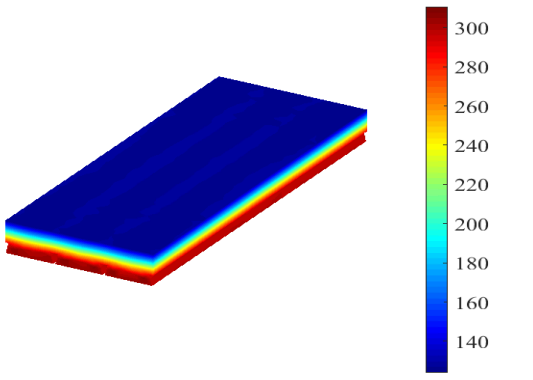 Slab76:h1=110mm Tmax=846Tave=642min

Steel deck: -Bondeck	**Natural Fire curve 2**
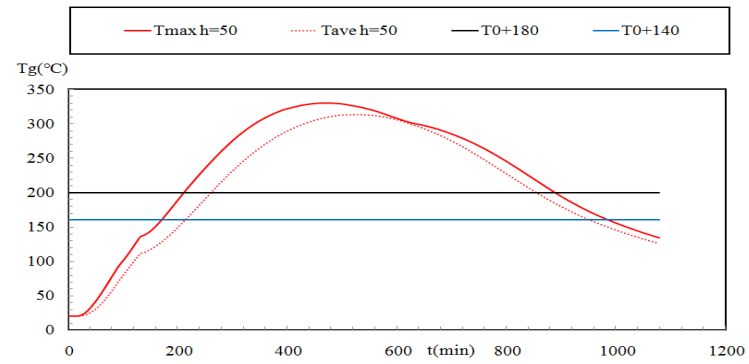	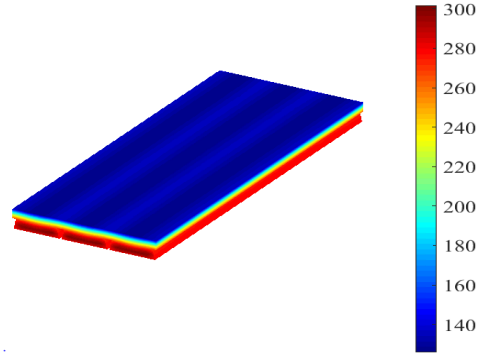 Slab77:h1=50mm Tmax=240Tave=228min
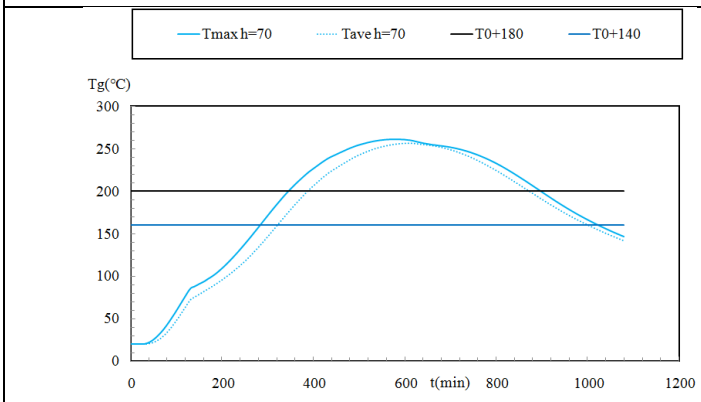	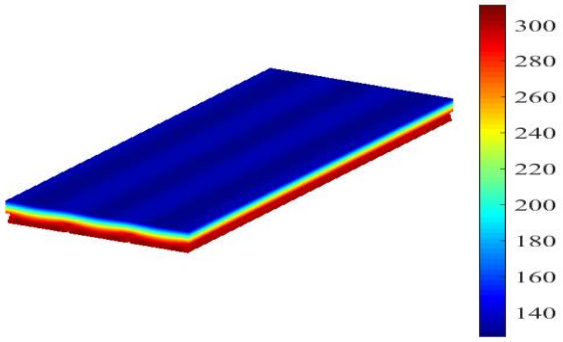 Slab78:h1=70mm Tmax=378Tave=348min
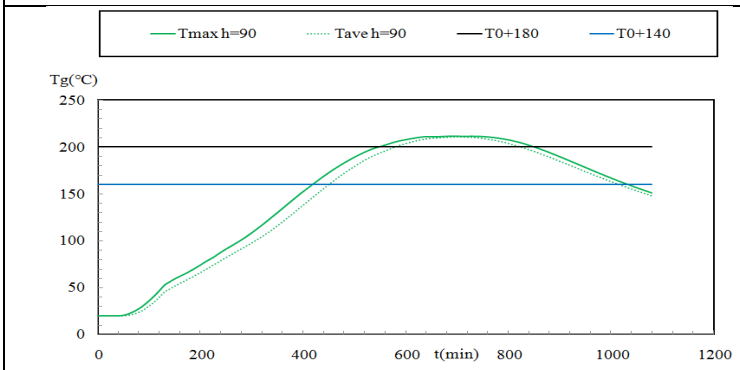	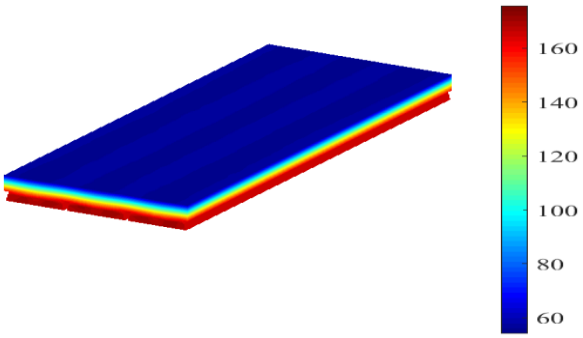 Slab79:h1=90mm Tmax=552Tave=480min
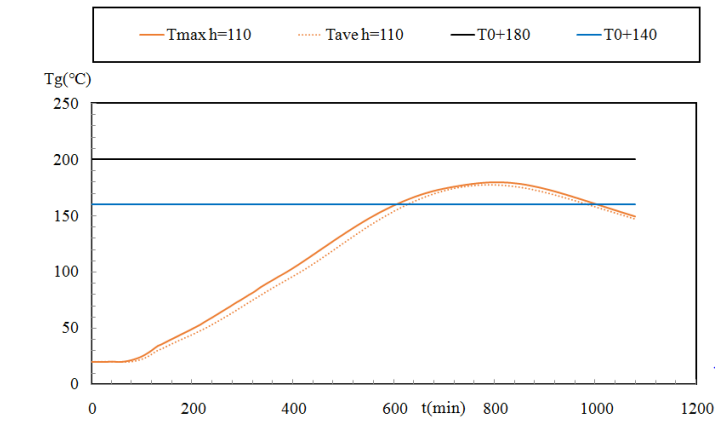	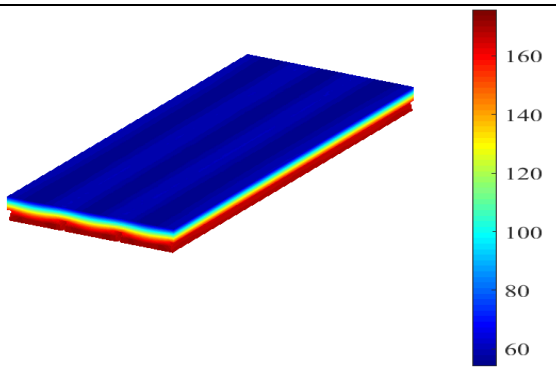 Slab80:h1=110mm Tave=624min

Steel deck: Bondeck	**Natural Fire curve 3**
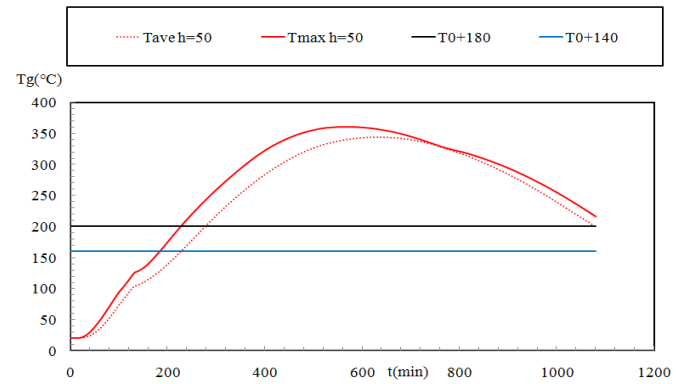	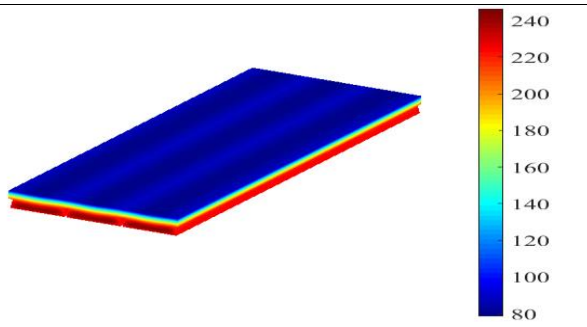 Slab81:h1=50mm Tmax=222 Tave=222min
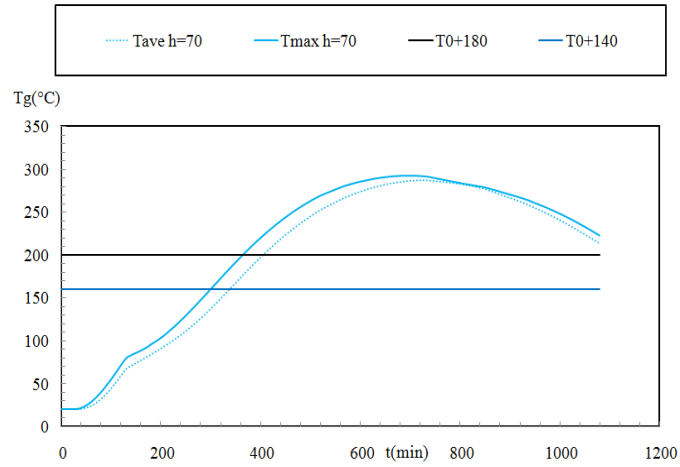	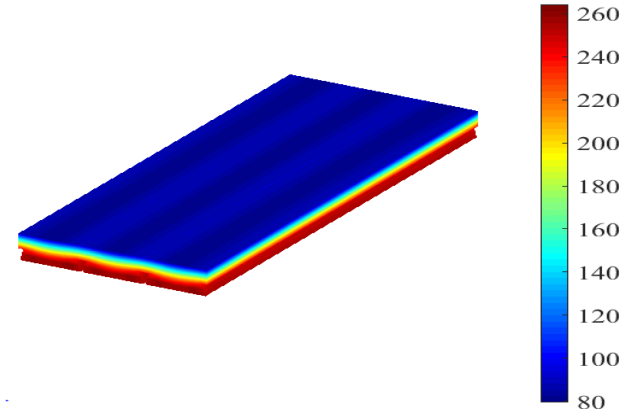 Slab82=70mm Tmax=360 Tave=330min
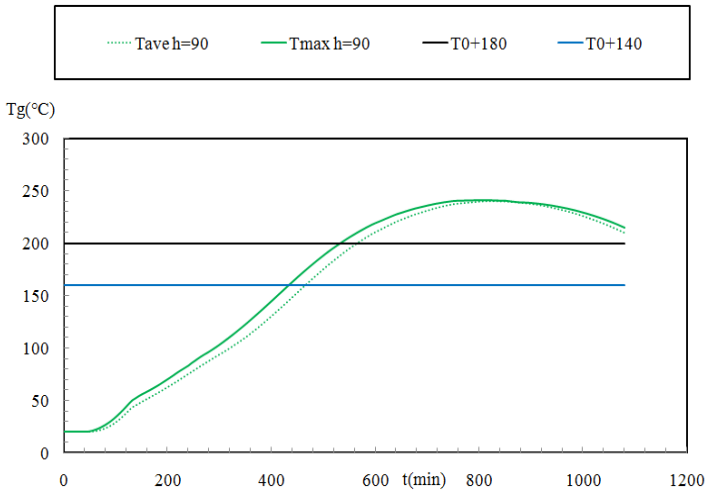	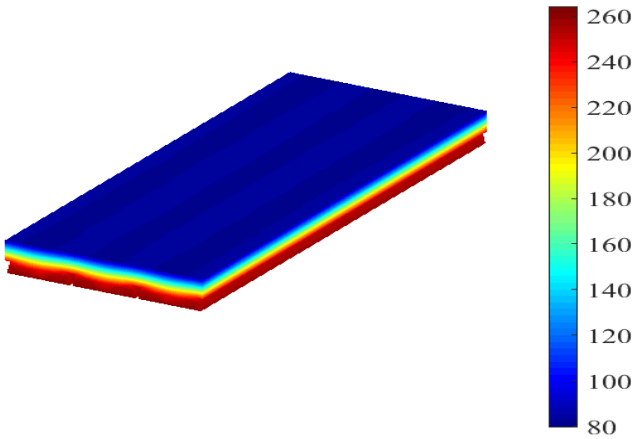 Slab83:h1=90mm Tmax=528 Tave=456min
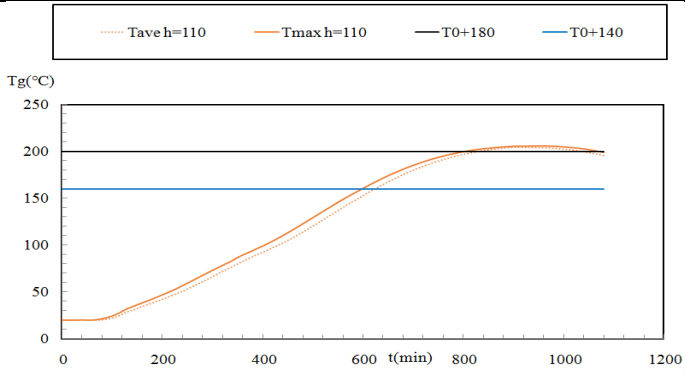	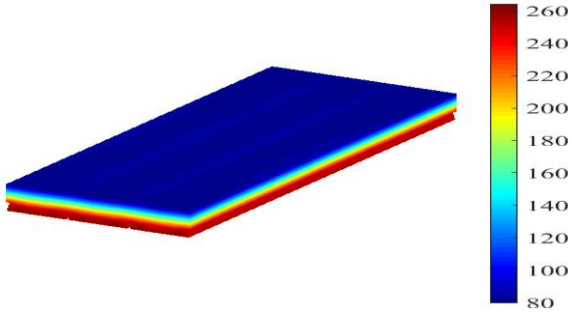 Slab84:h1=110mm Tmax=798 Tave=618min

Steel deck: -Bondeck	**Natural Fire curve 4**
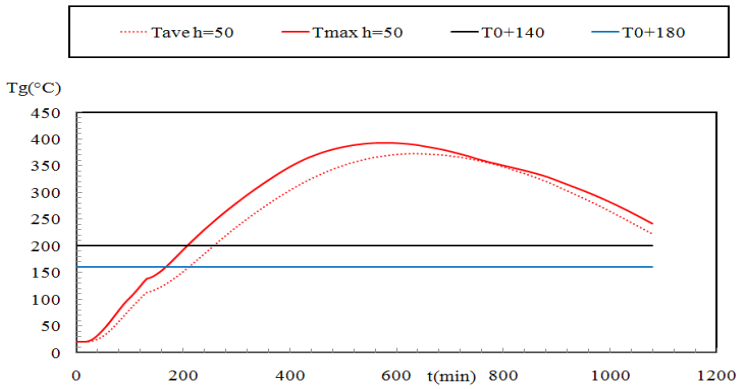	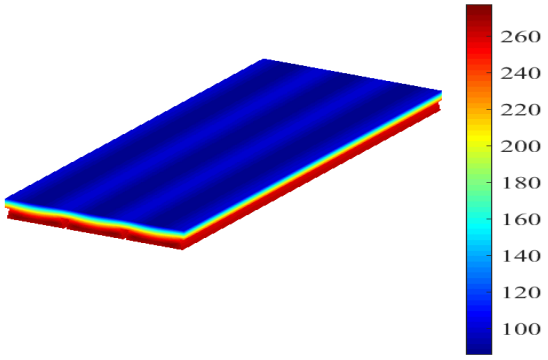 Slab85:h1=50mm Tmax=198 Tave=198min
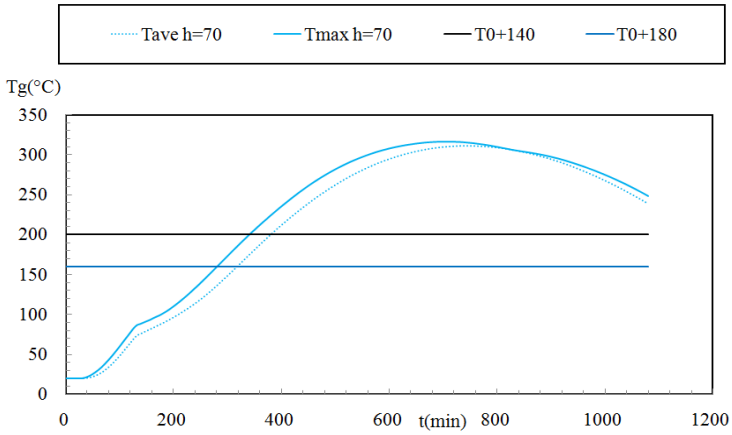	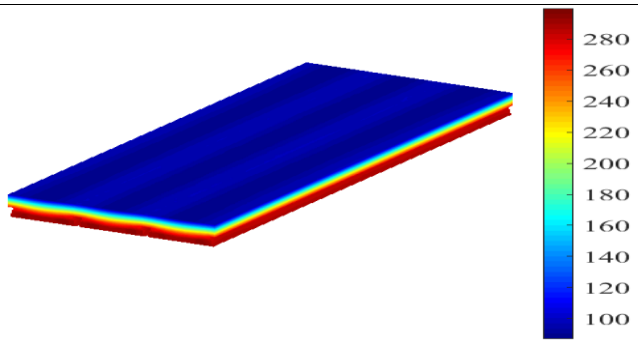 Slab86:h1=70mm Tmax=330 Tave=312min
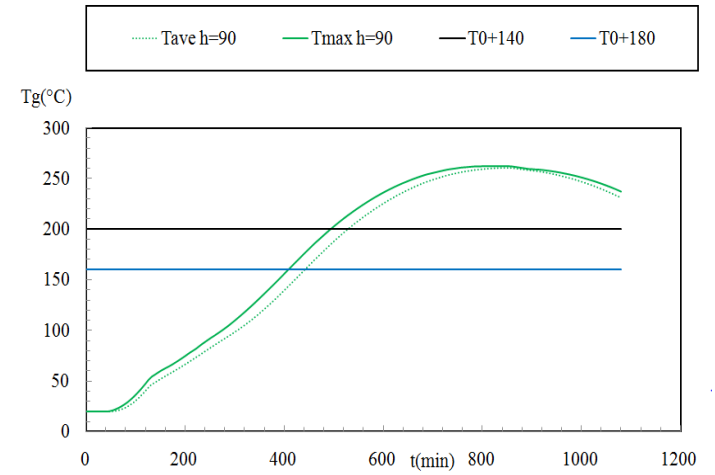	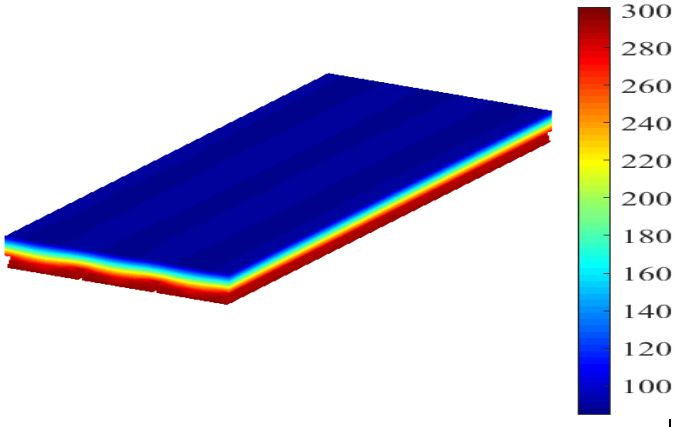 Slab87:h1=90mm Tmax=486 Tave=432min
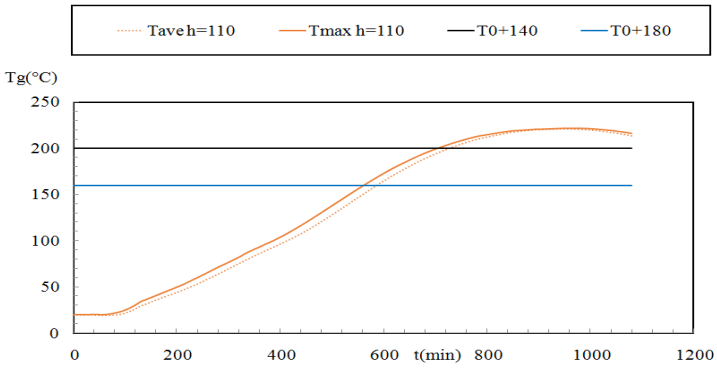	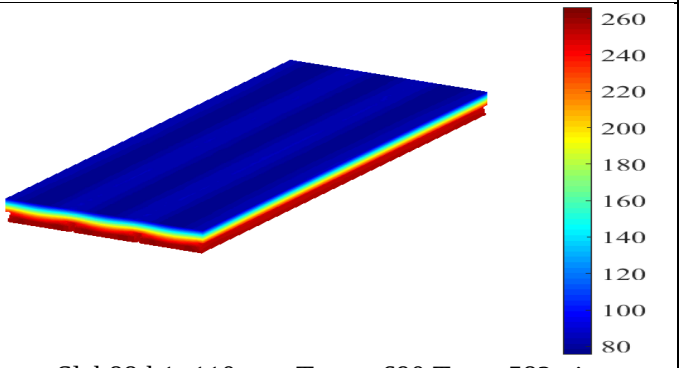 Slab88:h1=110mm Tmax=690 Tave=582min

steel deck: -Bondeck	**Natural Fire curve 5**
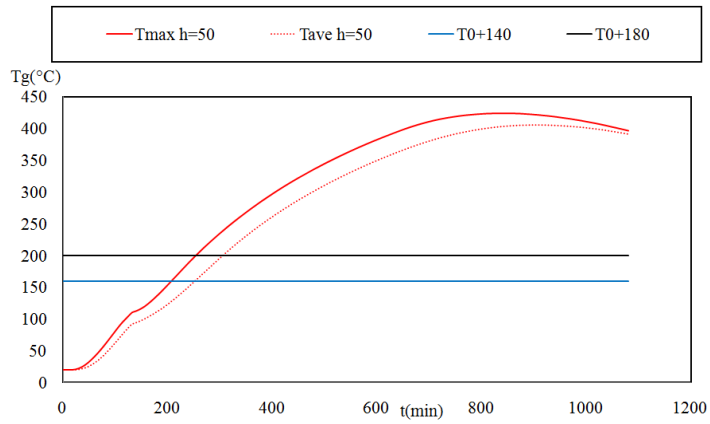	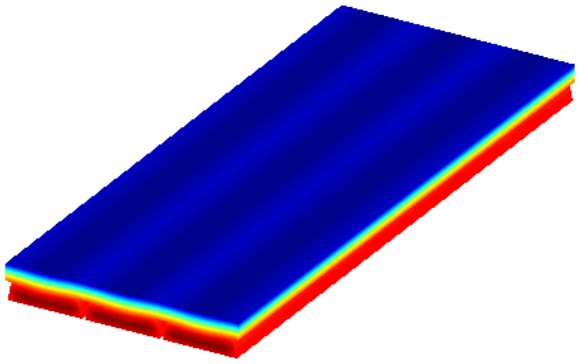 Slab89:h1=50mm Tmax=246 Tave=246min
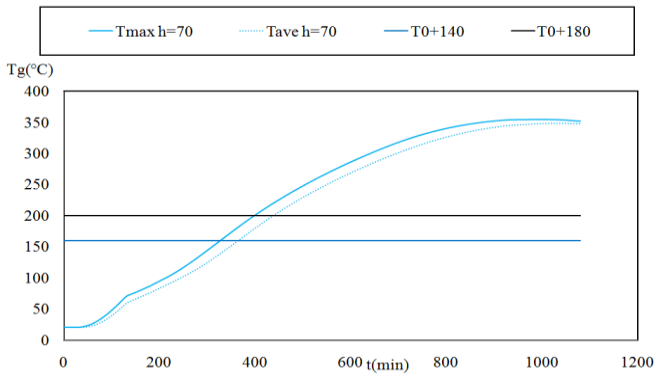	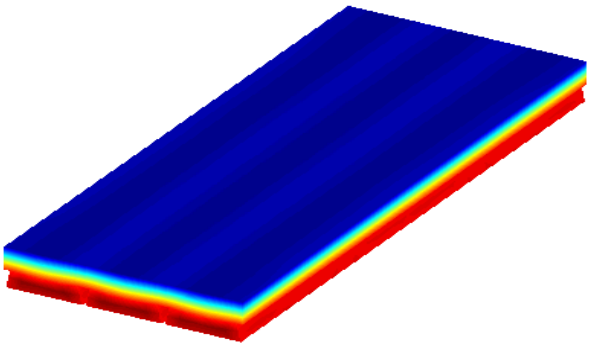 Slab90:h1=70mm Tmax=390Tave=360min
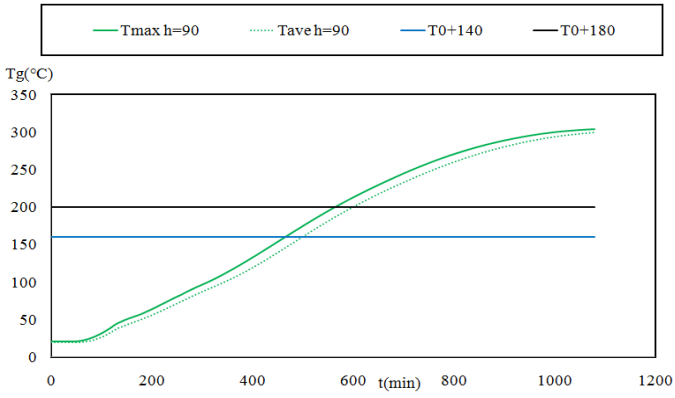	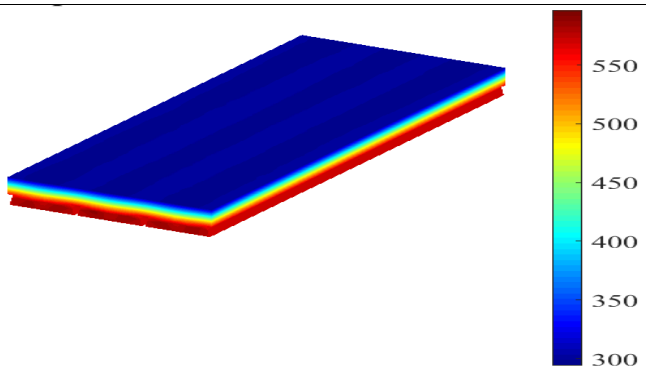 Slab91:h1=90mm Tmax=558 Tave=492min
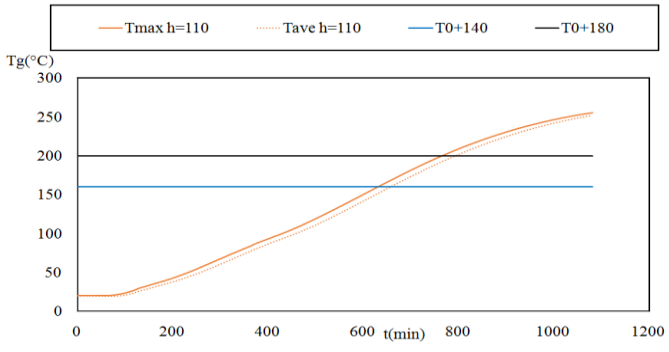	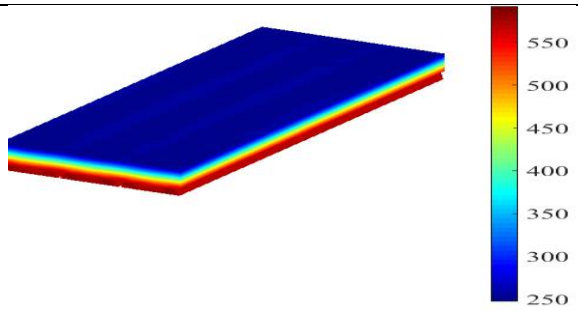 Slab92:h1=110mm Tmax=756 Tave=654min

steel deck: -Bondeck	**Natural Fire curve 6**
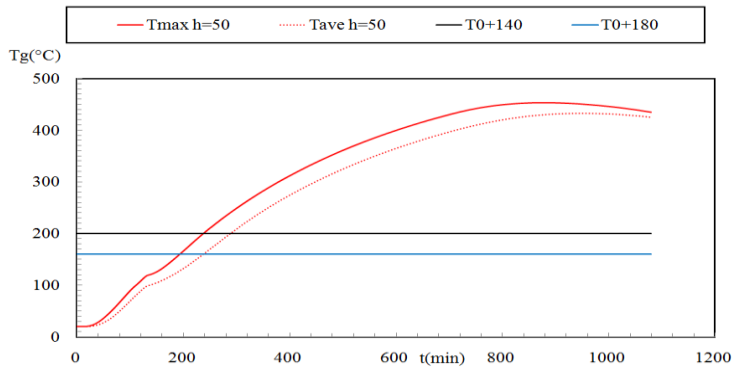	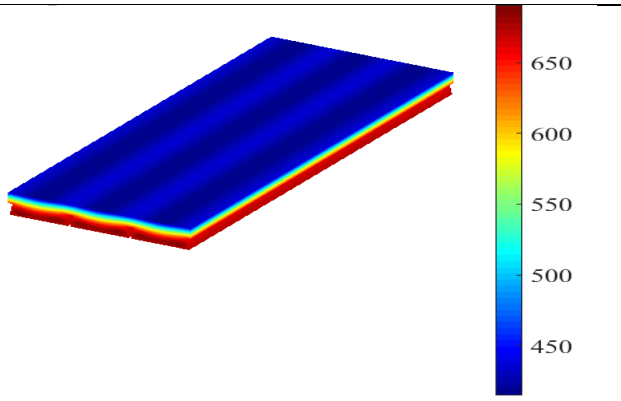 Slab93:h1=50mm Tmax=228 Tave=228min
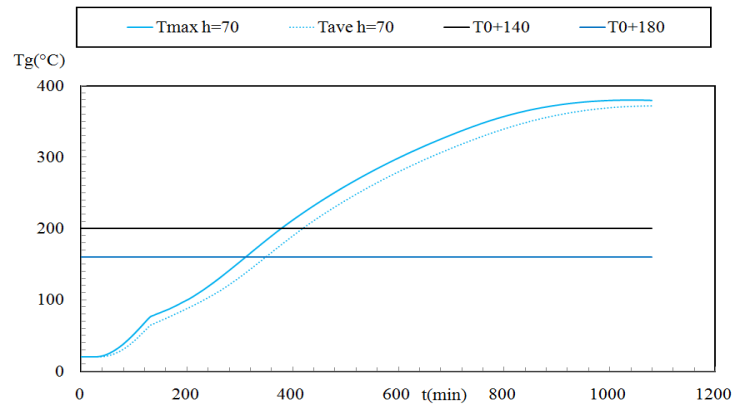	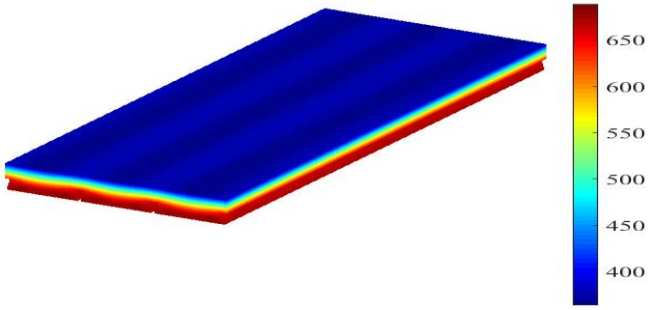 Slab94:h1=70mm Tmax=372 Tave=342min
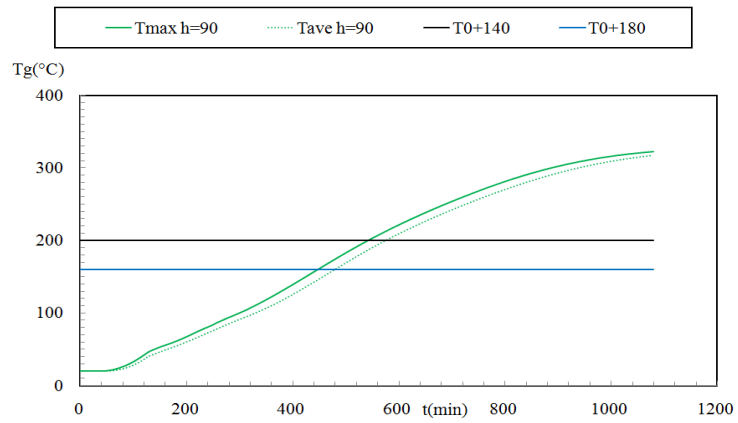	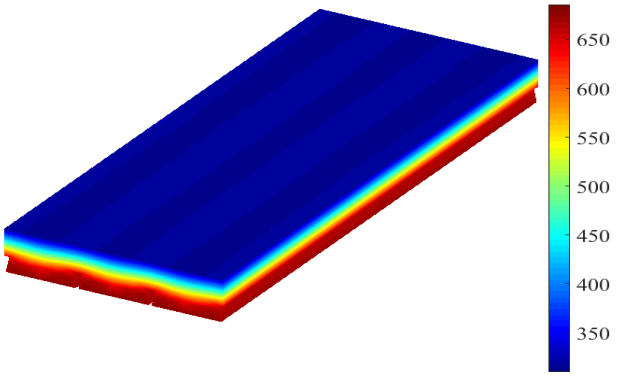 Slab95:h1=90mm Tmax=534 Tave=468min
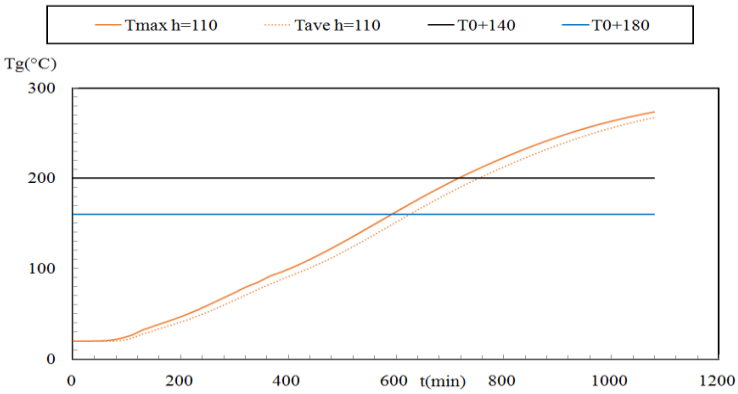	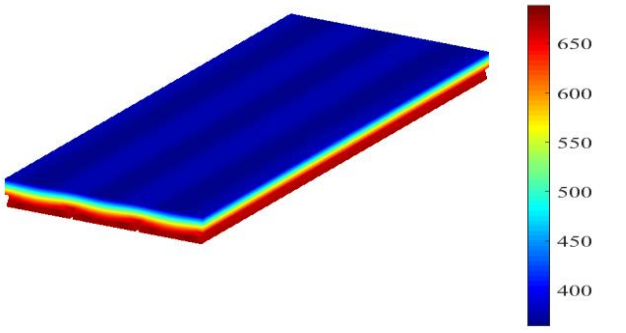 Slab96:h1=110mm Tmax=708 Tave=612min